Ministry of Higher Education & Scientific Research
Ninevah University
College of Electronics Engineering
Communication Engineering Department

Performance Investigation of the Null Steering Techniques in Linear Antenna Arrays

By

Mohammed Azhar Fakhri

M.Sc. Thesis

In

Communication Engineering

Supervised by

Prof. Dr. Jafar Ramadhan Mohammed

2022 A.D. **1444 A.H.**

Ministry of Higher Education & Scientific Research
Ninevah University
College of Electronics Engineering
Communication Engineering Department

Performance Investigation of the Null Steering Techniques in Linear Antenna Arrays

A thesis Submitted

By

Mohammed Azhar Fakhri

To

The Council of the College of Electronic Engineering

Ninevah University

As a Partial Fulfillment of the Requirements

for the Degree of Master of Science

In

Communication Engineering

Supervised by

Prof. Dr. Jafar Ramadhan Mohammed

2022 A.D. **1444 A.H.**

﴿ نَرۡفَعُ دَرَجَٰتٖ مَّن نَّشَآءُۗ

وَفَوۡقَ كُلِّ ذِي عِلۡمٍ عَلِيمٞ ٧٦ ﴾

صَدَقَ اللهُ العَظِيمُ

سورة يوسف – الآية 76

ACKNOWLEDGMENTS

First and foremost, praise and thanks be to Allah almighty, Who has given me strength, patience, and ability to complete this thesis.

I would like to express my sincere gratitude and thank to my supervisor Prof. Dr. Jafar R. Mohammed for his continuous guidance, useful suggestions, constant encouragement and assistance throughout preparing this research.

I would like to express my deep gratitude and thanks to the former Head of the Communications Engineering Department, Asst. Prof. Dr. Younis M. Abbosh, and the current Head, Asst. Prof. Dr. Mahmod A. Mahmod. I would also like to thank all the staff members of the Communication Engineering Department who have provided me with science and knowledge throughout the preparatory year. Thanks to all those who have given me advice and provided me with useful information during the research period.

Last but not least, I want to express my heartfelt gratitude to my family for their inspiration and support.

Mohammed Azhar Fakhri

ABSTRACT

The increasing interferences of the electromagnetic environment have prompted the study of array pattern nulling techniques. These techniques are very important in communication systems for minimizing degradation in signal-to-noise ratio performance due to undesired interference, which motivates advances in communication receiver antennas and hence synthesizing methods.

This thesis investigates three types of null steering methods: Schelkunoff polynomial, Godara, and the Adapted Side Lobe Canceller (ASLC) using a Matlab program. Two antenna array sizes (N) have been used: N=6 elements and N=11 elements, and the distances (d) between the elements are 0.2λ, 0.4λ, and 0.5λ for the three utilized methods. The performance of the null steering methods was compared to that of a broadside uniform linear array.

Simulation results show that the Schelkunoff method has the ability to offset N-1 nulls to the visible region at d=0.2λ, while the Godara method creates nulls at the specified angles at d=0.5λ. The ASLC method achieved the desired direction of the main beam and null position at a Signal to Interference noise Ratio (SIR) -30 dB, and the performance degraded at a SIR of 0 dB and 30 dB.

The Schelkunoff and ASLC achieved Average Side Lobe Level (ASLL) higher than the uniform array, while Godara achieved the same ASLL as the uniform array. The three techniques achieved higher Taper efficiency in comparison to a uniform array. Finally, it has been shown that the three utilized methods achieved higher directivity than that of uniform arrays, and the maximum obtained directivity is achieved in the ASLC.

TABLE OF CONTENTS

Subject		Page
ACKNOWLEDGMENTS		I
ABSTRACT		II
TABLE OF CONTENTS		III
LIST OF FIGURES		V
LIST OF TABLES		VIII
LIST OF ABBREVIATIONS		VIII
LIST OF SYMBOLS		IX
CHAPTER ONE - INTRODUCTION		
1.1	Overview	1
1.2	Literature Review	4
1.3	Aims of the Thesis	11
1.4	Outlines of the Thesis	11
CHAPTER TWO - BACKGROUND THEORY		
2.1	Introduction	12
2.2	Antenna Array	12
2.3	Parameters of Antenna Array	18
2.3.1	Radiation Pattern	18
2.3.1.1	Half Power Beam Width (HPBW)	19
2.3.1.2	First Null Beam Width (FNBW)	20
2.3.1.3	Side Lobe Level (SLL)	21
2.3.1.4	Average Side Lobe Level (ASLL)	22
2.3.1.5	Taper Efficiency	22
2.3.2	Directivity	23
2.4	Linear Array Configuration	23
2.4.1	Uniform Linear Array	24
2.4.2	Non-Uniform Linear Array	24
2.4.2.1	Binomial Array	26

2.5	Null Steering Technique	27
2.5.1	Schelkunoff Method	29
2.5.2	Godara Method	30
2.5.3	Sidelobe Canceller (SLC) Method	32
2.5.3.1	Conventional SLC - with separate auxiliary antennas	33
2.5.3.2	Adapted SLC - by using a number of the main antenna elements as an auxiliary antenna	34
CHAPTER THREE – NULL STEERING TECHNIQUES SIMULATION MODELING		
3.1	Introduction	35
3.2	Schelkunoff Method	36
3.3	Godara Method	37
3.4	Adapted Side Lobe Canceller (ASLC)	39
CHAPTER FOUR - SIMULATION RESULTS AND PERFORMANCE TESTING		
4.1	Introduction	40
4.2	Schelkunoff Method Performance	40
4.3	Godara Method Performance	51
4.4	Adapted Side Lobe Canceller (ASLC) Method Performance	59
4.5	Null Steering Method Maximum Directivity Result	69
4.6	Results Discussion	70
4.6.1	Regarding to Schelkunoff Method	70
4.6.2	Regarding to Godara method	71
4.6.3	Regarding to Adapted Side Lobe Canceller (ASLC)	71
CHAPTER FIVE- CONCLUSIONS AND FUTURE WORKS		
5.1	Conclusion	73
5.2	Future Works	74
REFERENCES		75

LIST OF FIGURES

Figure	Title	Page
1.1	Radiation pattern of a directional antenna	2
2.1	N-isotropic array elements geometry	14
2.2	The antenna arranged as an array with a distance of quarter wavelength between them	16
2.3	Broadside array beam pattern	17
2.4	End-Fire array beam pattern	17
2.5	Scanning array beam pattern	18
2.6	Circular radiation pattern shows the different types of lobes and null	19
2.7	Half-power beam width	20
2.8	The FNBW and HPBW	21
2.9	The first side lobe level	22
2.10	Linear array antenna topology	24
2.11	Non-uniform linear array with even and odd number	26
2.12	The excitation coefficients of the binomial arrays for up to 10 array elements	27
2.13	Null signal to the interference source	28
2.14	A three-element array that contains both favorable and unwanted signals	30
2.15	Block diagram of side lobe cancellation principle	32
2.16	Structure of the Conventional SLC technique	33
2.17	Structure of the Adapted SLC technique	34
3.1	Mechanism operation using Schelkunoff Method	36
3.2	Mechanism operation using Godara Method	37
3.3	Mechanism operation using ASLC Method	39
4.1	Amplitude excitation comparison between Schelkunoff and uniform array at N=6	42
4.2	Amplitude excitation comparison between Schelkunoff and uniform array at N=11	43
4.3	Phase excitation comparison between Schelkunoff and uniform array at N=6	43

4.4	Phase excitation comparison between Schelkunoff and uniform array at N=11	44
4.5	Schelkunoff and uniform arrays comparison radiation pattern (N=6, d=0.2 λ)	44
4.6	Schelkunoff and uniform arrays comparison radiation pattern (N=11, d=0.2λ)	45
4.7	Schelkunoff and uniform arrays comparison radiation pattern (N=6, d=0.4 λ)	46
4.8	Schelkunoff and uniform arrays comparison radiation pattern (N=11, d=0.4 λ)	46
4.9	Schelkunoff and uniform arrays comparison radiation pattern (N=6, d=0.5 λ)	47
4.10	Schelkunoff and uniform arrays comparison radiation pattern (N=11, d=0.5 λ)	47
4.11	ASLL comparison between Schelkunoff and uniform arrays at d=0.2λ	48
4.12	ASLL comparison between Schelkunoff and uniform arrays at d=0.4λ	48
4.13	ASLL comparison between Schelkunoff and uniform arrays at d=0.5λ	49
4.14	Taper efficiency comparison between Schelkunoff and uniform arrays at d=0.2λ	49
4.15	Taper efficiency comparison between Schelkunoff and uniform arrays at d=0.4λ	50
4.16	Taper efficiency comparison between Schelkunoff and uniform arrays at d=0.5λ	50
4.17	Amplitude excitation comparison between Godara and uniform array at N=6	51
4.18	Amplitude excitation comparison between Godara and uniform array at N=11	52
4.19	Phase excitation comparison between Godara and uniform array at N=6	52
4.20	Phase excitation comparison between Godara and uniform array at N=11	53
4.21	Godara and uniform arrays comparison radiation pattern (N=6, d=0.2 λ)	53
4.22	Godara and uniform arrays comparison radiation pattern (N=6, d=0.4 λ)	54
4.23	Godara and uniform arrays comparison radiation pattern (N=6, d=0.5 λ)	54
4.24	Godara and uniform arrays comparison radiation pattern (N=11, d=0.2λ)	55

4.25	Godara and uniform arrays comparison radiation pattern (N=11, d=0.4λ)	55
4.26	Godara and uniform arrays comparison radiation pattern (N=11, d=0.5λ)	56
4.27	ASLL comparison between Godara and uniform arrays at d=0.2λ	56
4.28	ASLL comparison between Godara and uniform arrays at d=0.4λ	57
4.29	ASLL comparison between Godara and uniform arrays at d=0.5λ	57
4.30	Taper efficiency comparison between Godara and uniform arrays at d=0.2λ	58
4.31	Taper efficiency comparison between Godara and uniform arrays at d=0.4λ	58
4.32	Taper efficiency comparison between Godara and uniform arrays at d=0.5λ	59
4.33	Amplitude excitation comparison between ASLC and uniform array at N=6	60
4.34	Amplitude excitation comparison between ASLC and uniform array at N=11	60
4.35	Phase excitation comparison between ASLC and uniform array at N=6	61
4.36	Phase excitation comparison between ASLC and uniform array at N=11	61
4.37	Geometry of the main and auxiliary elements and the beam pattern at N = 6, M = 2, d = 0.2λ, and SIR = -30 dB	62
4.38	Geometry of the main and auxiliary elements and the beam pattern at N = 6, M = 2, d = 0.4λ, and SIR = -30 dB	62
4.39	Geometry of the main and auxiliary elements and the beam pattern at N = 6, M = 2, d = 0.5λ, and SIR = -30 dB	63
4.40	Geometry of the main and auxiliary elements and the beam pattern at N = 11, M = 5, d = 0.2λ, and SIR = -30 dB	63
4.41	Geometry of the main and auxiliary elements and the beam pattern at N = 11, M = 5, d = 0.4λ, and SIR = -30 dB	64
4.42	Geometry of the main and auxiliary elements and the	64

	beam pattern at N = 11, M = 5, d = 0.5λ, and SIR = -30 dB	
4.43	Geometry of the main and auxiliary elements and the beam pattern at N = 11, M = 5, and SIR = 0 dB	65
4.44	Geometry of the main and auxiliary elements and the beam pattern at N = 11, M = 5, and SIR = 30 dB	65
4.45	ASLL comparison between ASLC and uniform arrays at d=0.2λ	66
4.46	ASLL comparison between ASLC and uniform arrays at d=0.4λ	66
4.47	ASLL comparison between ASLC and uniform arrays at d=0.5λ	67
4.48	Taper efficiency comparison between ASLC and uniform arrays at d=0.2λ	67
4.49	Taper efficiency comparison between ASLC and uniform arrays at d=0.4λ	68
4.50	Taper efficiency comparison between ASLC and uniform arrays at d=0.5λ	68

LIST OF TABLES

Table	Title	Page
3.1	Simulation Parameters	35
4.1	ASLC Simulation Parameters	59
4.2	Null Steering Methods Directivity	69

LIST OF ABBREVIATIONS

Abbreviation	Name
ASLC	Adapted Side Lobe Canceller
ASLL	Average Side Lobe Level
BA	Bat Algorithm
BFA	Bacterial Foraging Algorithm
BSO	Backtracking Search Optimization
CLONGALG	Clonal Selection Algorithm
FNBW	First Null Beam Width
GA	Genetic Algorithm
HPBW	Half Power Beam Width
MA	Memetic Algorithm
MTACO	Modified Touring Ant Colony Algorithm
MODE	Multiple Objective Differential Evolution
MVDR	Minimum Variance Distortion less Response

NSGA-2	Nondominated Sorting GA-2
PGSA	Plant Growth Stimulation
PSO	Particle Swarm Optimization
QPM	Quadratic Programming Methods
SLC	Sidelobe Canceller
SLL	Side Lobe Level
TSA	Tabu Search Algorithm
ULA	Uniform Linear Array

LIST OF SYMBOLS

Symbol	Name
λ	Wavelength of the transmit signal
D	Directivity
AF	Array Factor
N	Number of the Array Elements
ψ	Array Phase
k	Propagation constant
β	Phase constant
W	Weights
d	Spacing between the elements
M	Auxiliary element number
θ	Azimuth angle
a_n	non-uniform bounty excitation

CHAPTER ONE

INTRODUCTION

1.1 Overview

An Antenna is a transducer, which converts electrical power into electromagnetic waves and vice versa. An Antenna can be used either as a transmitting antenna or a receiving antenna. A transmitting antenna is one, which converts electrical signals into electromagnetic waves and radiates them. A receiving antenna is one, which converts electromagnetic waves from the received beam into electrical signals. In two-way communication, the same antenna can be used for both transmission and reception [1].

In general, antennas of individual elements may be classified as isotropic, omnidirectional, and directional according to their radiation characteristics. An isotropic radiator is one which radiates its energy equally in all directions. Even though such elements are not physically realizable, they are often used as references to compare to them the radiation characteristics of actual antennas [2]. Omnidirectional antennas are radiators having essentially an isotropic pattern in a given plane (the azimuth plane) and directional in an orthogonal plane (the elevation plane). Omnidirectional antennas are adequate for simple RF environments where no specific knowledge of the users directions is either available or needed [3]. Unlike an omnidirectional antenna, where the power is radiated equally in all directions in the horizontal (azimuth) plane, a directional antenna concentrates the power primarily in certain directions or angular regions [2]. The radiating properties of these antennas are described by a radiation pattern, which is a plot of the radiated energy from the antenna measured at various angles at a constant radial distance from the antenna. In the near

field the relative radiation pattern (shape) varies according to the distance from the antenna, whereas in the far field the relative radiation pattern (shape) is basically independent of distance from the antenna. The direction in which the intensity/gain of these antennas is maximum is referred to as the boresight direction [2,4]. The gain of directional antennas in the boresight direction is usually much greater than that of isotropic and/or omnidirectional antennas. The radiation pattern of a directional antenna is shown in figure 1.1 where the boresight is in the direction θ=0°. The plot consists of a main lobe (also referred to as major lobe), which contains the boresight and several minor lobes including side and rear lobes. Between these lobes are directions in which little or no radiation occurs. These are termed minima or nulls. Ideally, the intensity of the field toward nulls should be zero (minus infinite dBs). However, practically nulls may represent a 30 or more dB reduction from the power at boresight [5].

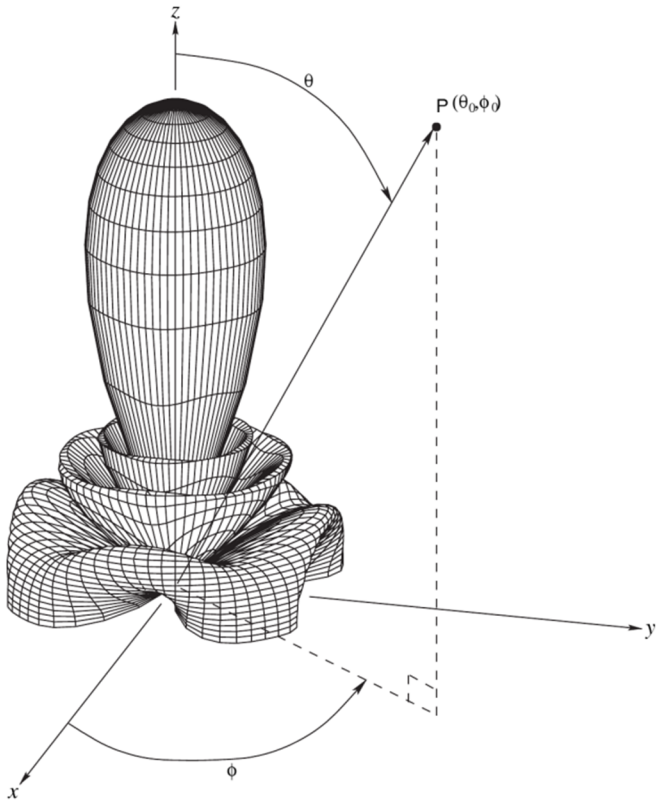

Figure (1.1) Radiation pattern of a directional antenna [6]

For long-distance communication, it is required to construct an antenna with high directional properties. This can be done by combining a number of antennas into an array. Array of antenna offers an improved directivity and the ability to steer its beam with control of excitation amplitude and phase of signal [7].

Antenna arrays may be referred to as phased arrays and adaptive arrays according to their functionality and operation. A phased array antenna uses an array of single elements and combines the signal induced on each element to form the array pattern. The direction where the maximum gain occurs is usually controlled by adjusting properly the amplitude and phase between the different elements [2]. Adaptive arrays for communication have been widely examined over the last few decades. The main thrust of these efforts has been to develop arrays that would provide both interference protection and reliable signal acquisition and tracking in communication systems [8]. The radiation characteristics of these arrays are adaptively changing according to changes and requirements of the radiation environment. Adaptive arrays provide significant advantages over conventional arrays in both communication and radar systems. They have well-known advantages for providing flexible, rapidly, configurable, beamforming and null-steering patterns [9]. The pattern of the array can be steered toward a desired direction space by applying phase weighting across the array and can be shaped by amplitude and phase weighting the outputs of the array elements [10]. A major reason for the progress in adaptive arrays is their ability to automatically respond to an unknown interfering environment by steering nulls and reducing side lobe levels in the direction of the interference, while keeping desired signal beam characteristics [11].

1.2 Literature Review

In 1983, H. Steyskal presented a method of sidelobe hulling, which involves perturbing the array illumination phase only. The general nonlinear problem was linearized by assuming the perturbations to be small, and an analytic solution was derived. Illustrative examples of sinc and Chebyshev patterns with imposed nulls were given [12].

In 1984, T. B. Vu achieved null steering without using phase shifters by forcing the zeros of the array factor to occur in conjugate pairs on the unit circle in the complex plane. It was shown that if the number of jammers is much smaller than half the total number of elements in the array, it is possible to optimise the pattern as well as suppressing the jammers. Alternatively, wide nulls in the radiation pattern can be easily approximated [13].

In 1986, H. Steyskal, R. Shore and R. Haupt reviewed several methods for synthesis of array antenna patterns with prescribed nulls. Methods based on full amplitude/phase control at each array element and methods with a restricted number of degrees of freedom were compared, with attention focused on the characteristic features of the resultant patterns. These features are largely independent of any algorithm for achieving the nulls, and therefore they also provide a perspective on the performance of adaptive antenna systems, which employ these various control architectures. [14]

In 1990, M. M. Dawoud and T. H. Ismail described a method for null steering based on the perturbations of element positions. This technique had a pattern cancellation with even symmetry that made it possible to induce nulls at symmetrical locations around the main beam. Additionally, it allowed the phase shifters to be utilized only to direct the main beam in the direction of the required signal [15].

In 1991, T. H. Ismail and M. M. Dawoud introduced a null steering method based on element position disruptions. By using this method, the phase shifters could be utilized to guide the main beam only in the direction of the required signal. By individually guiding the main beam and the nulls to arbitrary independent directions, it also eliminated the restrictions of the other approaches. Additionally, sidelobe cancellation and wide-band signal rejection could be achieved [16].

In the same year, I. Chiba and S. Mano presented a study in phased-array antennas, where nulls of the radiation pattern in phased-array antennas can be formed in the direction of undesired wave by controlling only the phase excitation without affecting the main beam. However, the computation time becomes very large when an antenna with a large number of elements is analyzed and it becomes very difficult to counteract the variation of wave boundary instantly. Based on the exact calculation of phase value by the method of plane-wave synthesis, the foremen-tioned elements were selected which contribute more to the null formation, and the method of controlling only the phase of the selected elements was presented. Using this method, the computation time had been reduced. Moreover, the depth of nulls and the gain of the main beam obtained in this way was the same as that produced by controlling the phase of all the antenna elements. As a result of numerical simulation and experiments of null forming in the phased-array antenna using a 5-bit phase shifter, deep nulls with the level of less than -40 dB had been formed without decreasing the gain of the main beam [17].

In 1995, M. M. Dawoud presented a method for null steering in scanned linear arrays by element position perturbations. The approach, which was based on the null only steering requirement, had been developed to enhance the performance of such arrays. Only minor adjustments were

made to the primary array characteristics, such as beam width and sidelobe levels. Results demonstrated this novel approach's advantages, particularly when used with phased arrays [18].

In 1999, T.H. Ismail and M.J. Mismar presented a new antenna configuration of dual phase shifters to steer multiple nulls by controlling the arbitrary phase perturbations. Consequently, the nonlinear problem of the perturbed element phases was transformed to a linear problem to obtain intermediate parameters, which are the cosine function of the perturbed phases. The linear programming approach was used to calculate the intermediate parameters. The computer simulations demonstrated the validity and the simplicity of this method [19].

In the same year, R. Vescovo introduced an iterative method for adding nulls in the array factor of linear arrays. This method just requires altering the phases or the amplitudes of the element excitations. Two synthesis problems for linear arrays that involve adding nulls to the array factor by adjusting simply the excitations' phase or amplitude, respectively, were taken into consideration. The method of consecutive projections was used to solve the issues repeatedly [20].

In 2000, Y. C. Chung and R. L. Haupt's paper introduced amplitude and phase nulling with a genetic algorithm with the intent of finding the optimum number of LSB of control needed to place multiple nulls while not significantly distorting the far field pattern. Many interference scenarios were modeled and individual runs were averaged to conclude that five LSB of amplitude and three LSB of phase control out of a total of eight bits were best for the linear array modeled. Representative samples of some of the interference scenarios modeled were shown [21].

In the same year, R. Vescovo presented a method for forming nulls in prescribed directions in the radiation pattern P_0 of an antenna array by

phase-only control. The method modified the excitation phases of P_0, allowing the construction of a sequence of patterns $\{P_n\}$ having increasingly deeper nulls. A solution was provided by terminating the sequence at a suitable step [22].

Also in 2000, J. R. Mohammed used a simple method to achieve cancellation or reduction in the sidelobes level in linear array by adding an auxiliary antenna that is consisting of two elements separated by a certain distance. The method depended on adding or subtracting between two responses obtained from main and auxiliary antennas. The suitable magnitude of the auxiliary antenna gave good reduction in sidelobe level and some sidelobes were cancelled [23].

J. A. Hejres in 2004, presented a technique that can steer nulls in the antenna pattern in the direction of powerful interference signals without impacting the main beam. The technique was based on the element position disturbances of selected antenna array elements. This technique allowed the phase shifters to be used for steering the main beam toward the required signal's direction. It also preserved the positions of those elements that contribute insignificantly to the nulls. The results were similar to those achieved using the method of controlling the locations of all elements [24].

In 2006, Moctar Mouhamadou, Patrick Vaudon, and Mohammed Rammal presented an efficient method for the pattern synthesis of the linear antenna arrays with the prescribed null and multi-lobe Beamforming. Multi-lobe pattern and adaptive nulling of the pattern was achieved by controlling only the phase of each array element. The proposed method was based on the Sequential Quadratic Programming (SQP) algorithm and the linear antenna array synthesis was modelled as a multi-ob jective optimization problem. Multi-objective optimization was concerned with the maximization (or minimization) of a vector of objectives functions in the

directions of desired signal that can be subject of a number of constraints (in our case, the constraints can be imposed as the null in the direction of interfering signal). To verify the validity of the technique, several illustrative examples of uniform excited array patterns with the main beam was placed in the direction of the useful signal and null was placed in the direction of potential interferers, and multi-beam patterns were demonstrated [25].

In 2007, M. J. Mismar, T. H. Ismail, and D. I. Abu-Al-Nadi devised an analytical synthesis approach that is based on the Schelkunoff's unit circle for phase-only control of linear antenna arrays. The array factor was defined as an array polynomial in the complex z-plane and the product of corresponding subpolynomials with roots on the unit circle. A constraint was developed such that the expansion of the subpolynomials generates current excitations with magnitudes of unity. The main beam properties were synthesized using the subpolynomial with the highest degree. The null steering for interference suppression was acquired by directing only one null with a single subpolynomial. The results validated the advanced analytical solution for synthesizing the recommended patterns with linear antenna array phase shifters [26].

In the same year, J. A. Hejres, A. Peng, and J. Hijres presented an approach for directing antenna pattern nulls in the direction of powerful interference signals. The process comprises separating a large array into two contiguous subarrays that were symmetrical about the array center. The nulls in the antenna pattern were formed using the element locations of one of the subarrays. This method allowed the phase shifters to be employed exclusively for steering the main beam [27].

In 2009, R. Ghayoula, N. Fadlallah, A. Gharsallah, and M. Rammal developed an effective method for synthesising directive beam and multi-

beam patterns and creating adaptive nulls in interference direction. The suggested approach relied on iterative minimization of a function that included constraints imposed in each direction with respect to excitation phases and a neural network technique. Several effects were presented to highlight the benefits and drawbacks of this approach. Back-propagation proved to be superior to previous phase-only adaptive algorithms. An eight-element array was constructed and experimented with different beam architectures to validate the proposed technique's performance [28].

In the same year, R. A. Qamar and N.M. Khan provided a thorough comparative analysis of the performance of the significant null steering techniques. It was found that Null Steering by Real-weight Control performs better other techniques including such Null Steering in Phased Arrays by controlling the Element Positions, Real-time Null Steering by the CLEAN Technique, and Null Steering Algorithm Based on Direction of Arrival Estimation. The observation was conducted utilising null depth, the maximum number of nulls which can be steered, computational complexity, and side lobe levels. [29]

In 2010, Dib et al. introduced a study of how to minimize the maximum side lobe level, and null steering for isotropic linear array antennas by controlling different array factors (amplitude, phase and positions). Two optimization methods had been performed: Taguchi’s optimization method and the adaptive self-differential evolution method. The results of these two methods provided better results for gradient-based methods and particle swarm optimization [30].

In 2014, J. R. Mohammed and K. H. Sayidmarie introduced a study that investigated an alternative strategy for null steering in adaptive arrays that is usually initiated by attempting to control the complex weights of all or most of the array elements, where only the two side elements of the

array were utilized for null steering. It was capable of changing the overall array pattern to put a wide angular null in the direction of unwanted interfering signals by appropriately adjusting the amplitude and phase excitations of these elements. With the exception of adaptive arrays, the suggested technique was much easier to implement in practice. [31]

In 2017, Mahmod A. Al Zubaidy, and Shatha M. Ali's paper discussed two types of beamforming systems. The first was the uniform phase and amplitude beamforming and the second was the non-uniform phase and amplitude. In this type the LMS algorithm was used to improve the signal to noise ratio. A Matlab Simulation results proved that the non – uniform amplitude and phase array is better than a uniform array in beam steering to get approach null at interference signals and get the desired signal with less noise [32].

In 2019, J. R. Mohammed in suggested a simple method for null steering by optimizing the positions of the last two edge elements of symmetrical uniformly spaced linear arrays. The steered nulls in the proposed array do not necessitate either the amplitude or phase weighting control of the element excitations. In practice, this characteristic is essential for avoiding null deviation caused by quantization errors in digital attenuators and/or digital phase shifters. The results demonstrated that the proposed array's interference rejection is comparable to that of fully non-uniform spaced arrays. Furthermore, by allowing a subset of the array's edge elements to be movable rather than the entire array. The proposed array has a lower cost, lower complexity, and shorter computational time [33].

In 2021, J. R. Mohammed, R. H. Thaher, and A. J. Abdulqader, conducted a study to perturb excitation of the minimum number of elements in such a way that the required number of nulls is obtained using

spares theory and convex optimization. The nulls generated are wide enough to cancel a whole specific sidelobe [34].

1.3 Aims of the Thesis

The main aims of this thesis can be summarized as:

1. Studying the performance of three null steering methods (Schelkunoff, Godara, and Sidelobe Canceller) in linear antenna arrays.
2. Simulating how to control the nulls in the three methods, and place them in specific directions by using the MATLAB program.
3. Studying the effect of the three methods on the directivity, the taper efficiency, and the average sidelobe level compared to that in uniform arrays.
4. Comparing the three methods, and demonstrating the pros and cons of each method.

1.4 Outlines of the Thesis

Chapter One: It gives an overview of the antenna and antenna arrays, the literature review, and the aims of the thesis.

Chapter Two: Illustrating the theoretical background of Antenna Array, Linear Array Configuration, and Null Steering Techniques.

Chapter Three: It provides a simulation modeling of the three null steering techniques that are investigated in this thesis.

Chapter Four: It presents the simulation results obtained using MATLAB.

Chapter Five: It gives the Conclusions and Future Works suggestions.

CHAPTER TWO

BACKGROUND THEORY

2.1 Introduction

An antenna array is a grouping of two or more antenna elements that can be arranged in a particular pattern. Antenna elements in a linear antenna array are arranged along a single axis. The antenna array generates a beam, which can be influenced by changing the geometry (linear, circular, spherical, etc.) as well as some other parameters such as inter-element spacing, excitation amplitude, and excitation phase of the individual element. Most wireless communications necessitate a more directive antenna with a high gain. An antenna array with high gain, greater directiveness, and spatial diversity [35].

In this chapter, the fundamentals of the antenna array are discussed. All the characteristic properties of the antenna array, and linear antenna array configurations are also introduced.

2.2 Antenna Array

As explained previously, an array antenna is a very important configuration for increasing the performance of the antennas. The antenna array is a set of multiple single-antenna elements connected in such a way to feed most of the power of the transmitter or receiver to a certain direction called the main beam.

In the antenna array, the distance between antennas is related to the wavelength of the transmitted signal. Changing this distance leads to a change in the radiation properties. The radio waves radiation of every single antenna is getting combined constructively (called main lobe or side

lobes) or destructively (called cancelation directions or nulls), such that the power will be focused in one direction more than the other directions. Steering the direction of a major power in a certain direction is needed which is where the receiver is located. Sometimes, need to steer the nulls in the direction of the interference receiver to reduce the impact of that on the main signal. In other words, the antenna array is to enhance the power radiated in the desired receiver direction and cancels or reduce the power of the radiated signal in other directions.

The scheme of the antenna array is intended to raise the gain, also called directivity, in that particular narrow beam more than what can get from a single element. Generally, the larger the number of the antenna in the array, the higher the gain and the narrower the beam will become.

The array pattern can be obtained based on the pattern multiplication theorem, which can be described as follows [36]:

$$Array\ Pattern = \ Element\ Pattern(EP) \times Array\ Factor(AF) \quad (2.1)$$

where, EP: the pattern of individual array elements, AF: function that depends on elements' excitation and array's geometry.

The most basic and useful array is created by aligning the components in a straight line. The geometry of the array isotropic elements in the uniform distribution is shown in Fig 2.1.

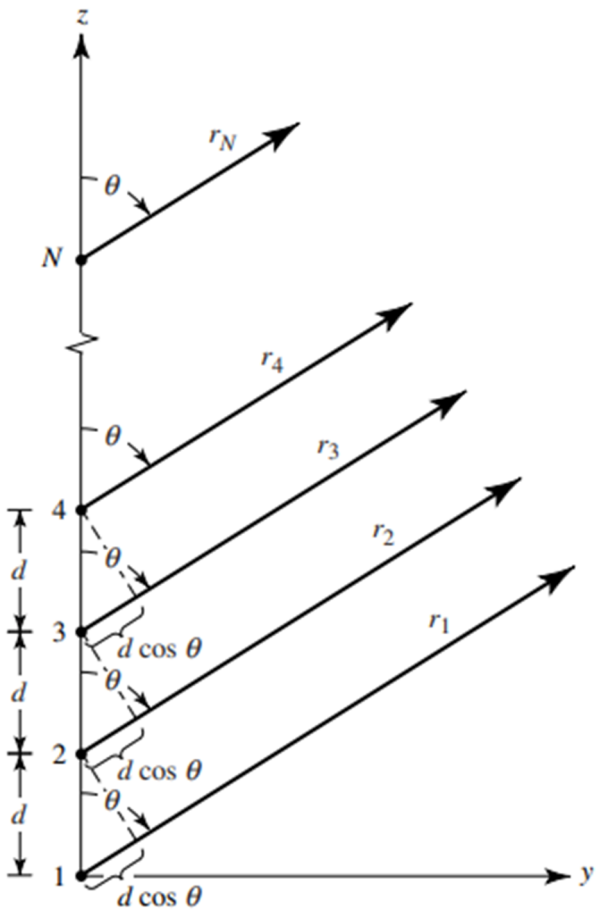

Figure (2.1) N-isotropic array elements geometry [36].

The array factor of the isotropic elements can be multiplied by the field of a single element to form the overall field. The array factor can be found in [36]:

$$AF = 1 + e^{+j(kd\cos\theta+\beta)} + e^{+j2(kd\cos\theta+\beta)} + e^{+j(N-1)(kd\cos\theta+\beta)}$$

$$AF = \sum_{n=1}^{N} e^{+j(n-1)(kd\cos\theta+\beta)} \quad (2.2)$$

where, k is the propagation constant, d is the distance between the elements, and β is the progressive phase. The array factor form can be written also as:

$$AF = \sum_{n=1}^{N} e^{j(n-1)\psi} \quad (2.3)$$

Where, $\psi = kd\cos\theta + \beta$

The array factor of (2.2) can alternatively be stated in a different, compact, and closed form with more recognized functions and distributions. The next is how it is done by multiplying the both (2.2) sides by $e^{j\psi}$ [36].

$$(AF)e^{j\psi}=e^{j\psi}+e^{j2\psi}+e^{j3\psi}+\cdots+e^{j(N-1)\psi}+e^{jN\psi} \tag{2.4}$$

Subtract (2.3) from (2.4), the result obtained as:

$$AF\left(e^{j\psi}-1\right)=\left(-1+e^{jN\psi}\right) \tag{2.5}$$

and also written:

$$AF=\left[\frac{e^{jN\psi}-1}{e^{j\psi}-1}\right]=e^{j\left[\frac{(N-1)}{2}\right]\psi}\left[\frac{e^{j(N/2)\psi}-e^{-j(N/2)\psi}}{e^{j(1/2)\psi}-e^{-j(1/2)\psi}}\right] \tag{2.6}$$

The final expression of the array factor is:

$$AF=\left[\frac{\sin\left(\frac{N}{2}\psi\right)}{\sin\left(\frac{1}{2}\psi\right)}\right] \tag{2.7}$$

and is approximated to:

$$AF\approx\left[\frac{\sin\left(\frac{N}{2}\psi\right)}{\frac{\psi}{2}}\right] \tag{2.8}$$

The normalized array factor form can be written as:

$$AF_n\approx\left[\frac{\sin\left(\frac{N}{2}\psi\right)}{N\frac{\psi}{2}}\right] \tag{2.9}$$

For N-elements of dipole, the total array field ($E_{\theta t}$) can be obtained by multiplying the single element field (E_θ) with the array factor.

$$E_{\theta t}=E_\theta\cdot(AF)_n \tag{2.10}$$

Where, $E_\theta=j\eta\frac{I_0e^{-jkr}}{2\pi r}\left[\frac{\cos\left(\frac{\pi}{2}\cos\theta\right)}{\sin\theta}\right]$ (2.11)

Figure (2.2) illustrates the geometry of the dipole array positioned at x-axis and λ/4 spaced between the elements [37].

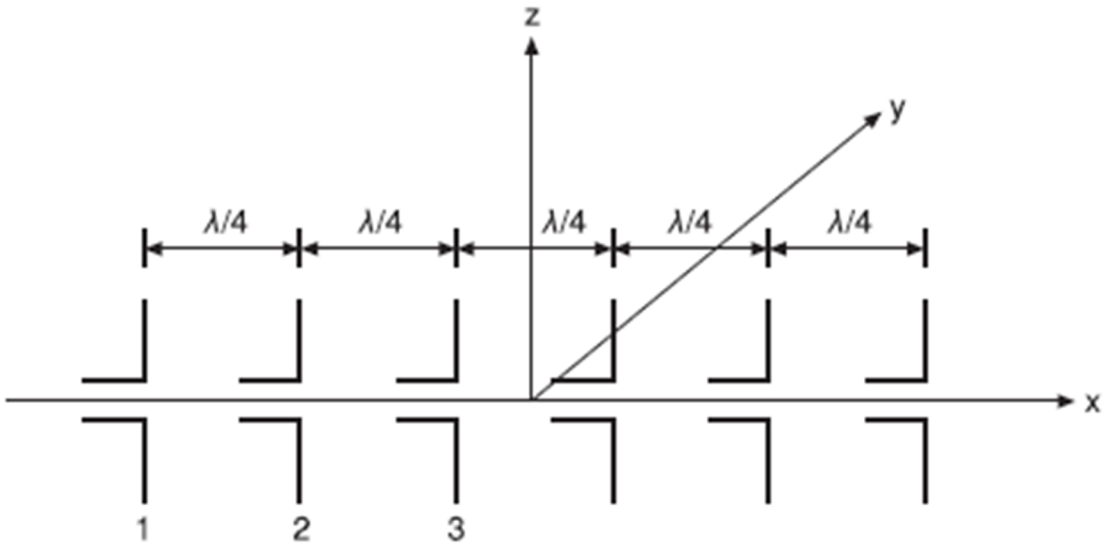

Figure (2.2) The antenna arranged as an array with a distance of quarter wavelength between them.

The maximum radiation of the array direction depends on the application. Three linear array types are designed based on the direction of the maximum radiation [36]:

1. Broadside Array: the maximum should be at $\theta_0 = 90^\circ$, see Figure 2.3.
2. Ordinary End-Fire Array: the maximum should be at $\theta_0 = 0^\circ$ or 180°, see Figure 2.4.
3. Phased (Scanning) Array: the maximum radiation can be directed in any direction, see Figure 2.5 example of scanning array.

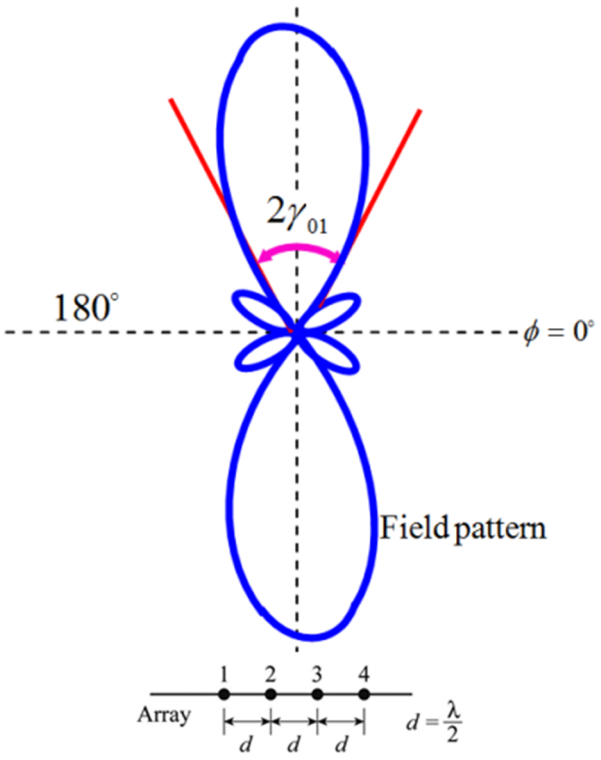

Figure (2.3) Broadside array beam pattern [38].

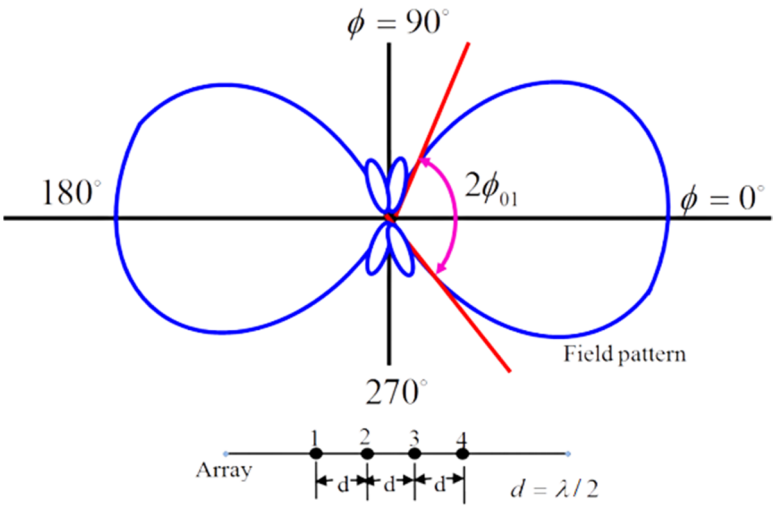

Figure (2.4) End-Fire array beam pattern [38].

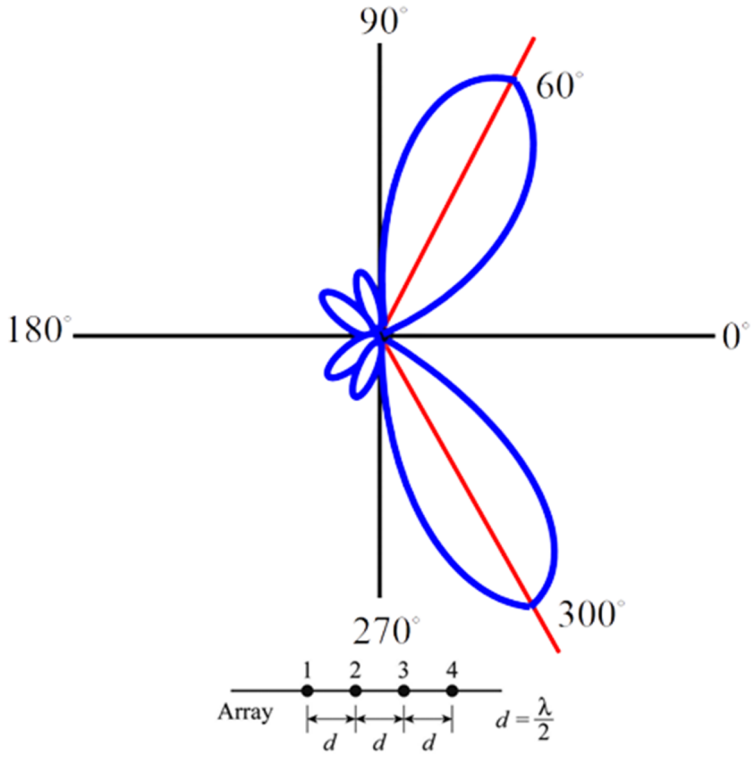

Figure (2.5) Scanning array beam pattern [38].

2.3 Parameters of Antenna Array

The performance of an antenna array must be explained in terms of many characteristics. The following are some of the parameters that are necessary for analysis in this thesis:

2.3.1 Radiation Pattern

Radiation patterns, also called antenna patterns or far-field patterns or power patterns, denote the power-strength in the particular direction (angle) from one antenna or array of antennas. The radiation pattern is defined as a mathematical function or a graphical representation of the radiation properties of the antenna as a function of space coordinates. Radiation pattern includes power flux density, radiation intensity, field strength, and directivity [36].

Radiation pattern lobes are classified into major lobe (main lobe) and side or back lobes, as shown in Fig. 2.6 [39].

The main lobe, also called major lobe, is defined as the lobe in the radiation pattern that contains maximum power radiated and the direction of that is called the direction of the main lobe. The direction of the main lobe is usually perpendicular on the antenna array layer. Now using some techniques, we can steer that lobe using phase difference in the excitation feeder. A side lobe is adjacent to the main lobe [40].

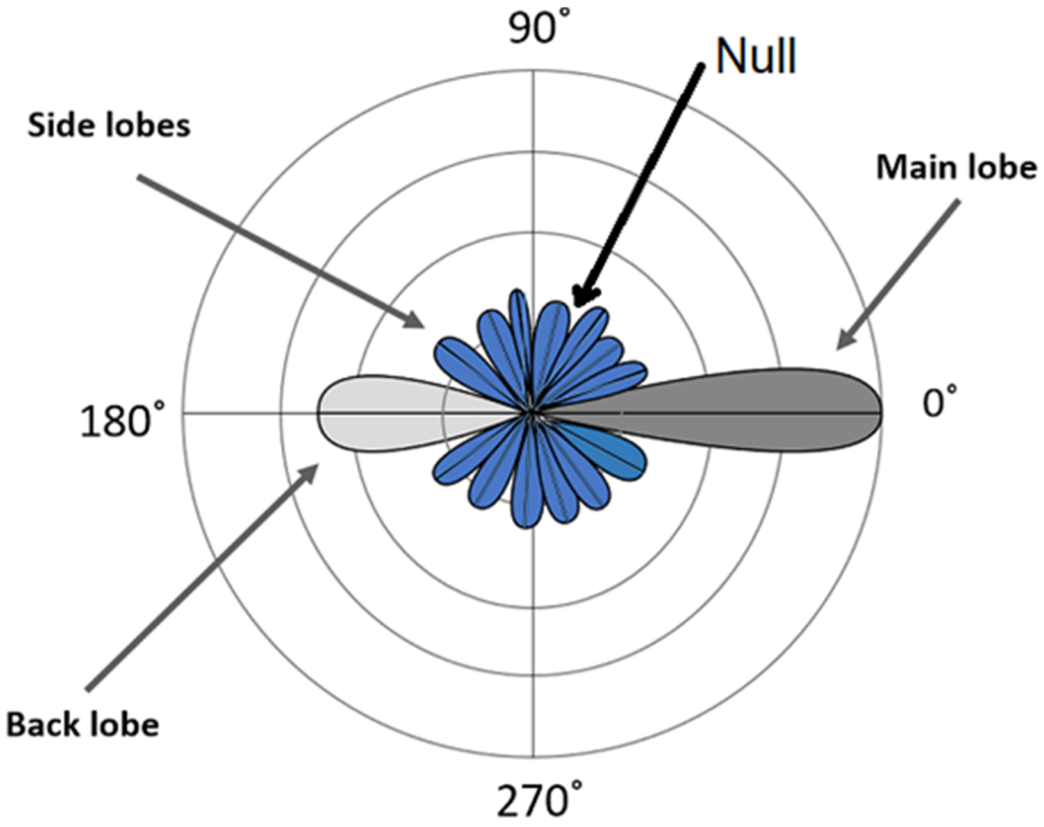

Figure (2.6) Circular radiation pattern shows the different types of lobes and null [39].

2.3.1.1 Half Power Beam Width (HPBW)

HPBW is the angle between which locates more than fifty percent of the maximum power in the effective radiated field of antennas. The smaller this angle is, the more focusing the main beam

will become and the higher the directivity will be. This angle is also called the 3 dB beam width, as the power at these two angles is smaller than the peak by 3 dB or 50 percent. Figure 2.7 shows the HPBW. Defining ($\theta_{HPBW}{}^{left}$) and ($\theta_{HPBW}{}^{right}$) as the angles measured from the maximum position of the main lobe to its left and right for which the angles measured, it is explained in equation (2.12) [36].

$$HPBW = \theta_{HPBW}{}^{right} + \theta_{HPBW}{}^{left} \tag{2.12}$$

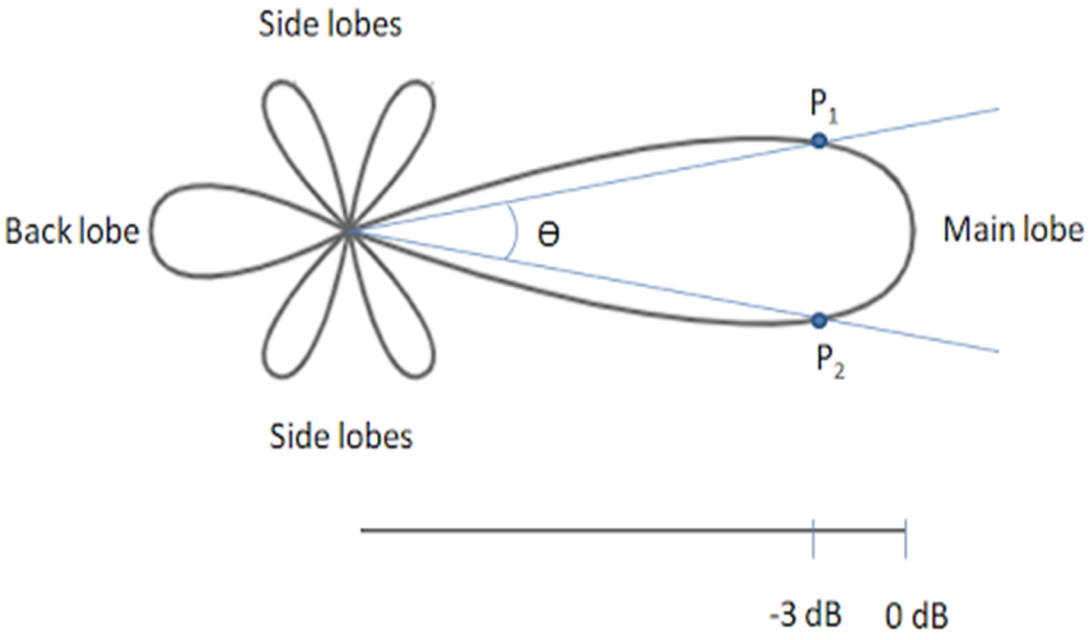

Figure (2.7) Half-power beam width

2.3.1.2 First Null Beam Width (FNBW)

The first null beam width is the angular separation between the first nulls around the main beam in the pattern. In other words, we can define FNBW as the angular span between the pattern first nulls that are adjacent to the main lobe. Figure 2.8 displays the FNBW. Defining ($\theta_{FNBW}{}^{right}$)and ($\theta_{FNBW}{}^{left}$) as the angles measured from the maximum position of the main lobe to its left and right for which the angles measured it is explained in equation (2.13) [36].

$$FNBW = \theta_{FNBW}{}^{right} + \theta_{FNBW}{}^{left} \tag{2.13}$$

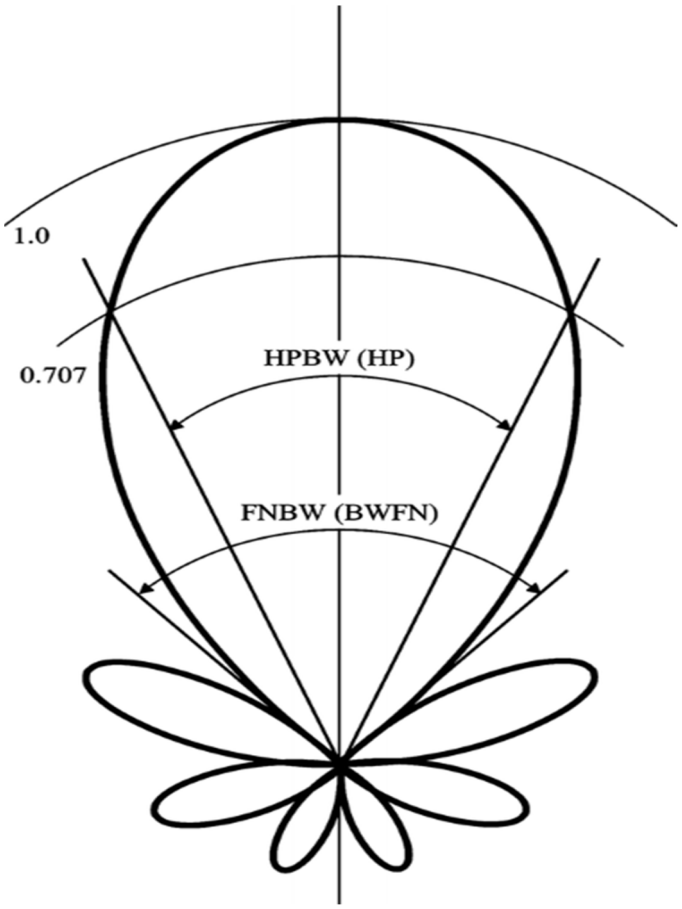

Figure (2.8) The FNBW and HPBW [41].

2.3.1.3 Side Lobe Level (SLL)

The ratio of the radiation intensity in the direction of the largest sidelobe which is usually, but not always the first sidelobe adjacent to the main antenna beam to the maximum radiation intensity is recognized as the sidelobe level (SLL) of an antenna as shown in Figure (2.9). It is explained in equation (2.14) [36].

$$SLL = \frac{U_{SLL} of\ Minor\ Lobe}{U_{Max} of\ Major\ Lobe} \tag{2.14}$$

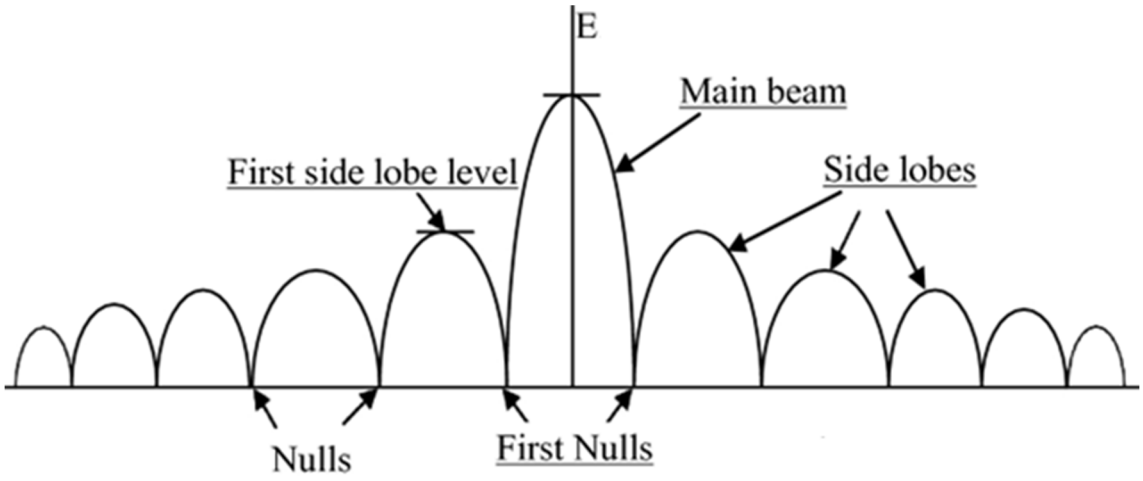

Figure (2.9) The first side lobe level [42].

2.3.1.4. Average Side Lobe Level (ASLL)

The ASLL is a power average created by combining the power in all minor lobes outside the major lobe and expressing it in decibels (dB). It is explained in equation (2.15) [35].

$$(ASLL) = 10 \log_{10} \begin{pmatrix} \text{average power of minor lobes} \\ \text{outside the major lobe} \end{pmatrix} \quad (2.15)$$

2.3.1.5 Taper Efficiency

The physical meaning of the taper efficiency of an array by starting from the communication link range is the ratio of beamformer signal gain to noise gain divided by the ratio of the same gains as the beamformer is uniformly weighted, where gain included the contributions from all active and passive components within the beamformer. It is explained in equation (2.16) [43].

$$Taper\ Efficiency = \frac{1}{M} \frac{|\sum W_n|^2}{\sum |W_n|^2} \quad (2.16)$$

where M is the number of elements, W_n is the coefficients weight.

2.3.2 Directivity

The main objective of an antenna array is to design a beam pattern such that radiation in a certain direction is strong and the reception in other directions is suppressed and it is a useful measure of the intensity. The array directivity is defined as the ratio of the intensity of radiation in a given direction from the antenna to the average intensity of radiation in all directions. The mean intensity of radiation is equal to the total power divided by 4π radiated by the antenna. The direction of maximum radiation intensity is inferred if the direction is not specified. More precisely put, the directness of a non-isotropic source is equal to the ratio in a given direction 14 of its radiation intensity to that of an isotropic source in the situation of array synthesis, as the losses in antennas and antenna circuits are not beholding, array gain is frequently used reciprocally with array directivity. It is explained in equation (2.17) [36].

$$D_0 = U_{max} / U_0 = 4\pi\, U_{max} / P_{rad} \quad (2.17)$$

where D_0 = directivity (dimensionless).

U_{max} = maximum radiation intensity (Watt/unit solid angle).

U_0= an isotropic source radiation intensity (Watt/unit solid angle).

P_{rad} = total radiated power (Watt).

2.4 Linear Array Configuration

There are different configurations for the antenna array based on the application. The linear antenna array is a very common configuration that is described as antenna elements that are placed along a single axis. Figure (2.10) shows the topology of the linear antenna array.

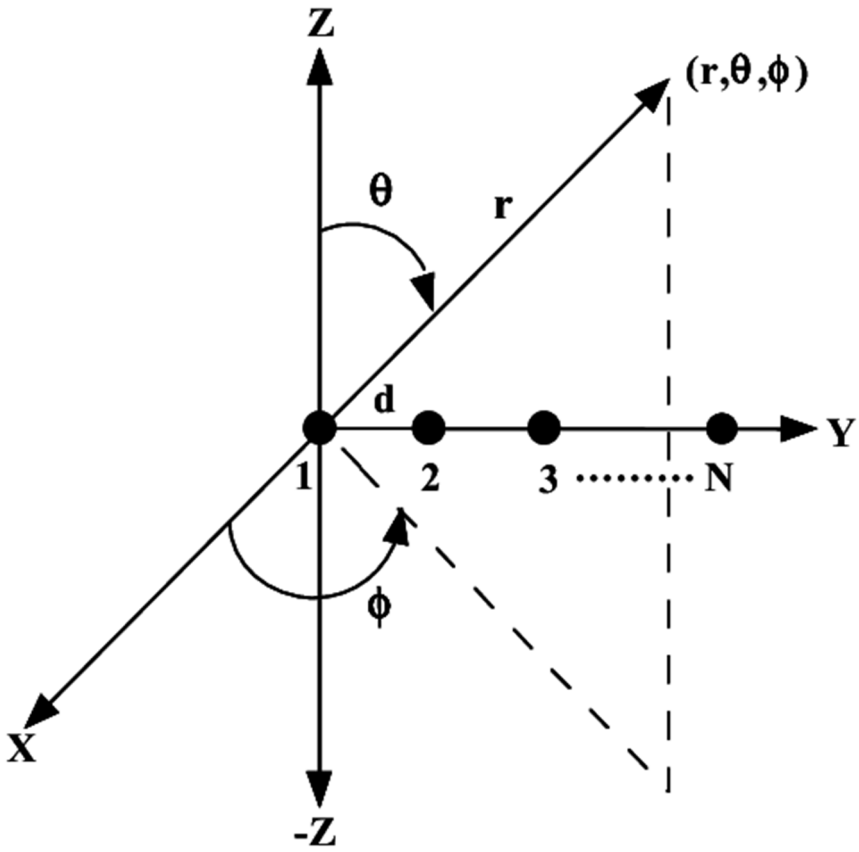

Figure (2.10) Linear array antenna topology [44].

2.4.1 Uniform Linear Array

The antenna array produces a beam that can be affected by varying the geometry such as linear, circular, or other geometry. Other parameters affecting the array are the inter-element spacing, excitation amplitude, and excitation phase of each antenna element. If the spacing is equal between elements and equal excitation, it is called a uniform linear array (ULA) [36].

2.4.2 Non-Uniform Linear Array

Another type of linear antenna array is a non-uniform amplitude linear array. This type of array is different by excitation amplitudes

(tapering). The main feature of this type is to produce the smallest side lobe levels compared to that in the uniform distribution. There are various types of a non-uniform linear array such binomial, Dolph-Tschebyscheff, and others. There are two shapes to arrange the array elements, the first is odd and the second is even as shown in Figs. 2.11 (a) and 2.11 (b) [36].

For the even isotropic array (2M), the elements arranged along the z-axis with the distance d between the elements M that are introduced on each of the reference sides. The array factor of the array can be derived as [36]:

$$\begin{aligned}(AF)_{2M} = {} & a_1 e^{+j(1/2)kd\cos\theta} + a_2 e^{+j(3/2)kd\cos\theta} + \cdots \\ & + a_M e^{+j((2M-1)/2)kd\cos\theta} + a_1 e^{-j(1/2)kd\cos\theta} \\ & + a_2 e^{-j(3/2)kd\cos\theta} + \cdots + a_M e^{-j((2M-1)/2)kd\cos\theta}\end{aligned}$$

$$(AF)_{2M} = 2\sum_{n=1}^{M} a_n \cos\left[\frac{(2n-1)}{2} kd\cos\theta\right] \tag{2.18}$$

where, a_n is the amplitude excitation. The normalized form written as:

$$(AF)_{2M} = \sum_{n=1}^{M} a_n \cos\left[\frac{(2n-1)}{2} kd\cos\theta\right] \tag{2.19}$$

When the isotropic elements odd number (2M+1), the array factor can be derived as:

$$\begin{aligned}(AF)_{2M+1} = {} & 2a_1 + a_2 e^{+jkd\cos\theta} + a_3 e^{j2kd\cos\theta} + \cdots + a_{M+1} e^{jMkd\cos\theta} \\ & + a_2 e^{-jkd\cos\theta} + a_3 e^{-j2kd\cos\theta} + \cdots + a_{M+1} e^{-jMkd\cos\theta}\end{aligned}$$

$$(AF)_{2M+1} = 2\sum_{n=1}^{M+1} a_n \cos[(n-1)kd\cos\theta] \tag{2.20}$$

The normalized array factor is:

$$(AF)_{2M+1} = \sum_{n=1}^{M+1} a_n \cos[(n-1)kd\cos\theta] \tag{2.21}$$

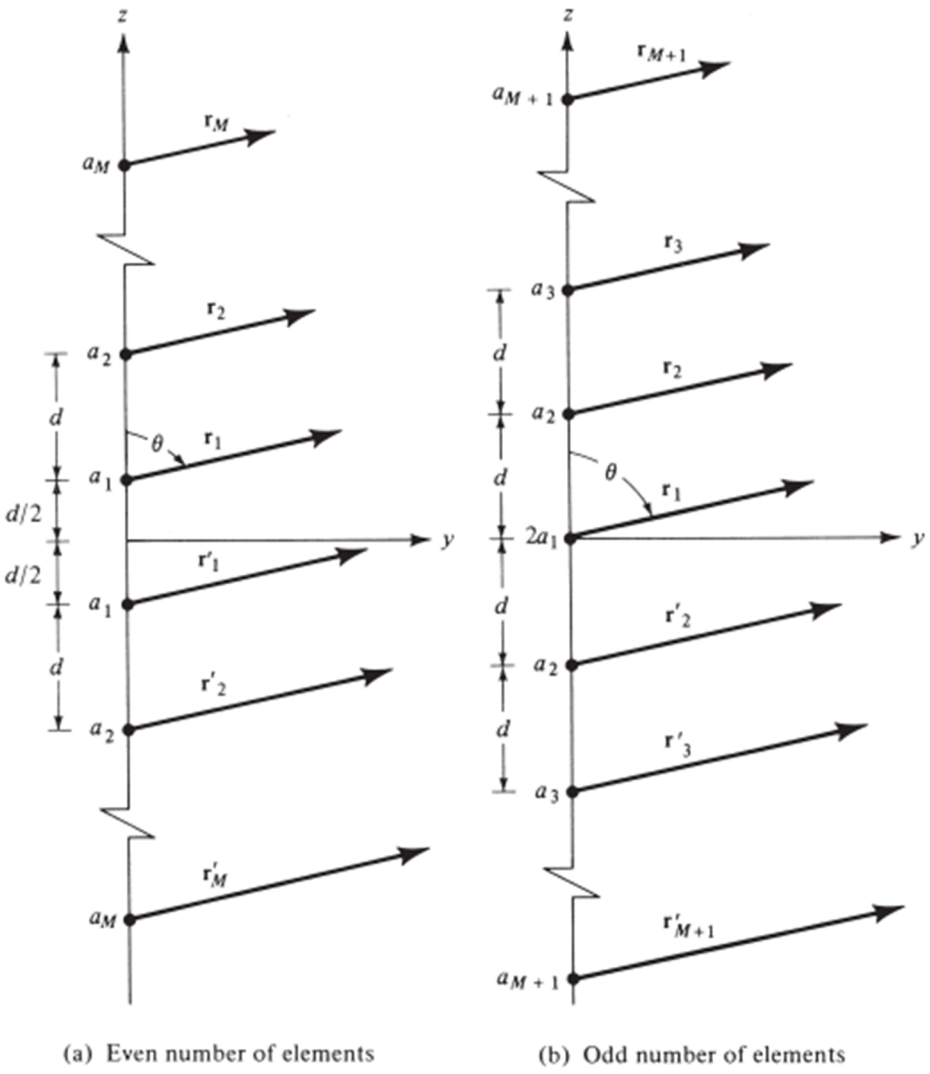

Figure (2.11) Non-uniform linear array with even and odd number [36].

2.4.2.1 Binomial Array

A binomial array is an array of n-isotropic sources with non-equal amplitudes and is a common example of a tapering approach. Also, the amplitude of the radiating sources arc is organized based on the binomial expansion. In the case of minor lobes shown in the array and required to be neglected, the radiating sources should have current amplitudes proportional to the coefficient of binomial series [36].

$$(1+x)^{m-1} = 1 + (m-1)x + \frac{(m-1)(m-2)}{2!}x^2 + \frac{(m-1)(m-2)(m-3)}{3!}x^3 \pm \cdots$$

(2.22)

The aforementioned relationship is equivalent to Pascal's Triangle as shown in figure (2.12). For instance, for the array of 1 to 10 radiating sources.

$N=1$									1									
$N=2$								1		1								
$N=3$							1		2		1							
$N=4$						1		3		3		1						
$N=5$					1		4		6		4		1					
$N=6$				1		5		10		10		5		1				
$N=7$			1		6		15		20		15		6		1			
$N=8$		1		7		21		35		35		21		7		1		
$N=9$	1		8		28		56		70		56		28		8		1	
$N=10$	1		9		36		84		126		126		84		36		9	1

Figure (2.12) The excitation coefficients of the binomial arrays for up to 10 array elements.

In binomial arrays, the element spacing is ≤ wavelength/2, the HPBW of the array becomes as follows [36]:

$$\text{HPBW} = \frac{1.06}{\sqrt{N-1}} = \frac{1.06}{\sqrt{\frac{2L}{\lambda}}} = \frac{0.75}{\sqrt{L\lambda}} \text{ (Radians)} \quad (2.23)$$

where, L= (N-1) λ/2, and directivity is formulated as the following equation [37]:

$$D_0 = 1.77\sqrt{N} = 1.77\sqrt{1 + 2L\lambda} \quad (2.24)$$

2.5 Null Steering Technique

Null steering strategies are essential in radar, sonar, and most of communication systems for reducing signal-to-noise ratio degradation caused by undesired interference [45].

The ever-increasing users is today's modern telecommunications challenge. This is in conflict with the provider's limited spectrum. With the available resources, the capacity that is proportional to the number of users served in a sector of the cellular station is limited. With an increasing number of users, detecting a signal coming from a specific direction permanently is an impossible task. Aside from these, the environment is becoming more polluted due to factors such as fading and co-channel interference. To overcome these, the solution lies in the use of adaptive antenna arrays in such environments. The adaptive arrays are designed to suppress interference signals, resulting in enhanced signal reception characteristics. As a result, the goals of such array synthesis are to yield radiation patterns that are formally defined by null steering and null positioning. This can be achieved by controlling the design parameters such as amplitude and phase excitation [46]. Figure 2.13 shows the steering of the null signal toward the interference to avoid the interference and stay only with the signal [47].

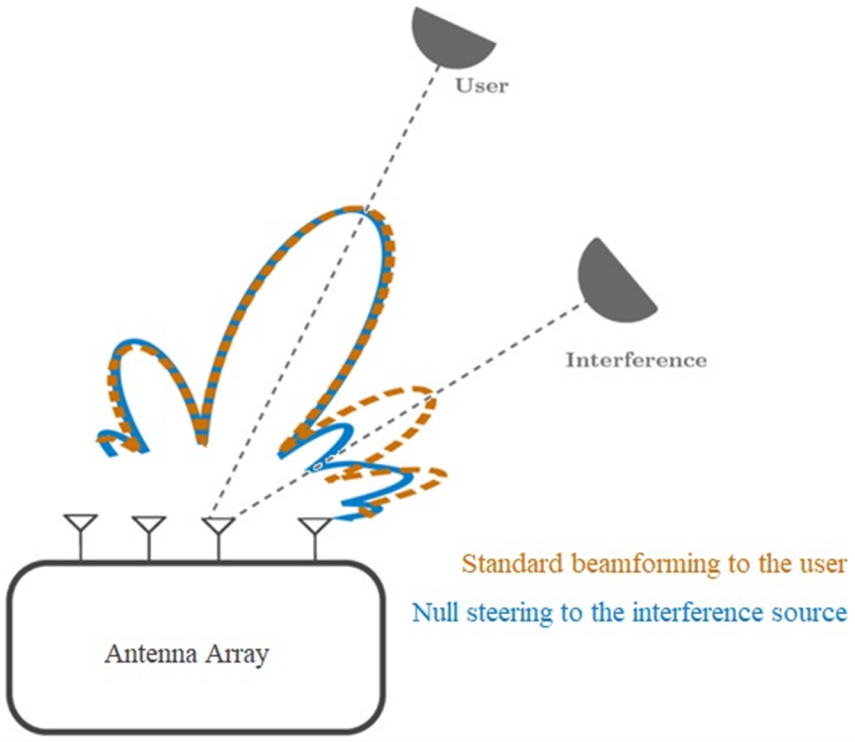

Figure (2.13) Null signal to the interference sources.

One of the antenna pattern synthesis classifications is to produce nulls in the desired locations, and this can be achieved using Schelkunoff, Godara, sidelobe canceller, and other methods. The main details of these methods will be explained in this chapter.

2.5.1 Schelkunoff Method

Since Schelkunoff demonstrated that linear arrays can be expressed as polynomials, this representation can be extremely helpful when analyzing and creating antenna arrays. Rather than directing an antenna array, they would like to make sure that only a small amount of energy travels in specific directions. An antenna array's weights can be chosen so that the radiation pattern has nulls in specific directions. Unwanted interference, jamming signals, and noise can be eliminated in this way. Generally speaking, an array of N elements can position N-1 separate nulls in the radiation pattern [26].

This approach requires information on the number of nulls and their positions to finish the design. Following that, the total number of components and their excitation coefficients are calculated. The following is how the technique is analytically formulated [36].

Assuming N elements, evenly distributed, non-uniform amplitude, and progressive phase excitation, the array factor is given by [36]:

$$AF = \sum_{n=1}^{N} a_n e^{j(n-1)(kd\cos\theta+\beta)} = \sum_{n=1}^{N} a_n \, e^{j(n-1)\psi} \tag{2.25}$$

Where a_n accounts for the non-uniform amplitude excitation of each element. The spacing between the elements is d and β is the progressive phase shift.

$$z = x + jy = e^{j\psi} = e^{j(kd\cos\theta+\beta)} \tag{2.26}$$

The Array Factor can rewrite it as:

$$AF = \sum_{n=1}^{N} a_n \, z^{n-1} = a_1 + a_2 z + a_3 z^2 + \cdots + a_N z^{N-1} \qquad (2.27)$$

This is a polynomial of (N-1) degree. Any polynomial of degree (N-1) has (N-1) roots and can be demonstrated as a product of (N-1) linear terms, according to the mathematics of multiple variables and algebra. So, may represent (2.27) as:

$$AF = a_n(z - z_1)(z - z_2)(z - z_3) \ldots (z - z_{N-1}) \qquad (2.28)$$

where $z_1, z_2, z_3, \ldots, z_{N-1}$ are the roots, which may be complicated, of the polynomial [36].

2.5.2 Godara Method

Considering an N = 3-element array with a known wanted source that is fixed and two static interferers that are not desirable. The assumption is that every transmission operates under the same carrier frequency. Assuming the intended signal and interference are present in a three-element array as shown in figure 2.14 [48]:

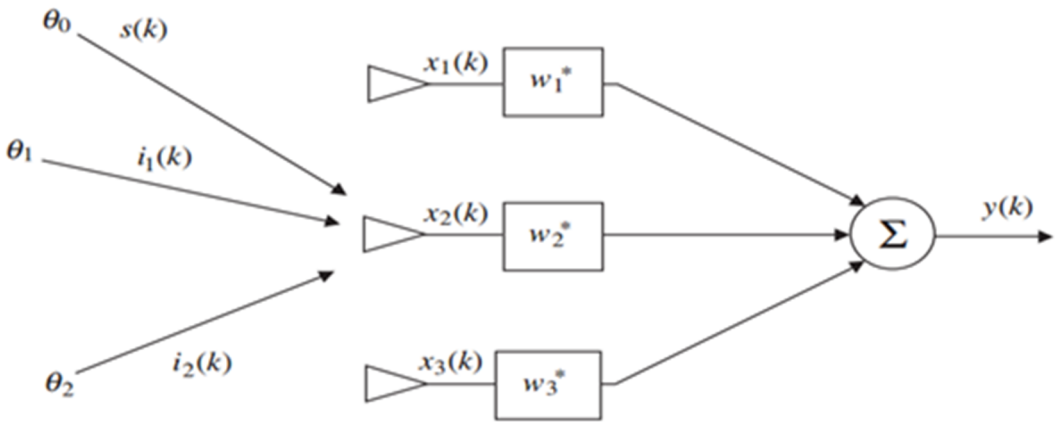

Figure (2.14) A three-element array that contains both favorable and unwanted signals.

The array vector can be found in:

$$\bar{a} = \left[e^{-jkdsin\theta}\ \ 1\ \ e^{jkdsin\theta}\right]^T \tag{2.29}$$

The array weights for optimization, which have not yet been calculated, are provided by:

$$\bar{w}^H = [w_1\ \ w_2\ \ w_3] \tag{2.30}$$

Consequently, the output of the general total array is provided as:

$$y = \bar{w}^H.\bar{a} = w_1 e^{-jkdsin\theta} + w_2 + w_3 e^{jkdsin\theta} \tag{2.31}$$

y_s will stand for the array outputs for the desired signal, while y_1 and y_2 will stand in for the conflicting or undesirable signals. There must be three conditions met because there are three unknown weights.

$$\text{Condition 1:}\quad y_s = \bar{w}^H \cdot \bar{a}_0 = w_1 e^{-jkd\sin\theta_0} + w_2 + w_3 e^{jkd\sin\theta_0} = 1$$
$$\text{Condition 2:}\quad y_1 = \bar{w}^H \cdot \bar{a}_1 = w_1 e^{-jkd\sin\theta_1} + w_2 + w_3 e^{jkd\sin\theta_1} = 0$$
$$\text{Condition 3:}\quad y_2 = \bar{w}^H \cdot \bar{a}_2 = w_1 e^{-jkd\sin\theta_2} + w_2 + w_3 e^{jkd\sin\theta_2} = 0$$

The intended signal can be obtained without modification because Condition 1 requires that $y_s = 1$ for it. The unwanted interfering signals are rejected under conditions 2 and 3. These criteria can be recast as a matrix to become:

$$\bar{w}^H.\ \bar{A} = \bar{u}_1^T \tag{2.32}$$

Where $\bar{A} = [\bar{a}_0\, \bar{a}_1\, \bar{a}_2]$ = matrix of steering vectors $\bar{u}_1 = [1\ \ 0\ \ \ldots\ \ 0]^T$ = Cartesian basis vector.

The matrix can be inverted to determine the necessary complex weights (w_1, w_2, and w_3) using:

$$\bar{w}^H = \bar{u}_1^T.\bar{A}^{-1} \tag{2.33}$$

A formula from Godara provides an approximation of the weights. However, because the matrix inversion would otherwise be single, his

formulation calls for the addition of noise to the system. Using the Godara approach,

$$\bar{w}^H = \bar{u}_1^T . \bar{A}^H (\bar{A} . \bar{A}^H + \sigma_n^2 \bar{I})^{-1} \quad (2.34)$$

where $\bar{u}_1{}^T$ is the vector's length in the Cartesian basis, which is equal to the number of sources [48].

2.5.3 Sidelobe Canceller (SLC) Method

Sidelobe cancellation is to use the interference signal received by the auxiliary antennas to suppress the directional interference coming in through the antenna sidelobe direction. The fundamental concept is to simultaneously send the interference signals received by the antenna's main lobe and side lobes to the adaptive processor, and calculate the ideal weight using a specific adaptive algorithm to reduce the total output power, and achieve the interference cancellation goal. The following block diagram illustrates the principle of side lobe cancellation [49]:

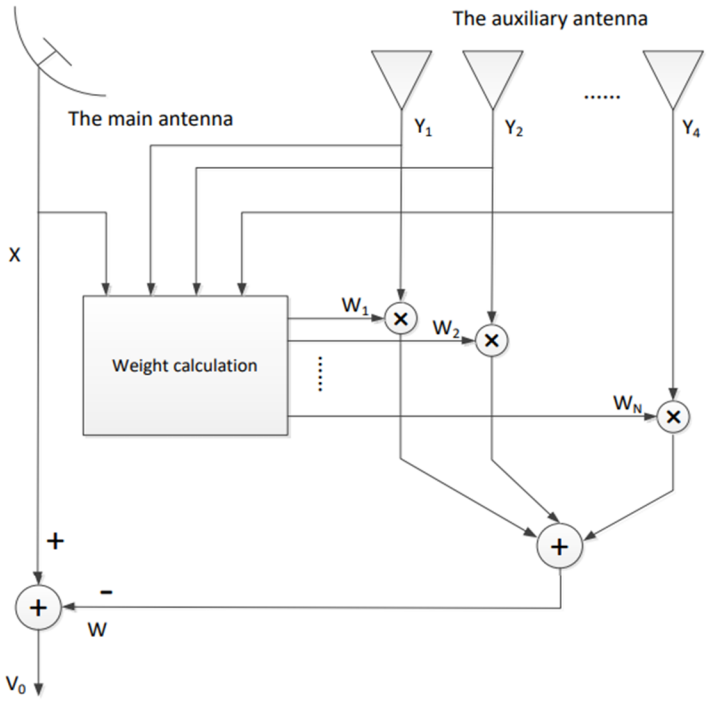

Figure (2.15) Block diagram of side lobe cancellation principle [49].

2.5.3.1 Conventional SLC - with separate auxiliary antennas

The need to guide a null in the direction of an assigned arrival direction is a common necessity when synthesizing beam patterns. This increases the signal-to-interference ratio and aids in suppressing interference coming from that direction. An airline radar system might need to minimize disturbance from a near radio station even though the disturbance is not always intentional. Since the radio station's location is known in this instance, the interference can be eliminated using a sidelobe cancellation technique [50].

The disturbance that enters through the sidelobes of the array can be suppressed with the aid of sidelobe cancellation. The technique is straightforward in this instance because the interference source is known. Create a beam that faces the interference direction, scale the weights for that beam, and then deduct the scaled weights from the weights for any other look-direction-pointing beam patterns. A significant null in the direction of the interference is always produced by this procedure. Figure (2.16) illustrates the structure of the conventional SLC technique [50].

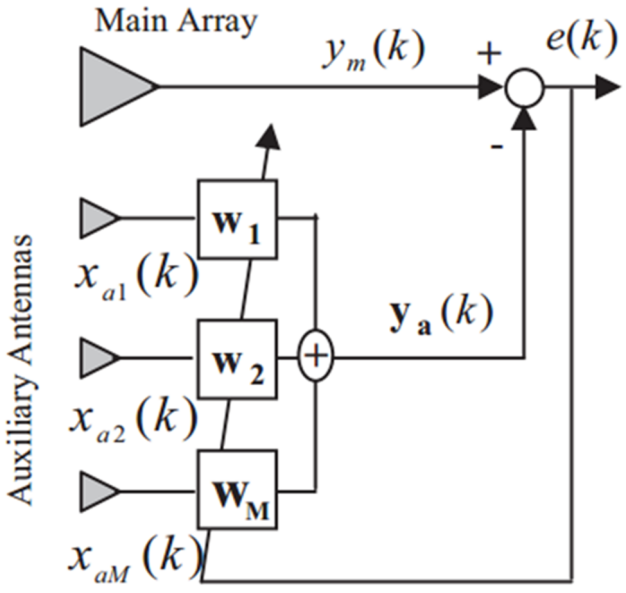

Figure (2.16) Structure of the Conventional SLC technique [50].

2.5.3.2 Adapted SLC - by using a number of the main antenna elements as an auxiliary antenna

By substituting several existing components of the primary antenna array for the independent auxiliary antennas, the standard sidelobe canceller is improved. The significant improvement and auxiliary channels' required signal components may be correlated, which distinguishes the modified SLC from the traditional one. When there are more elements reused from both the main array and the auxiliary antenna, the desired signal may be seriously attenuated by such correlation. By changing the weights of the repeated parts to create a certain cancellation pattern, the consequent malfunction of the desired signal suppression is eliminated [51].

The required cancellation pattern should have two features: first, the needed cancellation pattern must have a level at the interferer side that is equivalent to the level of the primary array pattern. Second, it should have a very low level or a null in the desired signal's direction. Figure (2.17) illustrates the structure of the adapted SLC technique [51].

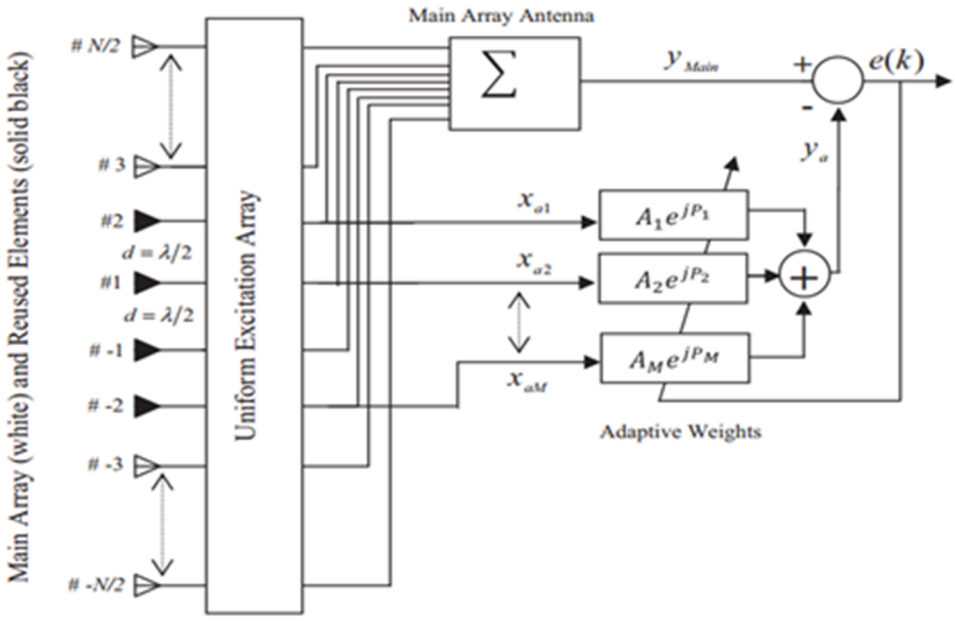

Figure (2.17) Structure of the Adapted SLC technique [51].

CHAPTER THREE

NULL STEERING TECHNIQUES SIMULATION MODELING

3.1 Introduction

To steer the direction of a particular null or nulls in the linear array antennas, three different methods have been used in this dissertation: the Schelkunoff method, the Godara method, and the Adapted sidelobe canceller method. Matlab program is used to simulate the null steering mechanisms and observed their performance.

In order to demonstrate the null steering capability, the experimentation is used several model assumptions:

1. Three different null steering methods are used, schelkunoff, Godara, and the Adapted sidelobe canceller.
2. The models used broadside linear array (the radiation is normal to the array axis) with uniform and non-uniform excitations.
3. Number of elements (N) used in each method is: 6 and 11.
4. The separation between the elements (d) is: 0.2λ, 0.4λ, and 0.5λ, where λ is the wavelength and assumed to equal 1.
5. Table 3.1 list the simulation parameter.

Table 3.1: Simulation Parameters

Parameter	**Setting**
Antenna Type	Broadside Linear (uniform, non-uniform)
Methods	Schelkunoff, Godara, Adapted Sidelobe Canceller
Number of elements (N)	6,11
Distance between elements (d)	0.2λ, 0.4λ, 0.5λ
λ	1

3.2 Schelkunoff Method

The first method used to steer the positions of the nulls to be exist in the visible region. The performance is compared with that of uniform excited array. Figure (3.1) illustrates block diagram to the operation mechanism.

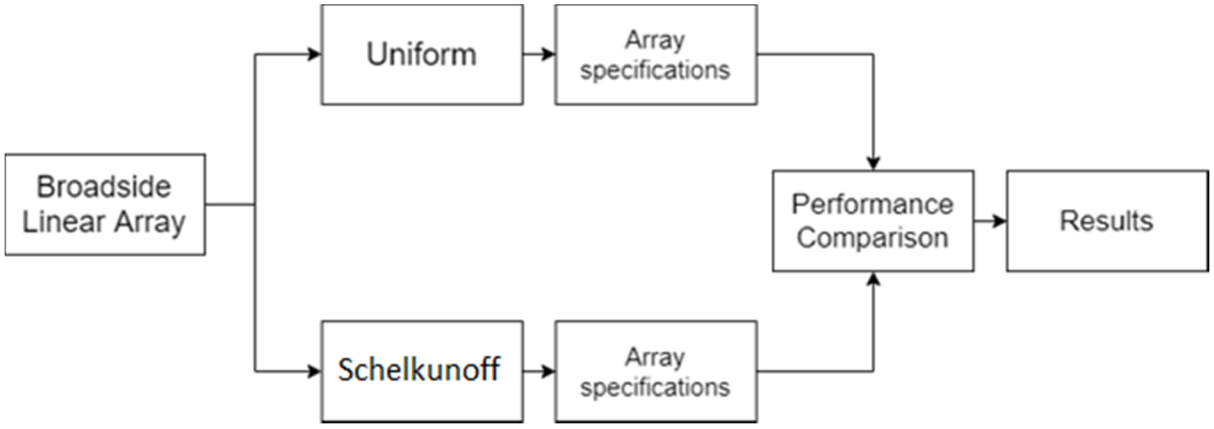

Figure (3.1) Mechanism operation using Schelkunoff Method

The Schelkunoff method is designed with N equal to 6 in the first case, and 11 in the second with d equal to 0.2λ, 0.4λ, 0.5λ. The performance compared with uniform linear array as shown in Figure 3.1. The Matlab simulation code used to specify the number of elements and the distance between the elements is:

```
kd = 2*pi*d ;
ii = 1:(N-1);
psi = -2*kd*ii/(N-1);
```

To perform the excitation for both uniform and Schelkunoff method, the Matlab code below is used:

```
w_uniform = ones(1,N);
z = exp(1j*psi);
zz = mypoly2(z);
w_schelkunoff = fliplr(zz);
```

The main beams of the uniform array and the Schelkunoff array were directed towards the 90° as follows:

```
w_uniform = steer(d,w_uniform,90);
w_schelkunoff = steer(d, w_schelkunoff, 90);
```

To draw the array pattern for the uniform array as well as for the Schelkunoff array, the amplitude and phase for each of them were found as follows:

```
[a_uniform, ph_uniform] = array(d, w_uniform, 400);
[a_schelkunoff, ph_schelkunoff] = array(d, w_schelkunoff, 400);
```

3.3 Godara Method

The second method used to steer the positions of the nulls based on specified angles. The performance is also compared with that of uniform excited array as shown in Figure (3.2).

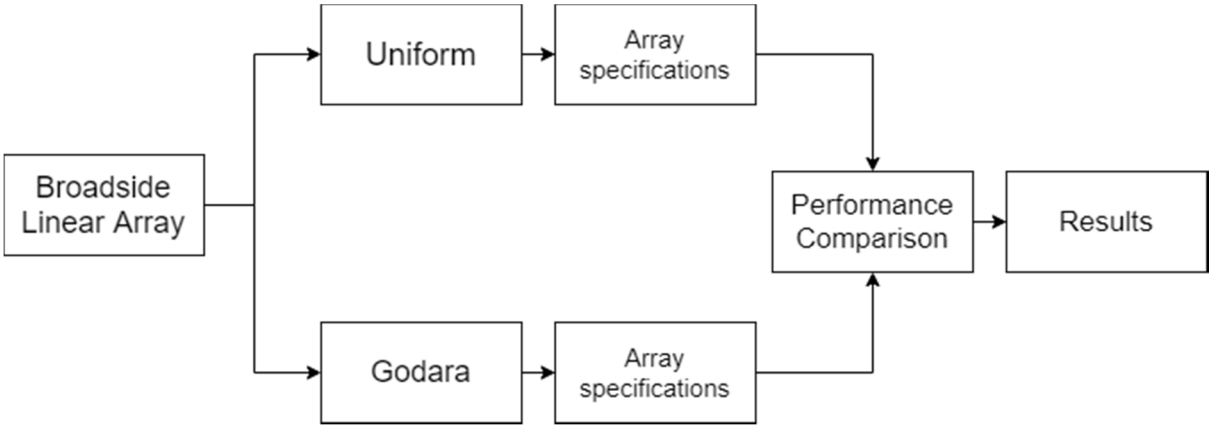

Figure (3.2) Mechanism operation using Godara Method

The Godara method is designed with N equal to 6 in the first case, and 11 in the second with d equal to 0.2λ, 0.4λ, 0.5λ. The performance compared with uniform linear array. As can be seen in Figure (3.2), the uniform array and Godara are designed and compared their performance.

The unwanted signal angles are imposed as follows: In the first case, one angle θ_1 = 105°, and in the second case, there are three angles θ_1=55° , θ_2=105° , θ_3=130°. The Matlab code that used to simulate this step is:

```
th0 = 90;
th1 = 55*pi/180;
th2 = 105*pi/180;
th3 = 130*pi/180;
```

The steering vector has been calculated for all required angles through the following equations:

```
n = 0:(N-1);
a0 = [ exp(-1j*(((N-1)/2)-n)*pi*sin(th0)) ]';
a1 = [ exp(-1j*(((N-1)/2)-n)*pi*sin(th1)) ]';
a2 = [ exp(-1j*(((N-1)/2)-n)*pi*sin(th2)) ]';
a3 = [ exp(-1j*(((N-1)/2)-n)*pi*sin(th3)) ]';
```

The weights of the uniform array were calculated through the following equation:

```
w_uniform = ones(1,N);
```

The weights of the Godara array are calculated using the following equation:

```
Sig2 = 0.001;
A = [a0 a1 a2 a3];
I = eye(length(A(1,:)));
u1 = I(:,1);
w_godara = u1'*A'*inv(A*A'+sig2*eye(N));
```

To draw the array pattern for both the uniform array and the Godara array, the array factor was calculated and multiplied by the weights of each array, as follows:

```
theta = 0:0.01:pi;
for m = 1:length(theta)
    th = theta(m);
    aa = [ exp(-1j*(((N-1)/2)-n)*2*pi*d*sin(th))
]';
    y_godara(m) = w_godara*aa;
    y_uniform(m) = w_uniform*aa;
end
```

3.4 Adapted Sidelobe Canceller (ASLC)

The final null steering method that has been used is the ASLC method, and the performance is also compared with that of uniform excited array. Figure (3.3) shows the mechanism that was adopted in the simulation. The simulation used Auxiliary array with size (M) of 2 and 5. In addition, SIR (dB) of -30, 0, and 30.

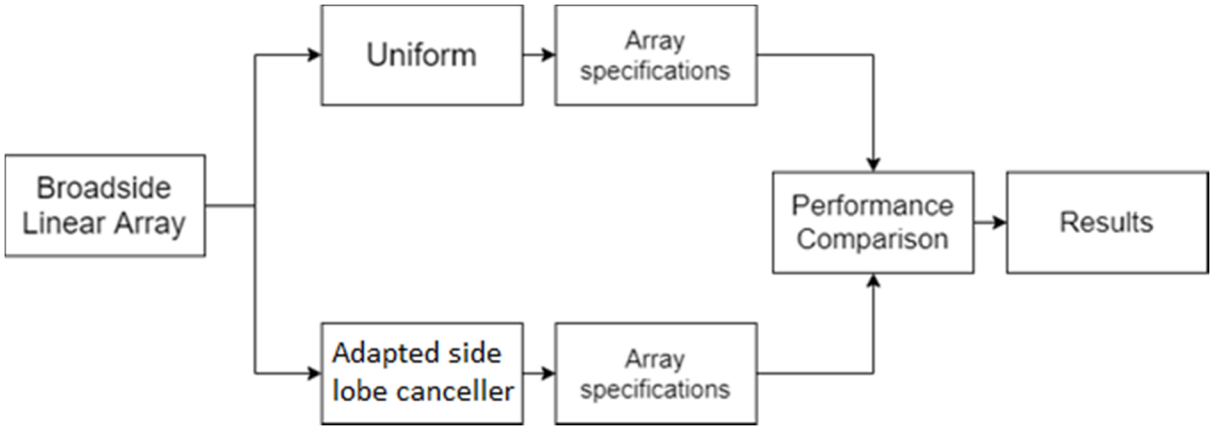

Figure (3.3) Mechanism operation using ASLC Method

The Matlab code used to specify the signal to interference noise ratio as follow:

```
SIR = 10*log10(sig2s/(sig2i));
```

```
% sig2s = σs^2 (signal variance)
% sig2i = σi^2 (interferer variance)
```

The desired signal angle is assumed to be $\theta_s = 90°$ and the unwanted signal angle is assumed to be $\theta_i = 105°$ as follow:

```
thS = 90*pi/180;
thI = 105*pi/180;
```

The steering vector of the main array is calculated for both the desired signal and the unwanted signal through the following equation:

```
n = 1:Nmain;
vSmain = exp(1j*2*pi*(n-1)*d*sin(thS)).';
vImain = exp(1j*2*pi*(n-1)*d*sin(thI)).';
```

The steering vector of the auxiliary array is calculated for both the desired signal and the unwanted signal through the following equation:

```
nn = 1:Naux;
vSaux = exp(1j*2*pi*((nn-1))*d*sin(thS)).';
vIaux = exp(1j*2*pi*((nn-1))*d*sin(thI)).';
```

The weights of the main array and auxiliary elements are calculated using the following Matlab code:

```
wq = (1/(Nmain))*vSmain;
waux = zeros(Naux,1);
```

The array factor equation was used to draw the array pattern for the main array as follow:

```
theta = 0:0.01:pi;
AFmain = zeros(1,length(theta));
```

```
for i = 1:Nmain
    AFmain = AFmain + wq(i)'.*exp(1j*(i-1) * 2*pi*d *sin(theta));
end
```

The array factor equation is used to draw the array pattern for the auxiliary array, which represents the cancellation pattern:

```
theta = 0:0.01:pi;
AFaux = zeros(1,length(theta));
for ii = 1:Naux
    AFaux = AFaux + waux(ii)'.*exp(1j*((ii-1)) *2*pi*d*sin(theta));
end
```

The adapted pattern is drawn by subtraction between the array factor of the main array (AF_{main}) and the array factor of the auxiliary array (AF_{aux}).

CHAPTER FOUR

SIMULATION RESULTS AND PERFORMANCE TESTING

4.1 Introduction

Most communication systems use linear arrays to steer the nulls in the desired directions. In this chapter, the simulation results and analysis are produced for various null steering techniques with several comparisons. The presentation of the utilized techniques is assessed in relation to numerous constraints such as power shape, directivity, tapering efficiency, and Achieved Side Lobe Level (ASLL).

4.2 Schelkunoff Method Performance

Based on the simulation assumptions proposed in chapter three, the Schelkunoff method is compared to the uniform array performance. Figures (4.1) and (4.2) show the amplitude excitation of the Schelkunoff compared to uniform array at N=6 and N=11 array size.

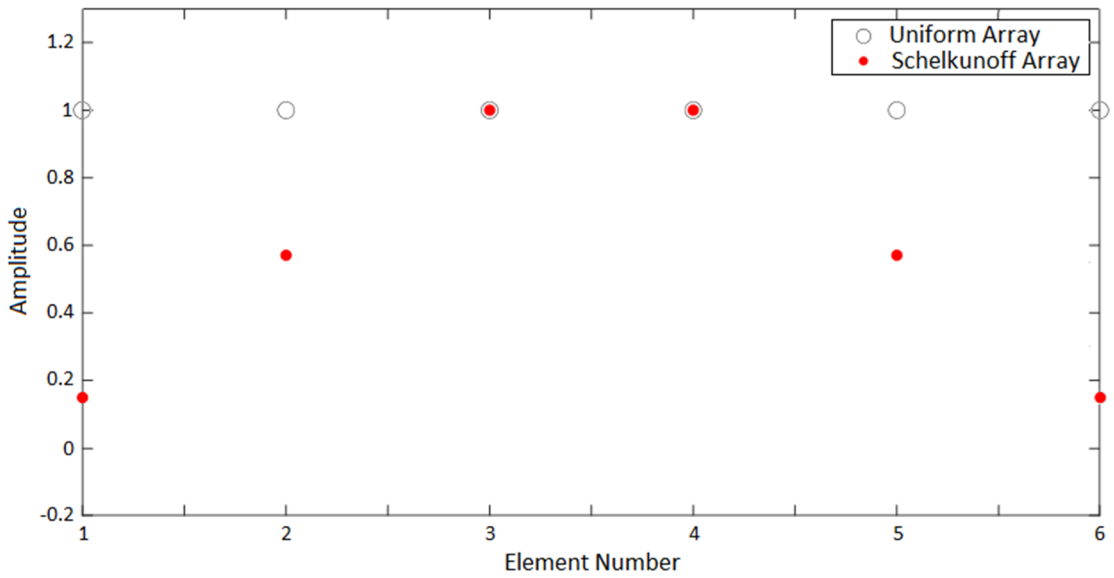

Figure (4.1) Amplitude excitation comparison between Schelkunoff and uniform array at N=6

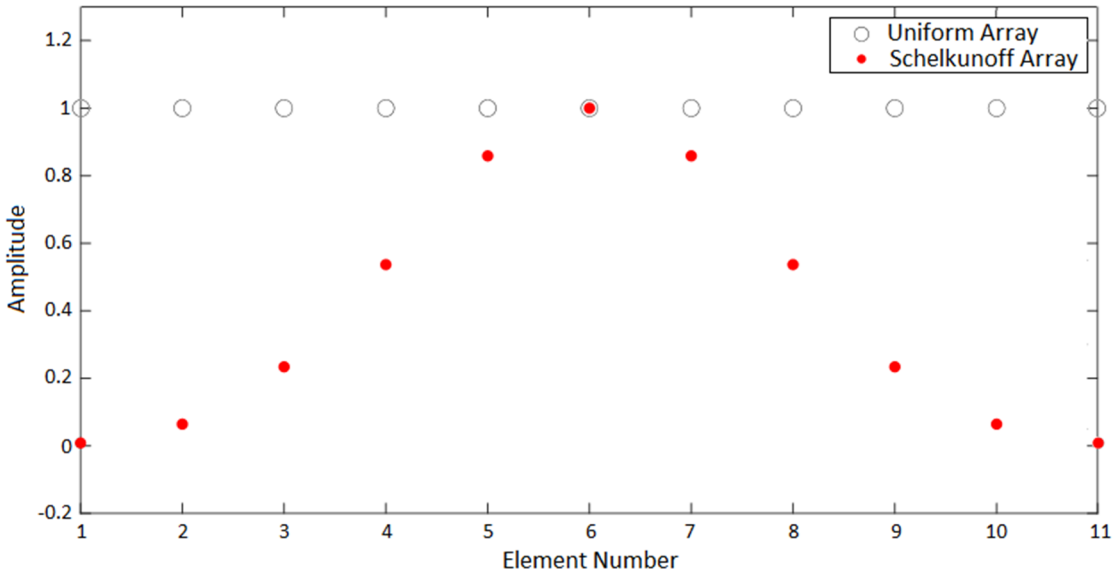

Figure (4.2) Amplitude excitation comparison between Schelkunoff and uniform array at N=11

Figures (4.3) and (4.4) compares the phase excitation between Schelkunoff and uniform array at N=6 and N=11. It can be seen there is a difference phase excitation between the two arrays.

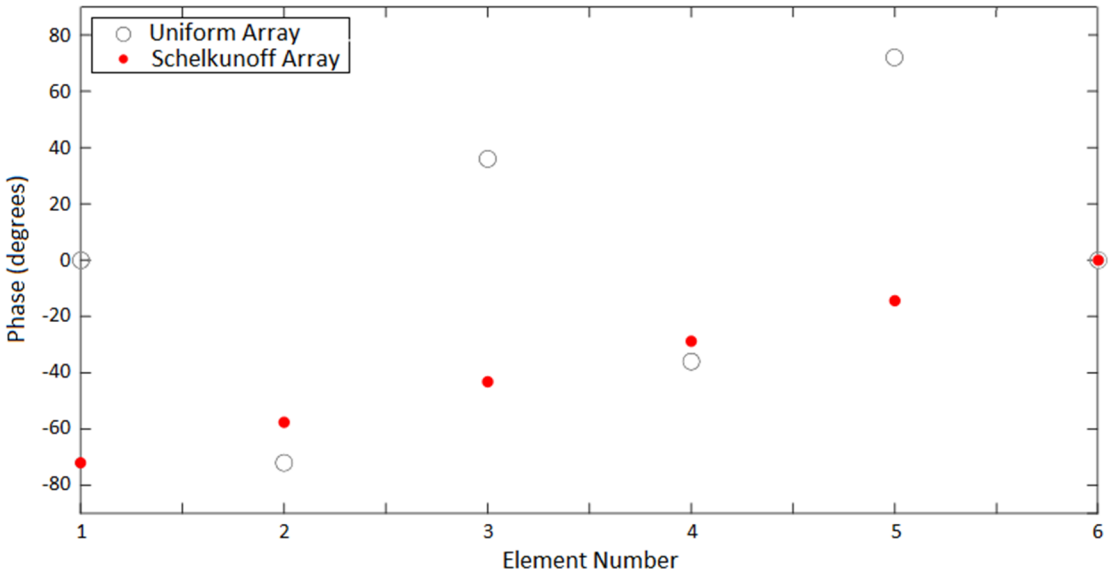

Figure (4.3) Phase excitation comparison between Schelkunoff and uniform array at N=6

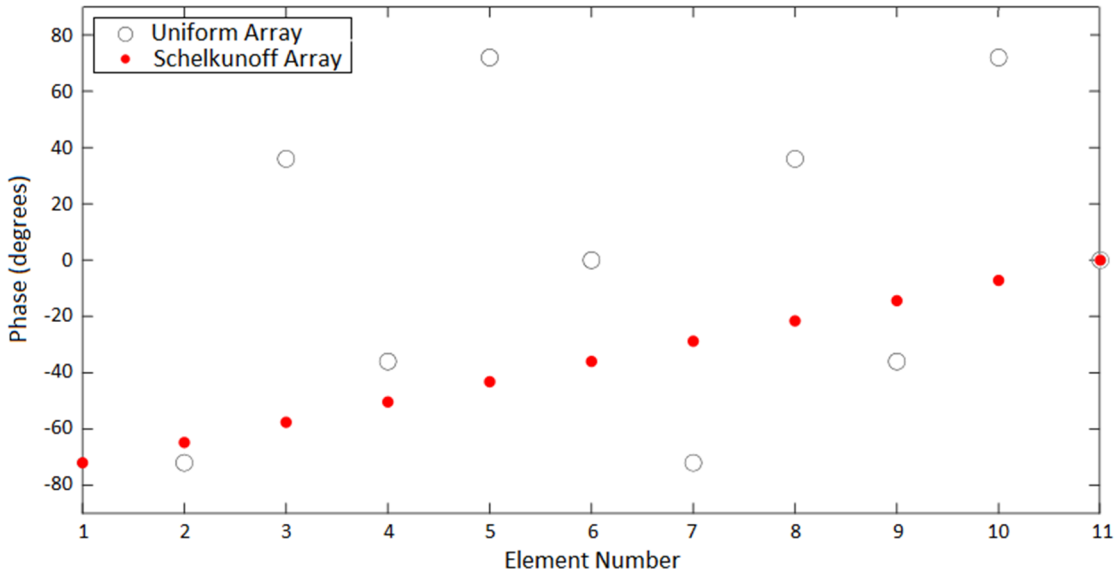

Figure (4.4) Phase excitation comparison between Schelkunoff and uniform array at N=11

Figures (4.5) and (4.6) illustrate the radiation patterns at N=6 elements and N=11 elements, respectively, when the distance between the elements d=0.2λ.

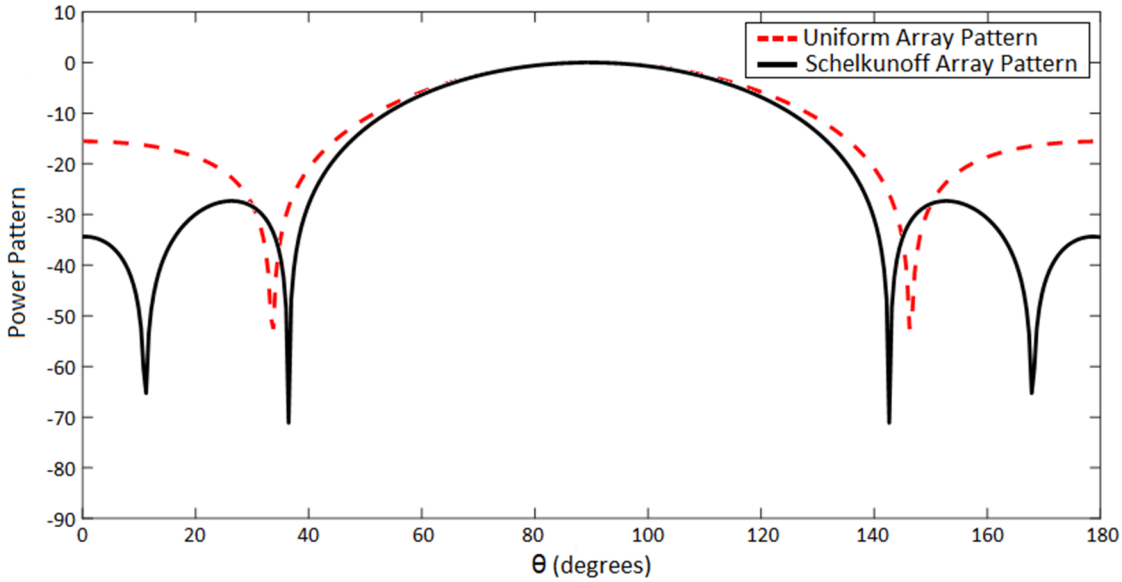

Figure (4.5) Schelkunoff and uniform arrays comparison radiation pattern (N=6, d=0.2 λ)

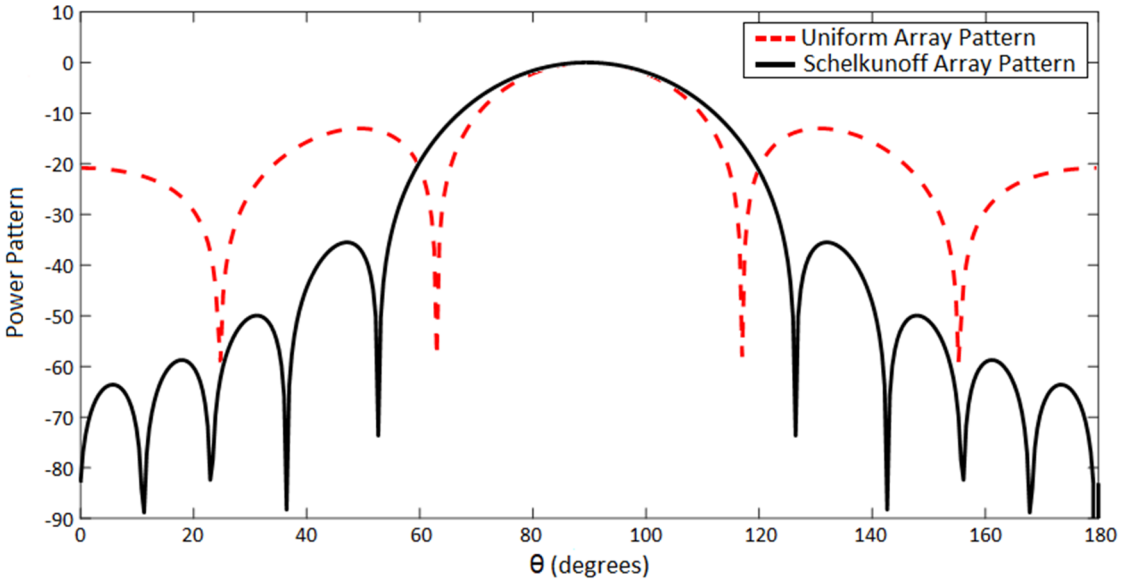

Figure (4.6) Schelkunoff and uniform arrays comparison radiation pattern (N=11, d=0.2λ)

It can be seen from the results, the schelkunoff array shifts the N-1 nulls to the visible region of the antenna radiation pattern in comparison to the uniform array. Where, the number of nulls in the uniform array in the first case is equal to 2 and 4 in the second, while in the Schelkunoff the numbers of nulls achieved are 5 and 10 for N=6 and N=11 array, respectively.

For the same length of the array but at d=0.4λ, the radiation patterns also compared to the uniform array. Figures (4.7) and (4.8) illustrates the radiation patterns for N=6 and N=11 arrays respectively. It can be noticed that, the Schelkunoff method achieved the nulls in the visible region of the antenna radiation pattern. It can also observed that, at this distance d=0.4λ, the side lobe levels increase compared to the uniform array.

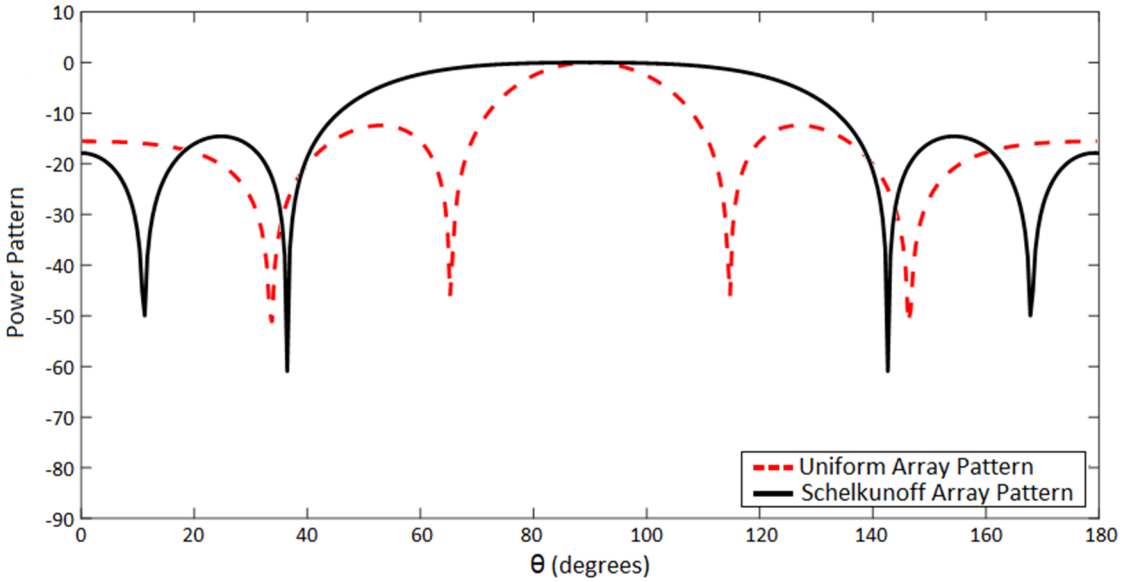

Figure (4.7) Schelkunoff and uniform arrays comparison radiation pattern (N=6, d=0.4 λ)

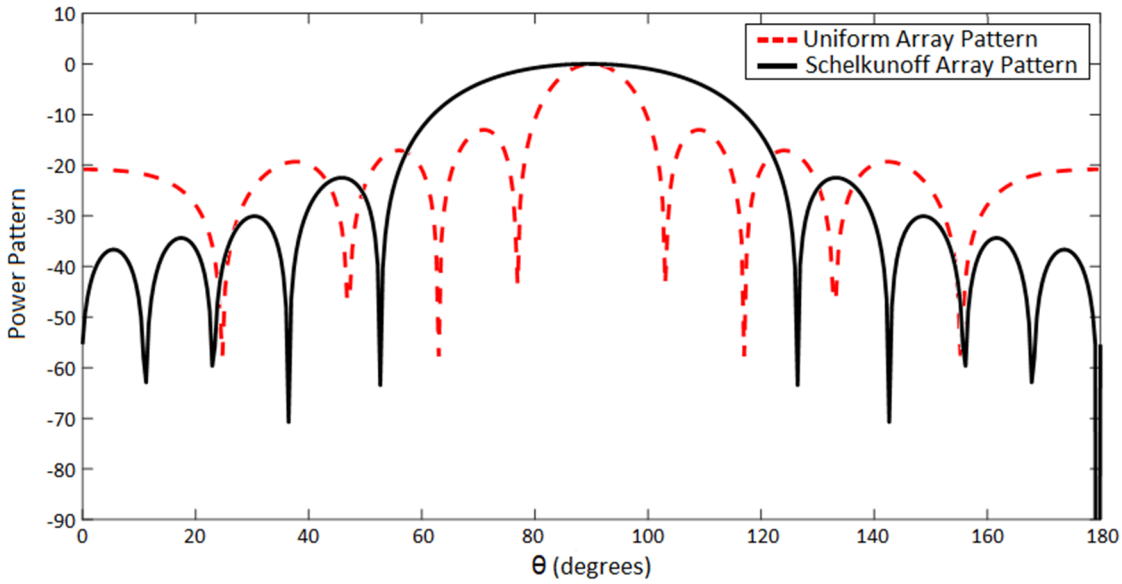

Figure (4.8) Schelkunoff and uniform arrays comparison radiation pattern (N=11, d=0.4 λ)

Figures (4.9) and (4.10) compare the radiation patterns of Schelkunoff and uniform arrays of N=6 and N=11 at 0.5λ. It can be seen that, the Schelkunoff achieved nulls in the visible region but at the expense of distortion in the main beam.

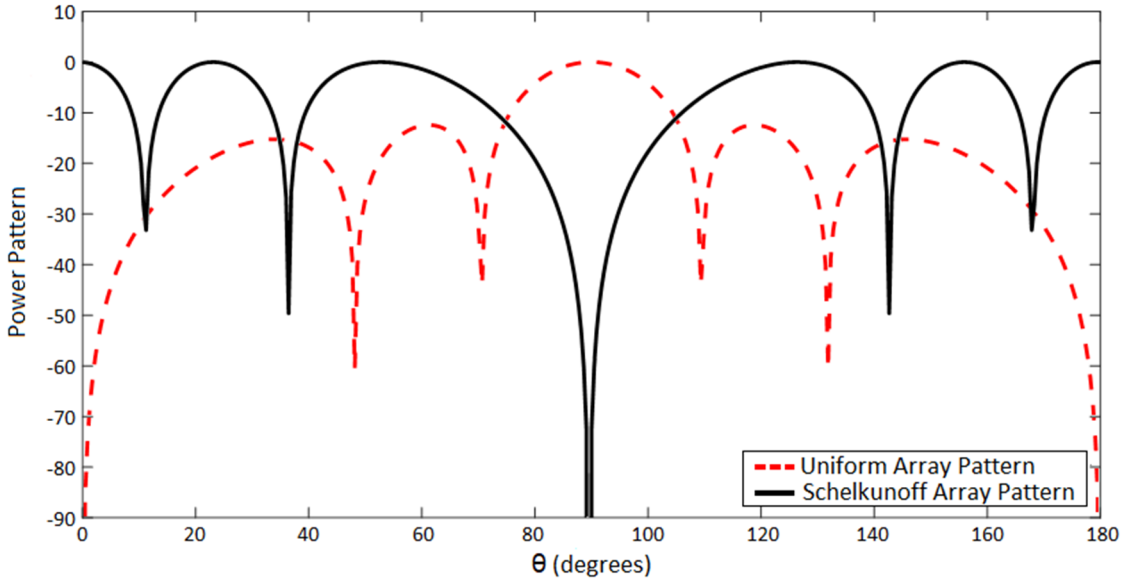

Figure (4.9) Schelkunoff and uniform arrays comparison radiation pattern (N=6, d=0.5 λ)

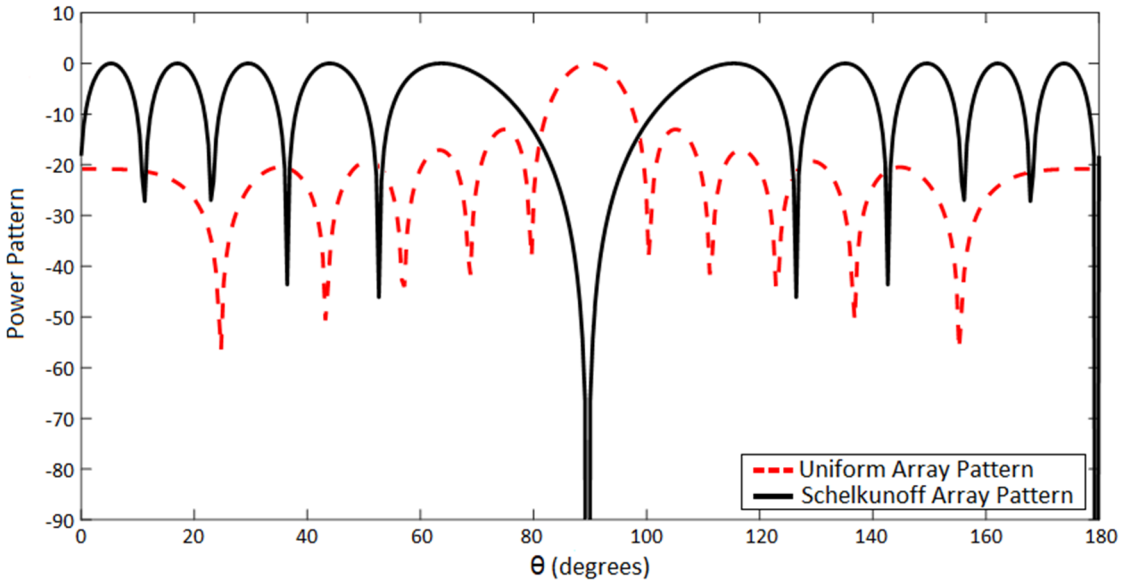

Figure (4.10) Schelkunoff and uniform arrays comparison radiation pattern (N=11, d=0.5 λ)

Figures (4.11), (4.12) and (4.13) illustrate the comparisons of the Average Side Lobe Level (ASLL) between the Schelkunoff and uniform arrays at 0.2λ, 0.4λ, and 0.5λ, respectively. It can be noticed that at 0.2λ and 0.4λ, the ASLL in Schelkunoff outperform uniform array when the number of element is increased. while at 0.5λ the ASLL in Schelkunoff is increased to that in uniform array.

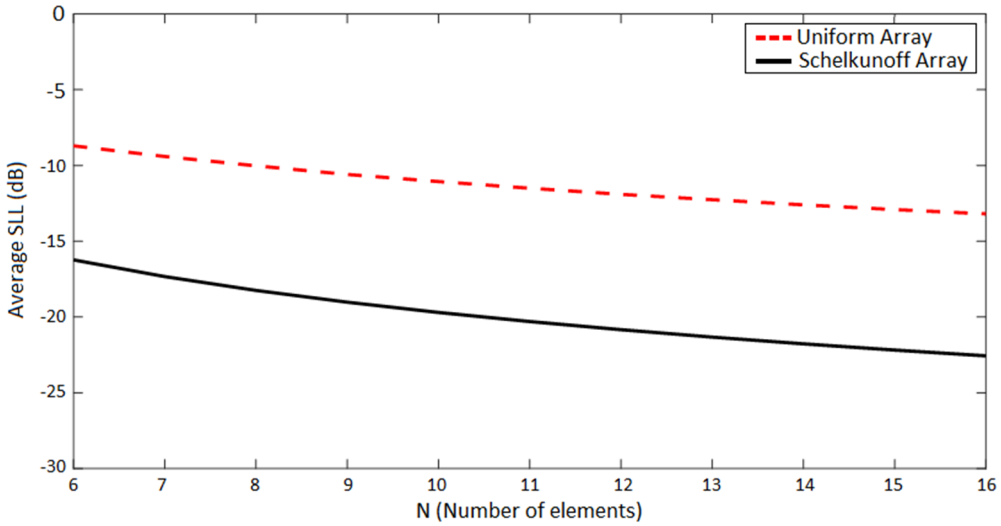

Figure (4.11) ASLL comparison between Schelkunoff and uniform arrays at d=0.2λ

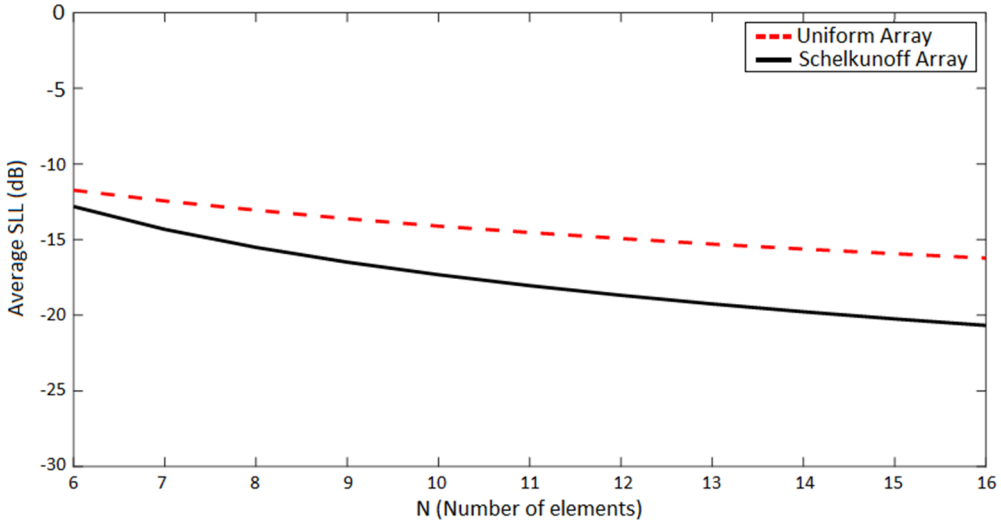

Figure (4.12) ASLL comparison between Schelkunoff and uniform arrays at d=0.4λ

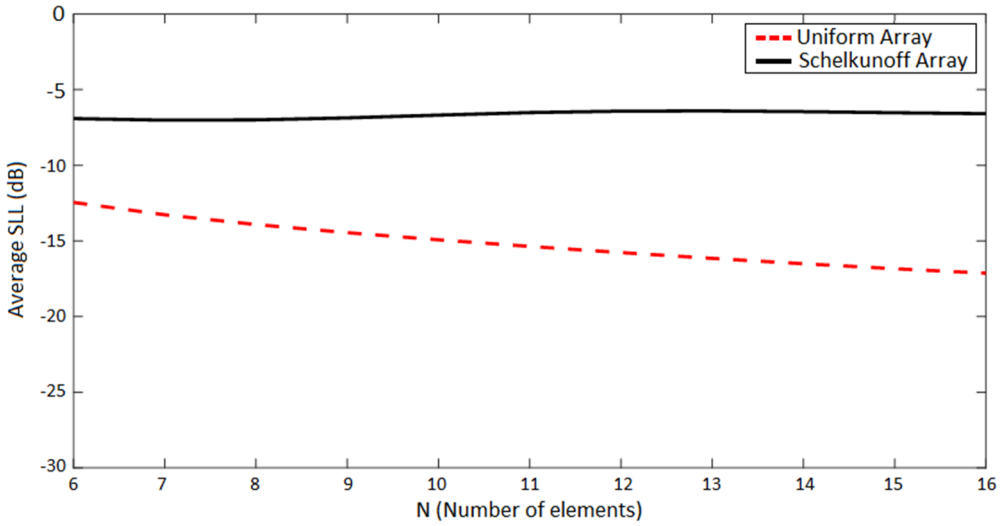

Figure (4.13) ASLL comparison between Schelkunoff and uniform arrays at d=0.5λ

Figures (4.14), (4.15), and (4.16) compared the Taper efficiency between Schelkunoff and uniform arrays at 0.2λ, 0.4λ, and 0.5λ, respectively. It can be seen that, at the distances 0.2λ and 0.4λ, the Taper efficiencies are increase in Schelkunoff to that in uniform array when the number of elements are increase. While the Taper efficiency is decrease in Schelkunoff at distance d= 0.5λ.

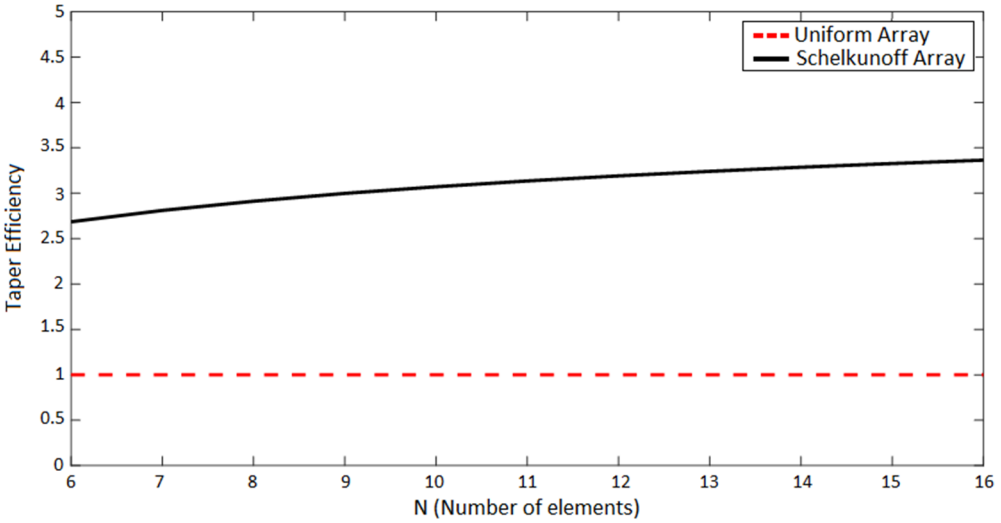

Figure (4.14) Taper efficiency comparison between Schelkunoff and uniform arrays at d=0.2λ

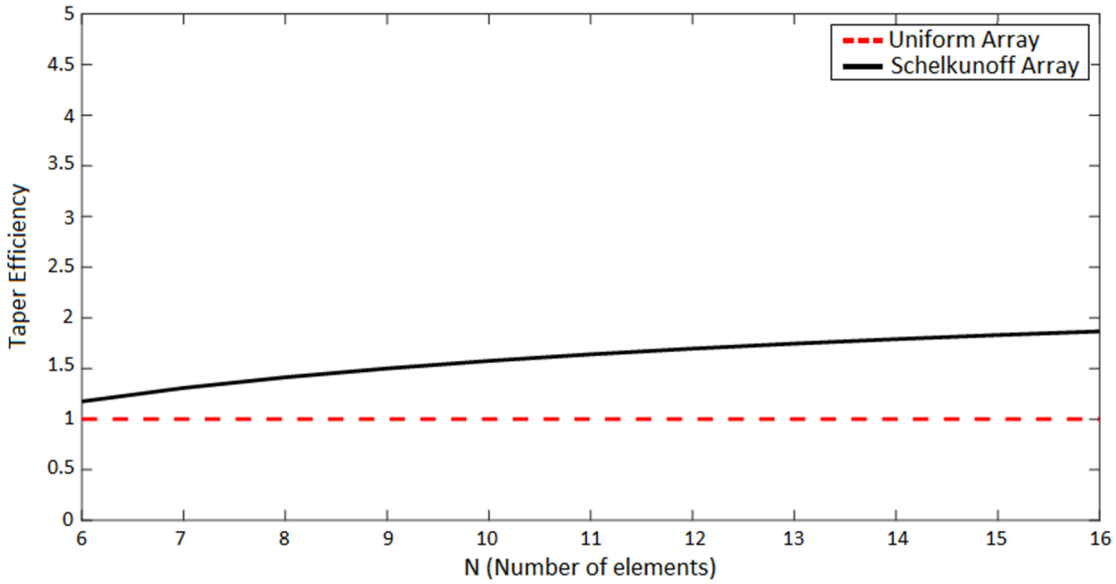

Figure (4.15) Taper efficiency comparison between Schelkunoff and uniform arrays at d=0.4λ

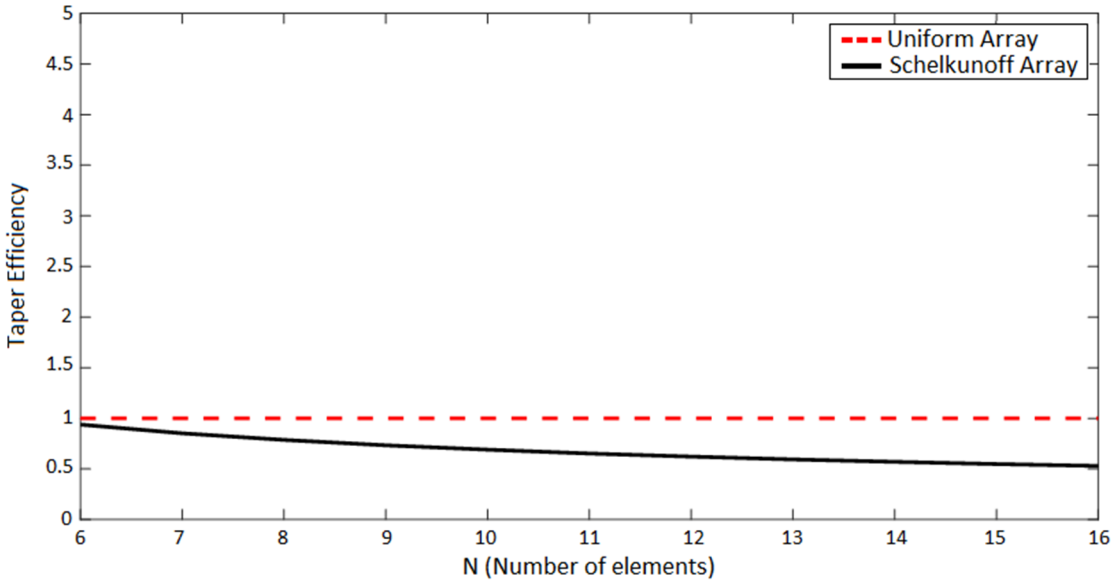

Figure (4.16) Taper efficiency comparison between Schelkunoff and uniform arrays at d=0.5λ

4.3 Godara Method Performance

Based on the specifications proposed in chapter three, the simulation results of Godara method are compared to that in uniform array. Figures (4.17) and (4.18) illustrates the amplitude excitation comparison between the uniform and Godara array at N=6 and N=11 elements. Figures (4.19) and (4.20) show the phase excitation comparison between the uniform and Godara array at N=6 and N=11 elements.

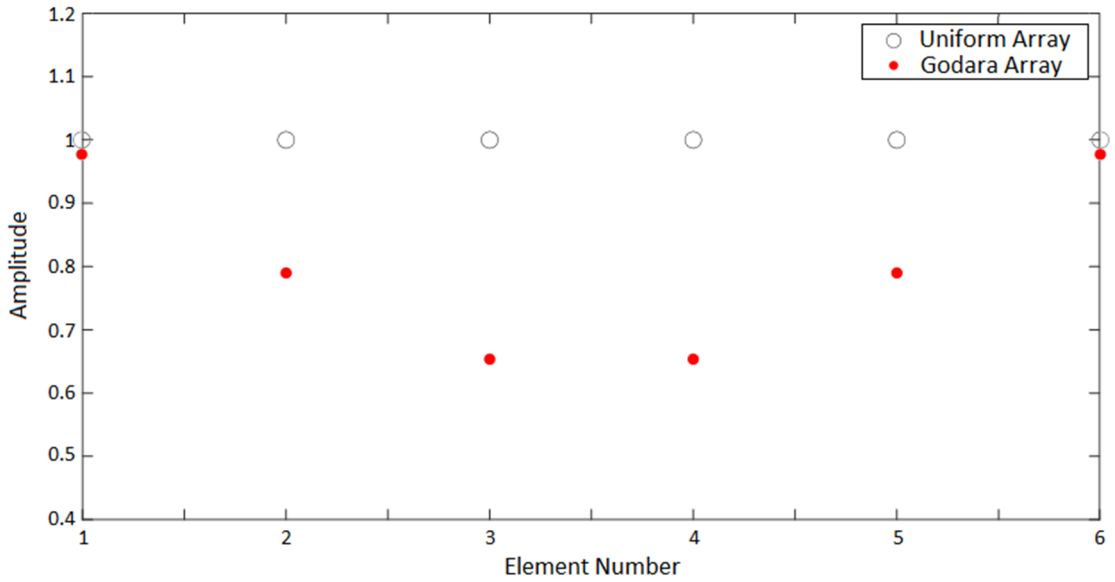

Figure (4.17) Amplitude excitation comparison between Godara and uniform array at N=6

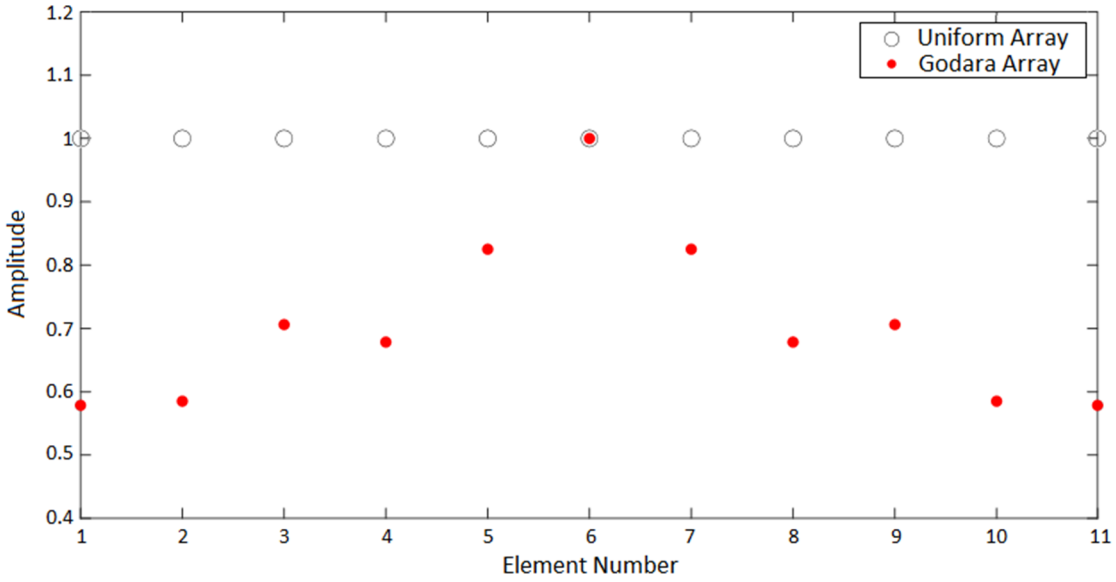

Figure (4.18) Amplitude excitation comparison between Godara and uniform array at N=11

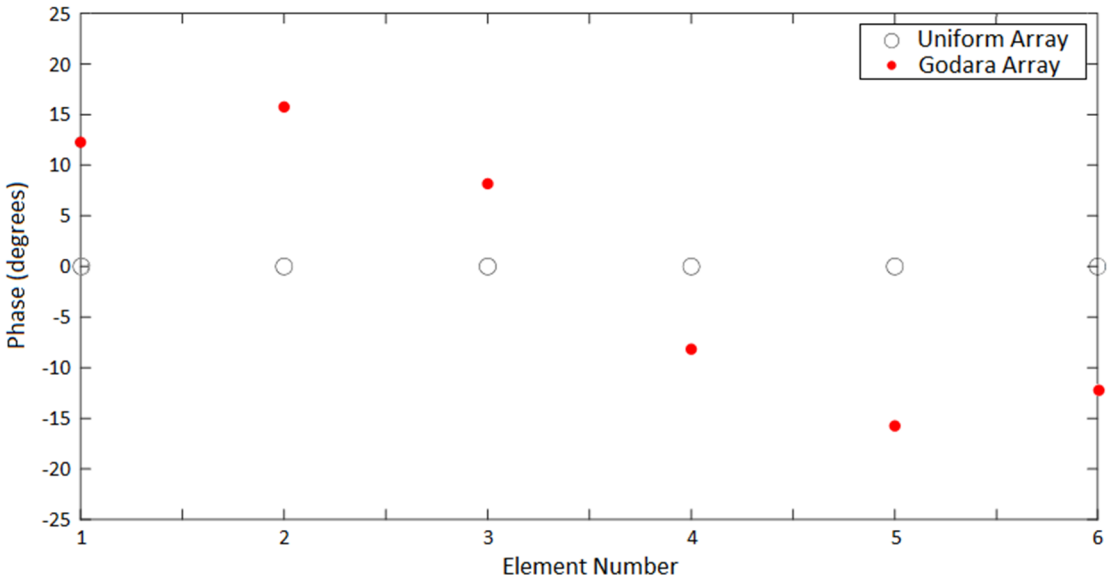

Figure (4.19) Phase excitation comparison between Godara and uniform array at N=6

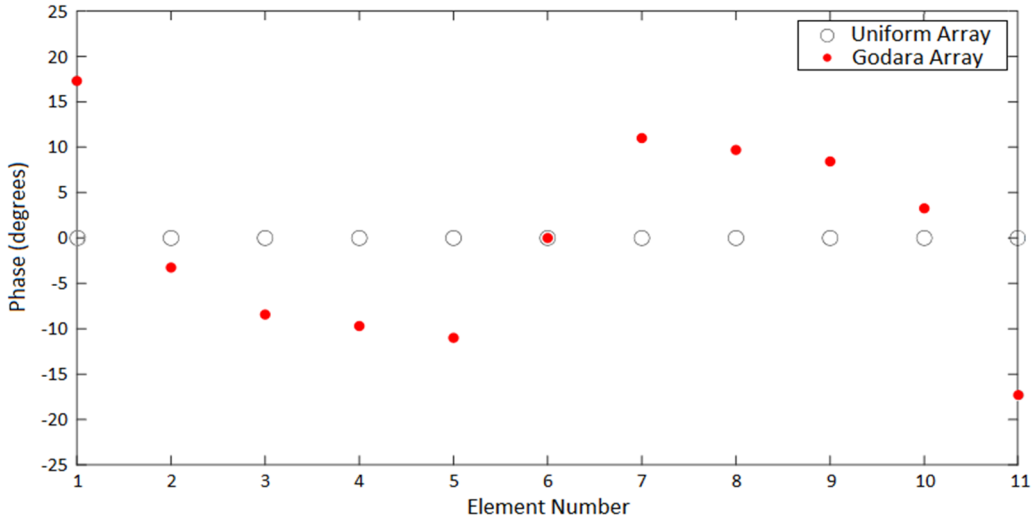

Figure (4.20) Phase excitation comparison between Godara and uniform array at N=11

Figures (4.21), (4.22) and (4.23) illustrates the radiation patterns of Godara method compared to uniform array for N=6 elements at distances 0.2λ, 0.4λ, and 0.5λ, respectively. The green line specified null at Θ_n=105˚.

It can be seen that the Godara array at d=0.2λ and 0.4λ, does not achieved the null at the specified angle, while at d= 0.5 λ the specified null position is achieved as shown in Figure (4.23).

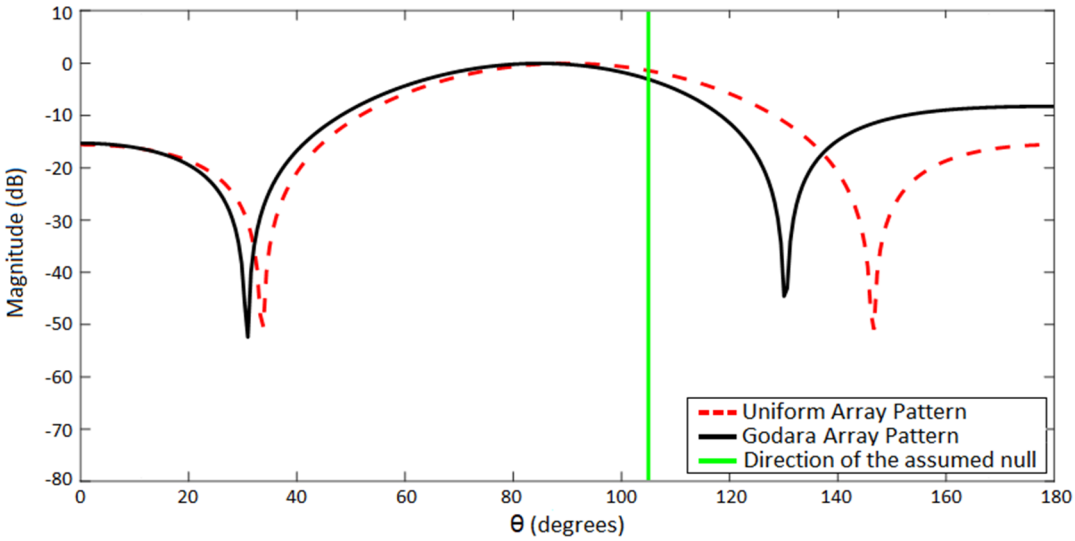

Figure (4.21) Godara and uniform arrays comparison radiation pattern (N=6, d=0.2 λ)

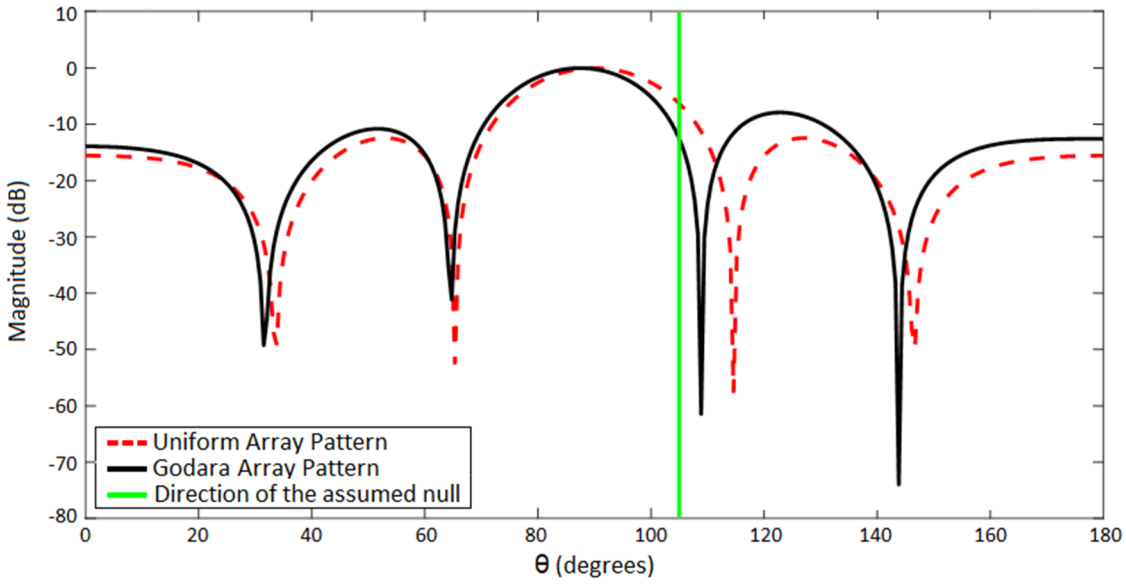

Figure (4.22) Godara and uniform arrays comparison radiation pattern (N=6, d=0.4 λ)

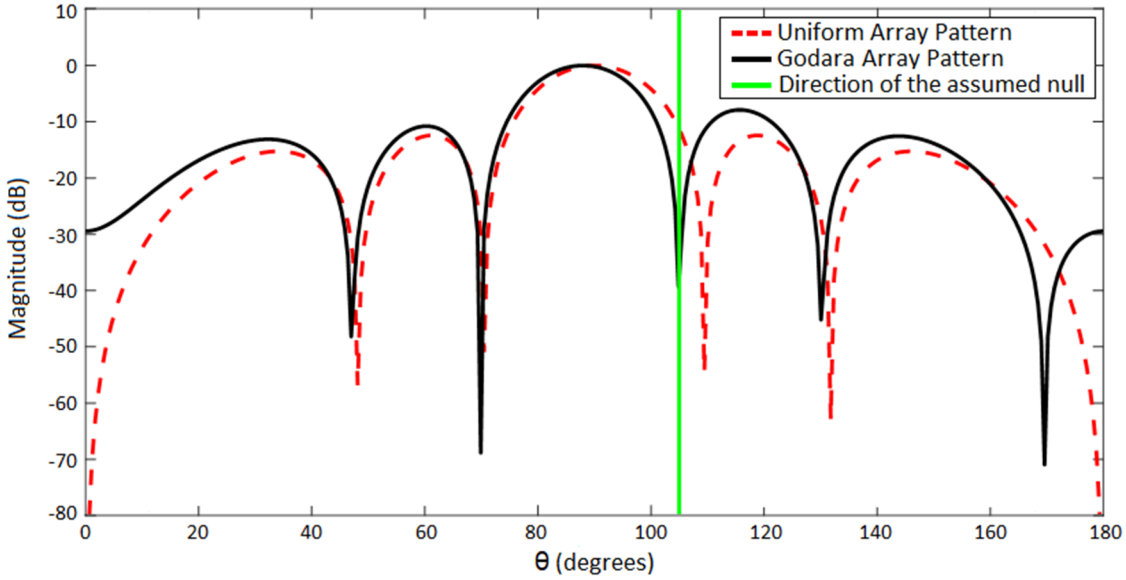

Figure (4.23) Godara and uniform arrays comparison radiation pattern (N=6, d=0.5 λ)

Figures (4.24), (4.25), and (4.26) illustrates the radiation patterns of the Godara method compared to uniform array at N=11 elements at distances 0.2λ, 0.4λ, and 0.5λ, respectively. The nulls specified at three angles, Θ_n= 55˚, 105˚, and 130˚.

It can be seen that at distances 0.2λ and 0.4λ, the Godara method does not achieved the specified null positions, while at d=0.5λ the nulls achieved as shown the green line in Figure (4.26).

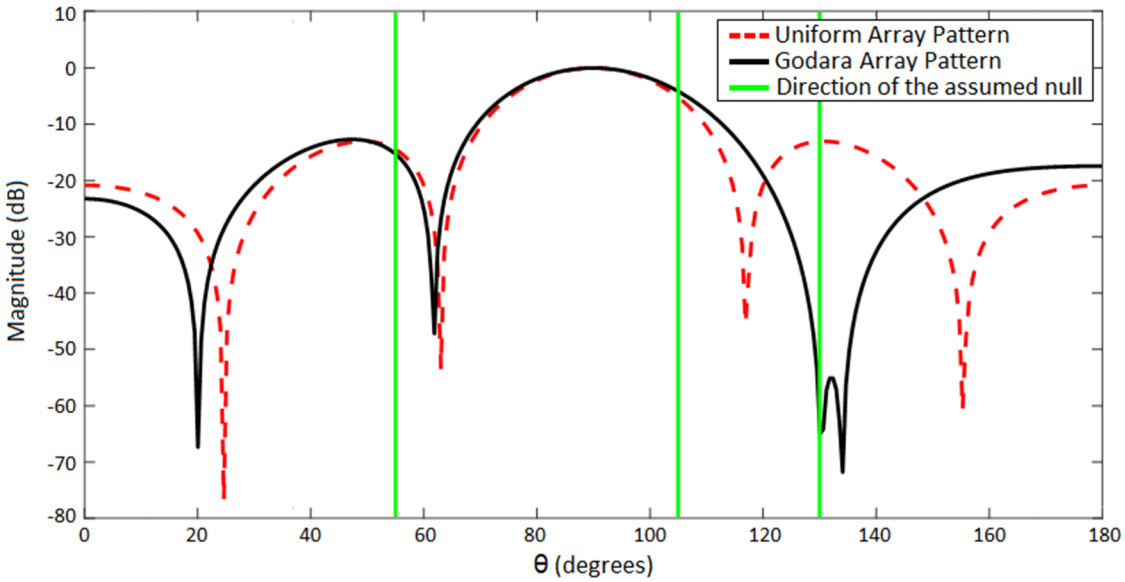

Figure (4.24) Godara and uniform arrays comparison radiation pattern (N=11, d=0.2λ)

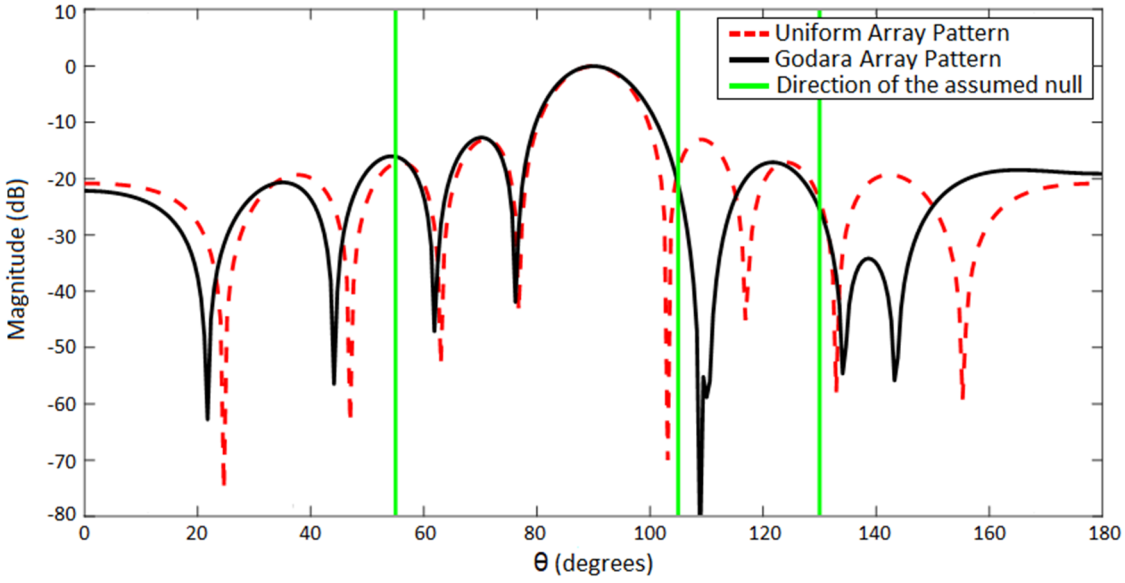

Figure (4.25) Godara and uniform arrays comparison radiation pattern (N=11, d=0.4λ)

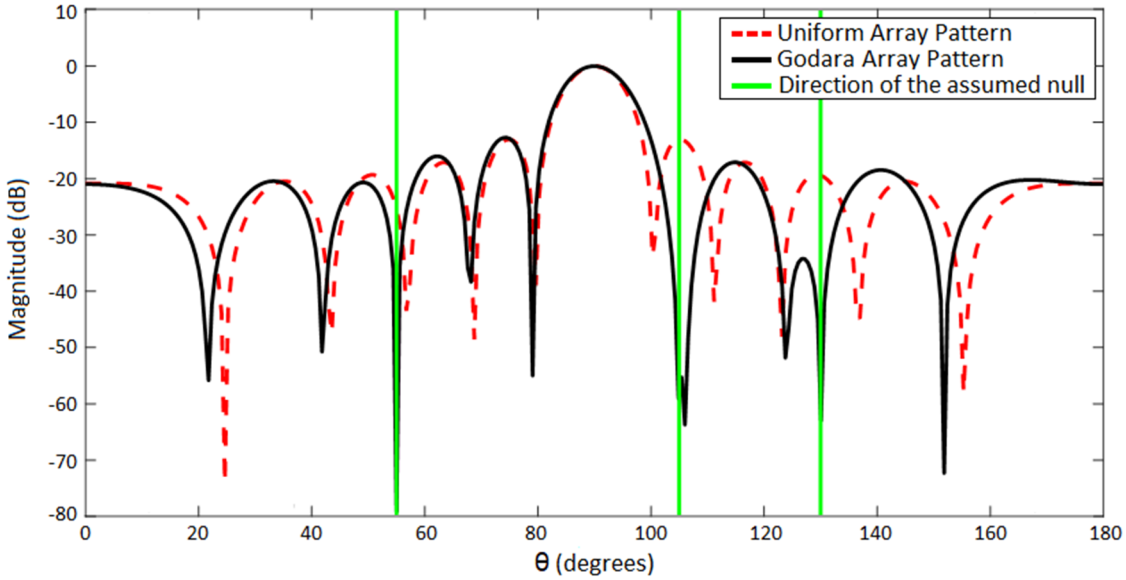

Figure (4.26) Godara and uniform arrays comparison radiation pattern (N=11, d=0.5λ)

The ASLL in Godara method is also compared to that in uniform array with the increases of array elements. Figures (4.27), (4.28), and (4.29) illustrate that Godara method achieved the same ASLL performance to that in uniform array at distances 0.2λ, 0.4λ, and 0.5λ, respectively.

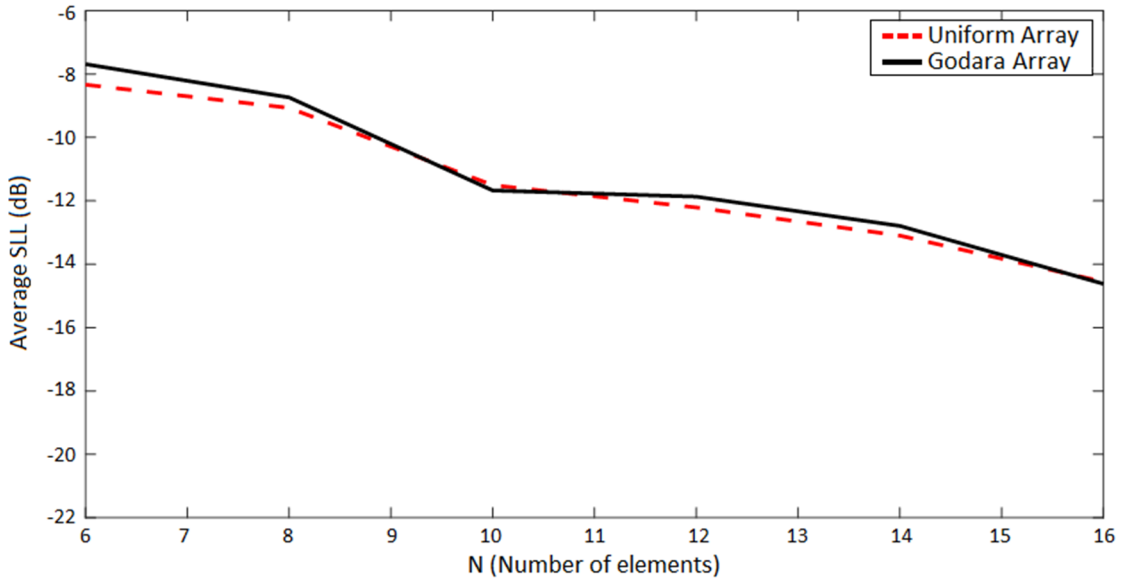

Figure (4.27) ASLL comparison between Godara and uniform arrays at d=0.2λ

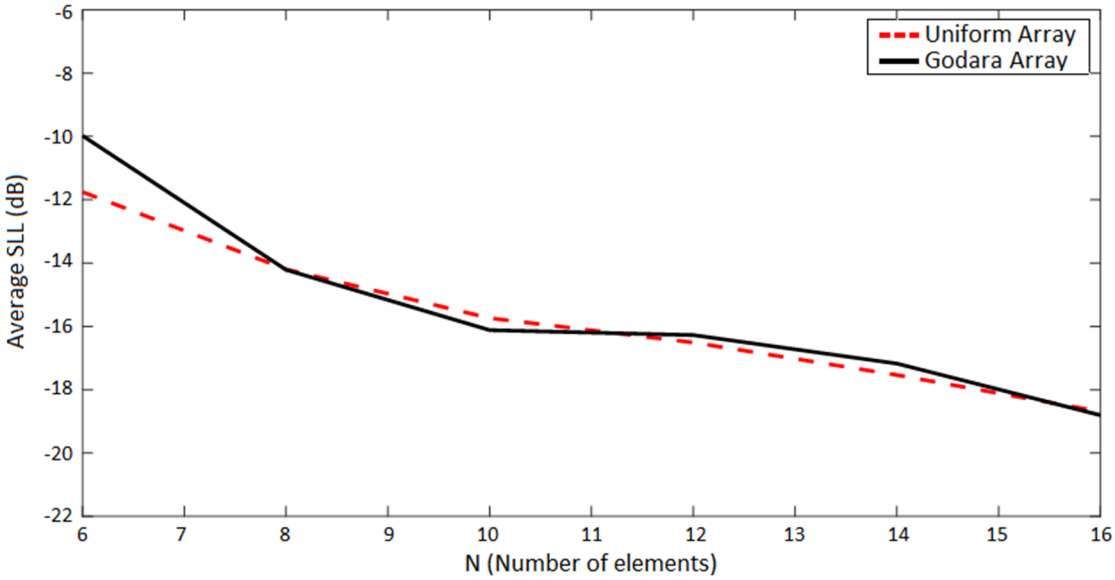

Figure (4.28) ASLL comparison between Godara and uniform arrays at d=0.4λ

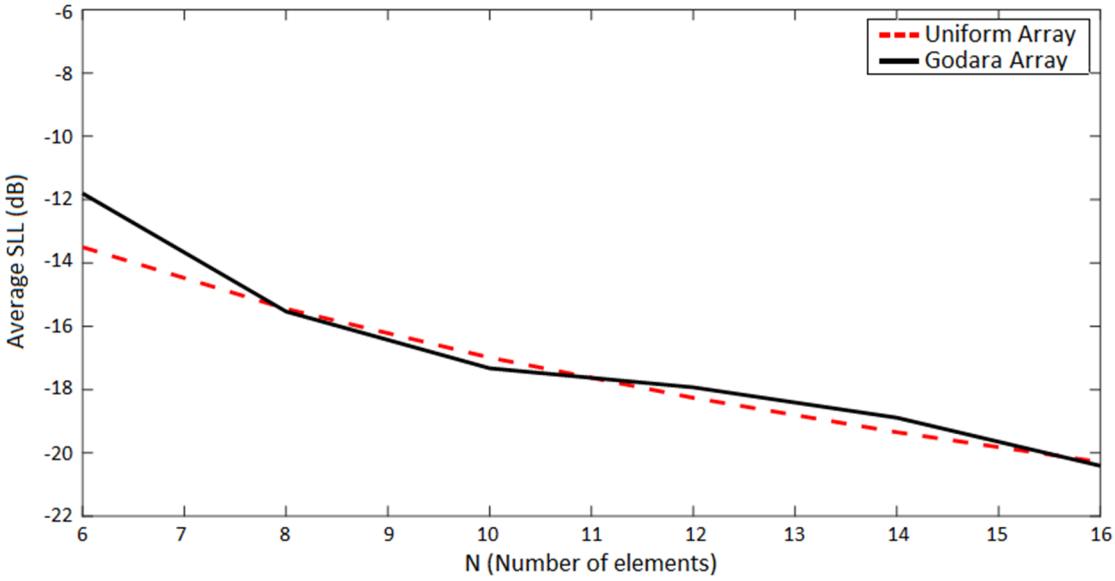

Figure (4.29) ASLL comparison between Godara and uniform arrays at d=0.5λ

Finally, the Taper efficiency of Godara array method compared to that in uniform at increases of the array elements. Figures (4.30), (4.31), and (4.32) illustrate the Taper efficiency at distances 0.2λ, 0.4λ, and 0.5λ,

respectively. It can be seen that in uniform array, the Taper efficiency is fixed with increases of the array size, while Godara array Taper efficiency is increased when the array size is increased.

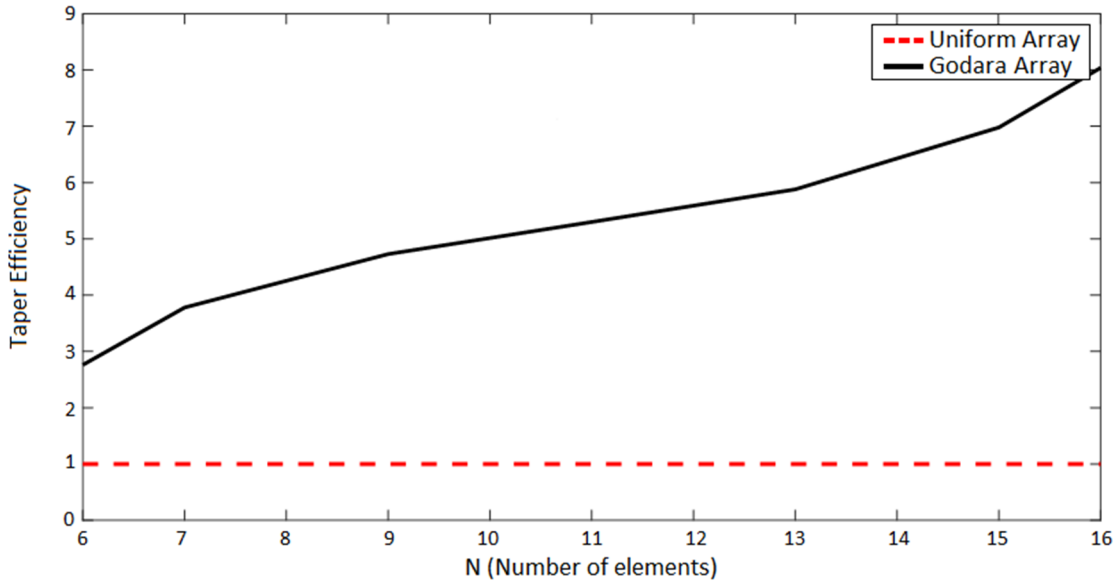

Figure (4.30) Taper efficiency comparison between Godara and uniform arrays at d=0.2λ

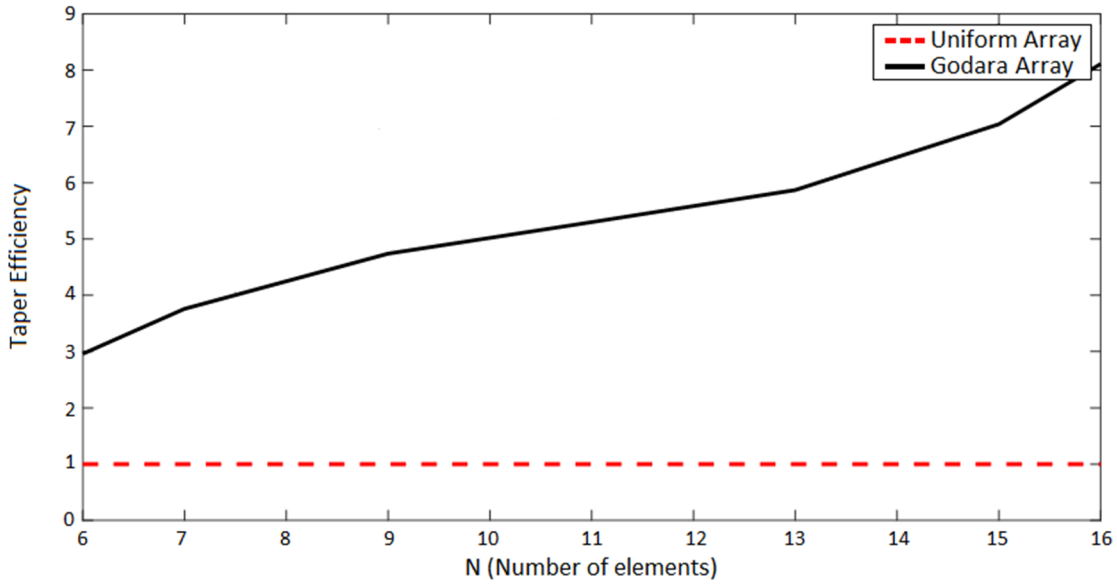

Figure (4.31) Taper efficiency comparison between Godara and uniform arrays at d=0.4λ

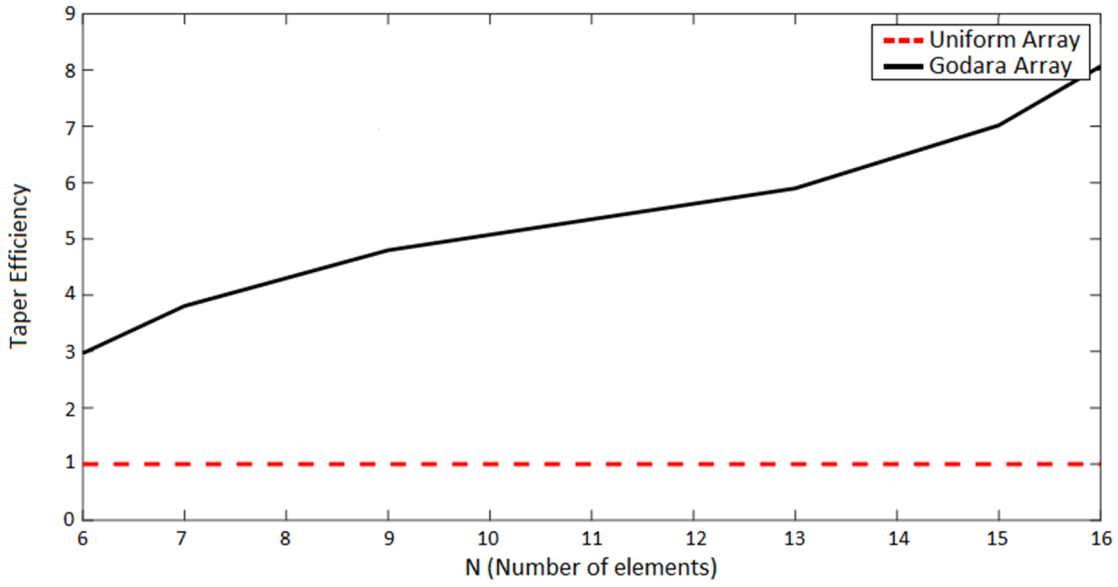

Figure (4.32) Taper efficiency comparison between Godara and uniform arrays at d=0.5λ

4.4 Adapted Side Lobe Canceller (ASLC) Method Performance

In this way, some of the primary antenna elements were used by the ASLC as an auxiliary antennas to produce nulls at specified angles for cancel out the unwanted signals. The simulation specifications parameters of this method are listed in Table (4.1).

Table (4.1) ASLC Simulation Parameters

Parameter	Setting
SIR	-30, 0, 30 (dB)
Noise variance	0.0005 (watts)
Number of Auxiliary array M	2, 5

The amplitude and phase excitations of ASLC method compared to the uniform array at N=6 and N=11 elements as shown in Figures (4.33)

and (4.34) for amplitude excitation and Figures (4.35) and (4.36) for phase excitation.

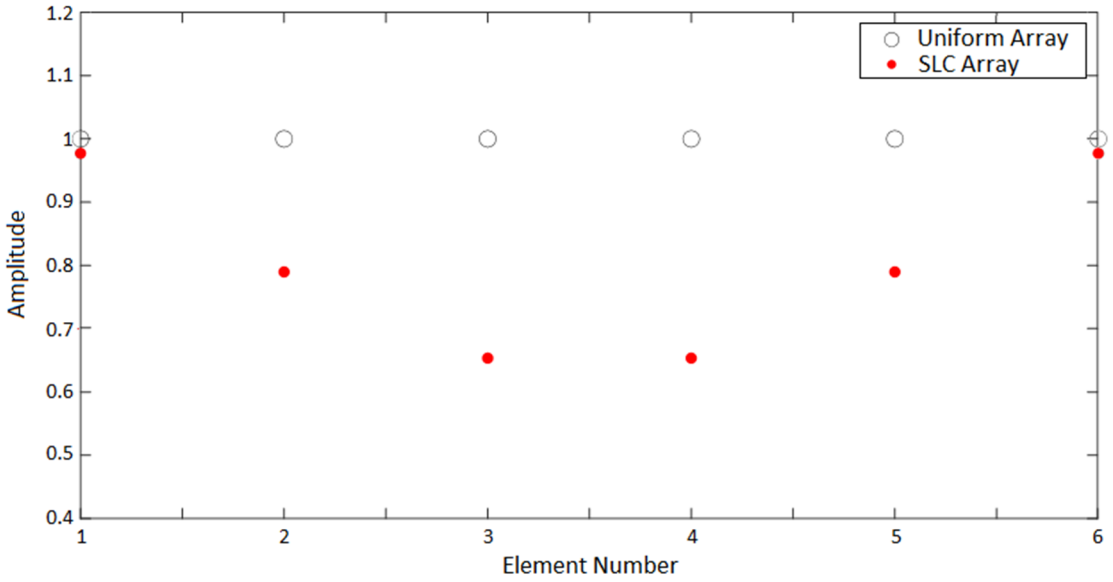

Figure (4.33) Amplitude excitation comparison between ASLC and uniform array at N=6

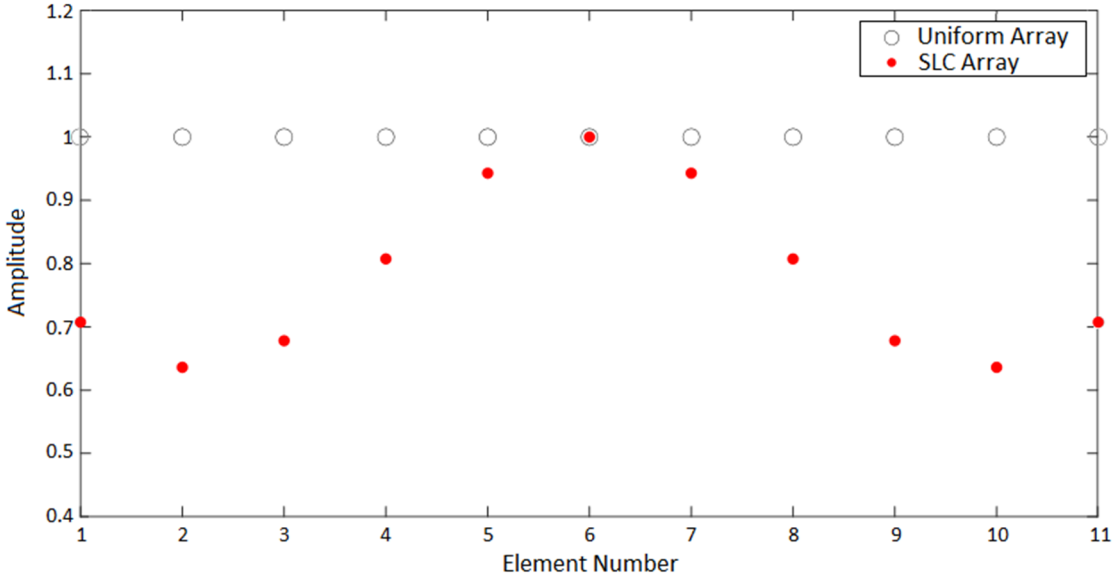

Figure (4.34) Amplitude excitation comparison between ASLC and uniform array at N=11

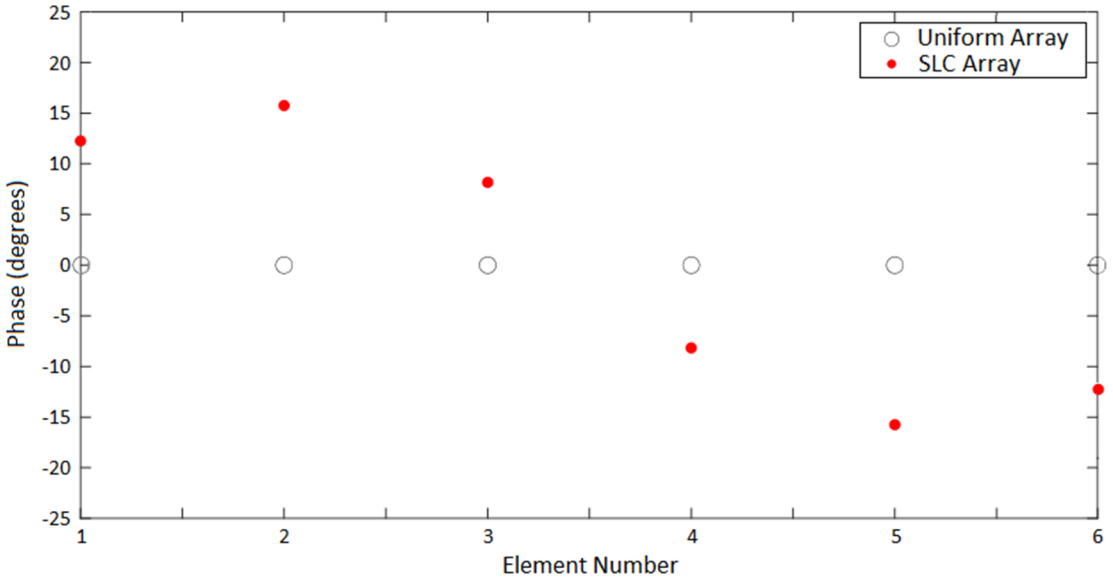

Figure (4.35) Phase excitation comparison between ASLC and uniform array at N=6

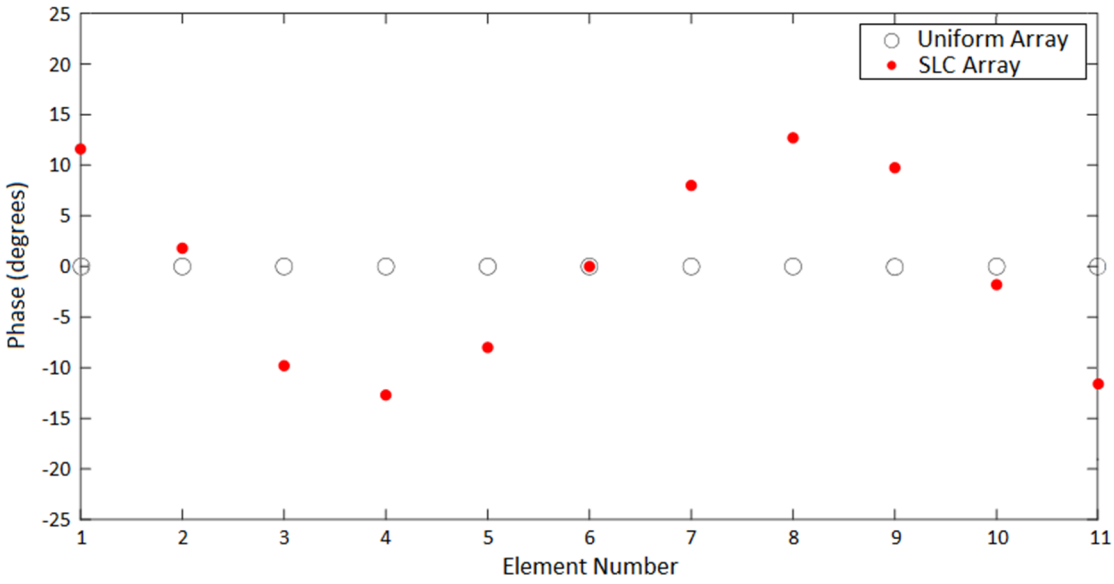

Figure (4.36) Phase excitation comparison between ASLC and uniform array at N=11

For N=6 elements and M=2 elements, the adapted array radiation patterns compared to the main array radiation patterns at distances d= 0.2λ, 0.4λ, and 0.5λ. Figures (4.37), (4.38) and (4.39) illustrate the radiation pattern of the main and adapted arrays at N=6 elements, where the black

pattern represents the adapted array pattern that achieved from the subtraction of the cancellation pattern (blue) from the main array pattern (red). It can be seen there is a slight distortion in the main beam in the adapted array compared to the main array pattern.

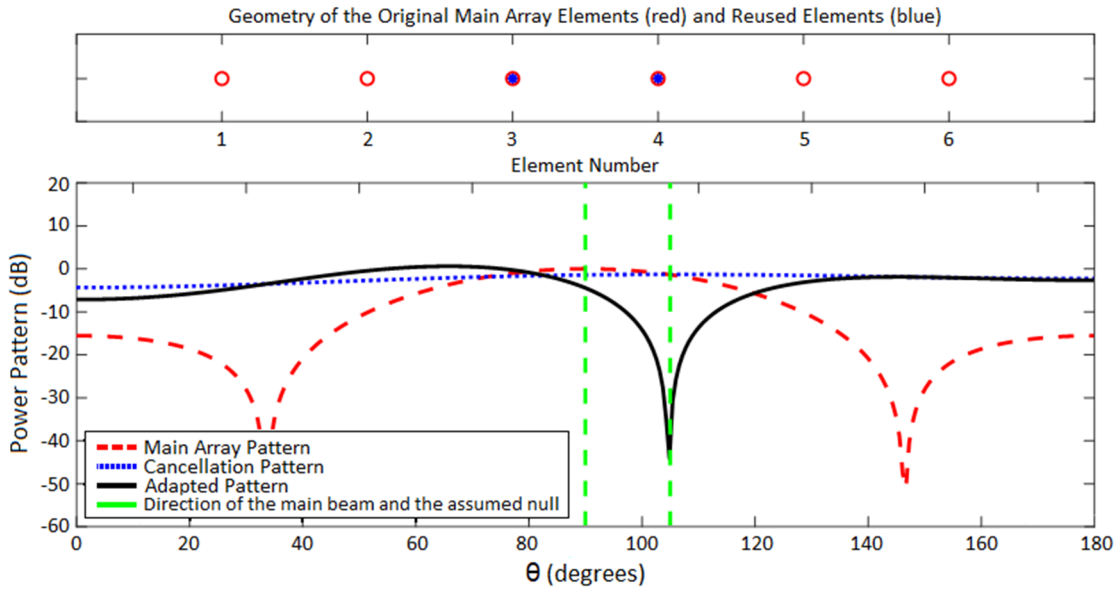

Figure (4.37) Geometry of the main and auxiliary elements and the beam pattern at N = 6, M = 2, d = 0.2λ, and SIR = -30 dB.

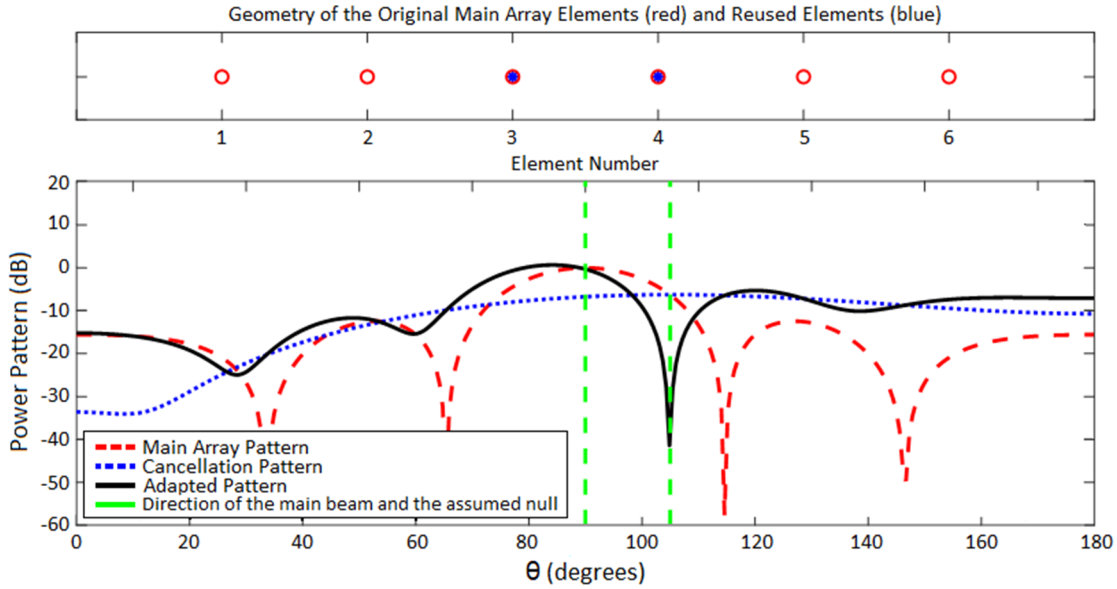

Figure (4.38) Geometry of the main and auxiliary elements and the beam pattern at N = 6, M = 2, d = 0.4λ, and SIR = -30 dB.

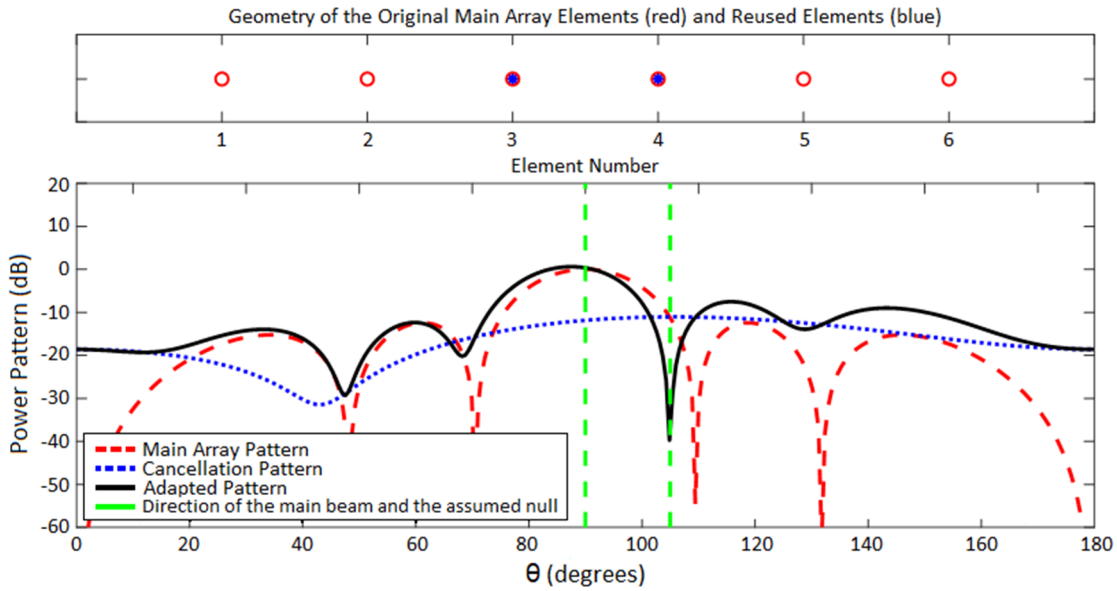

Figure (4.39) Geometry of the main and auxiliary elements and the beam pattern at N = 6, M = 2, d = 0.5λ, and SIR = -30 dB

Figures (4.40), (4.41) and (4.42) show Geometry of the radiation pattern of the main and auxiliary elements of ASLC method at N=11 elements. It can be seen that at 0.4λ in Figure (4.42) the adapted array achieved the desired specification with a minimum distortion to that in 0.2λ and 0.5λ.

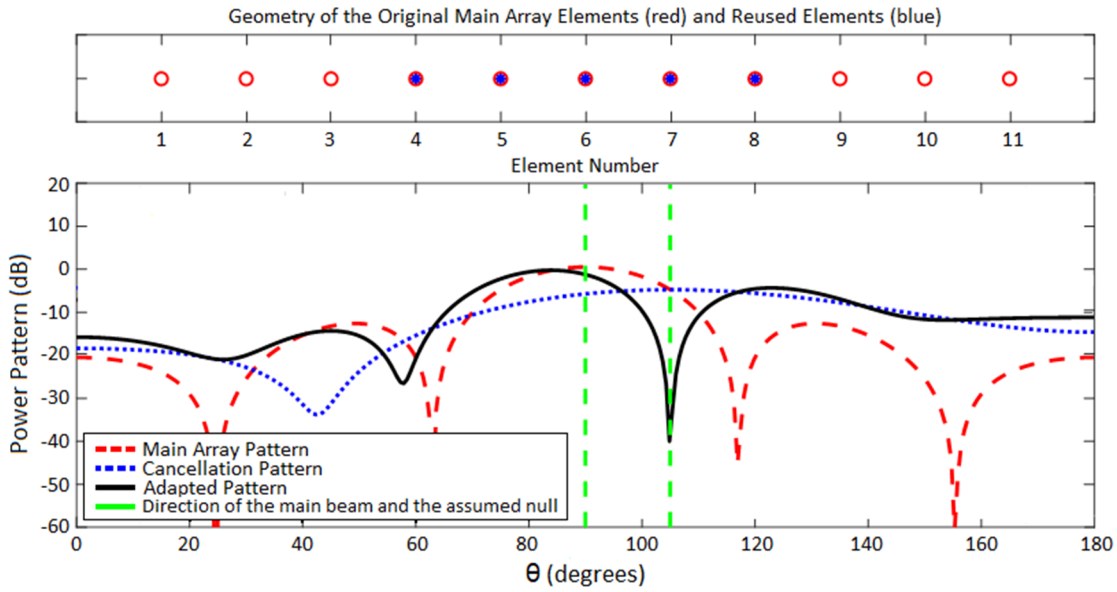

Figure (4.40) Geometry of the main and auxiliary elements and the beam pattern at N = 11, M = 5, d = 0.2λ, and SIR = -30 dB

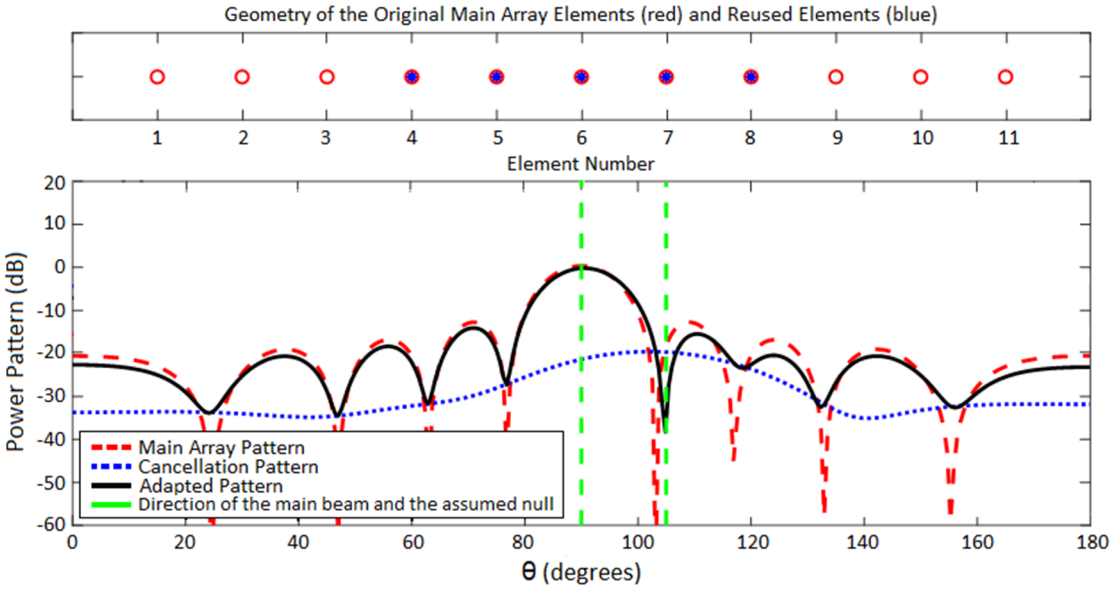

Figure (4.41) Geometry of the main and auxiliary elements and the beam pattern at N = 11, M = 5, d = 0.4λ, and SIR = -30 dB

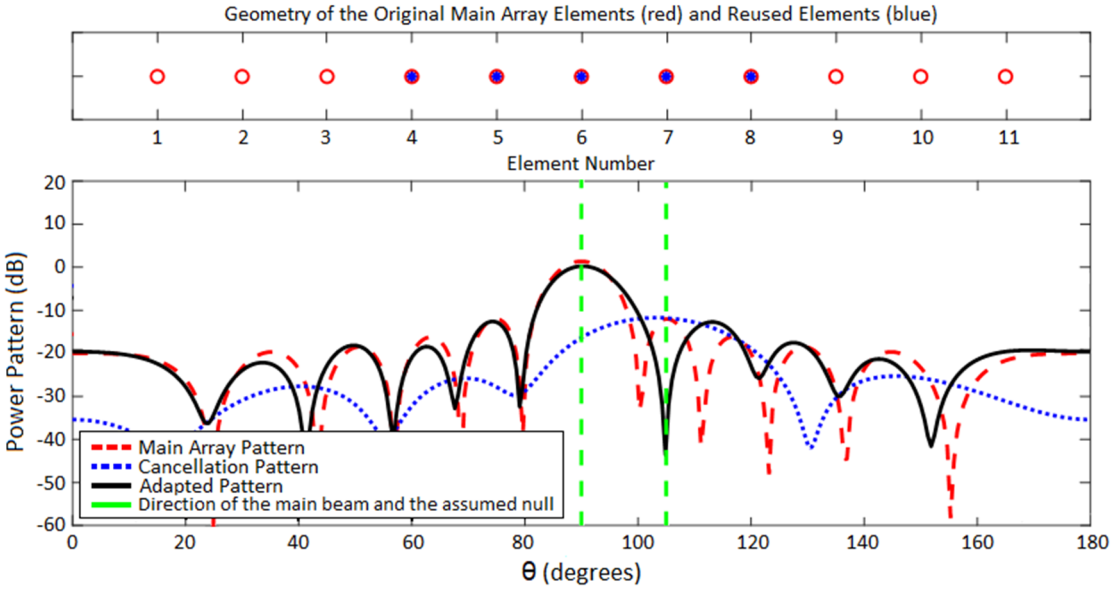

Figure (4.42) Geometry of the main and auxiliary elements and the beam pattern at N = 11, M = 5, d = 0.5λ, and SIR = -30 dB.

Figures (4.43) and (4.44) show the effect of the SIR on the performance of ASLC method at SIR=0 dB and SIR=30 dB, respectively, for N=11 elements and 0.5λ. It can be seen in Figure (4.43) that the null is achieved at 106˚ of level equal to -34.71 dB. The main beam is distorted of

about 17.77 dB. Figure (4.44) shows that the beam pattern is distorted at SIR=30 dB and the null is created at 90˚.

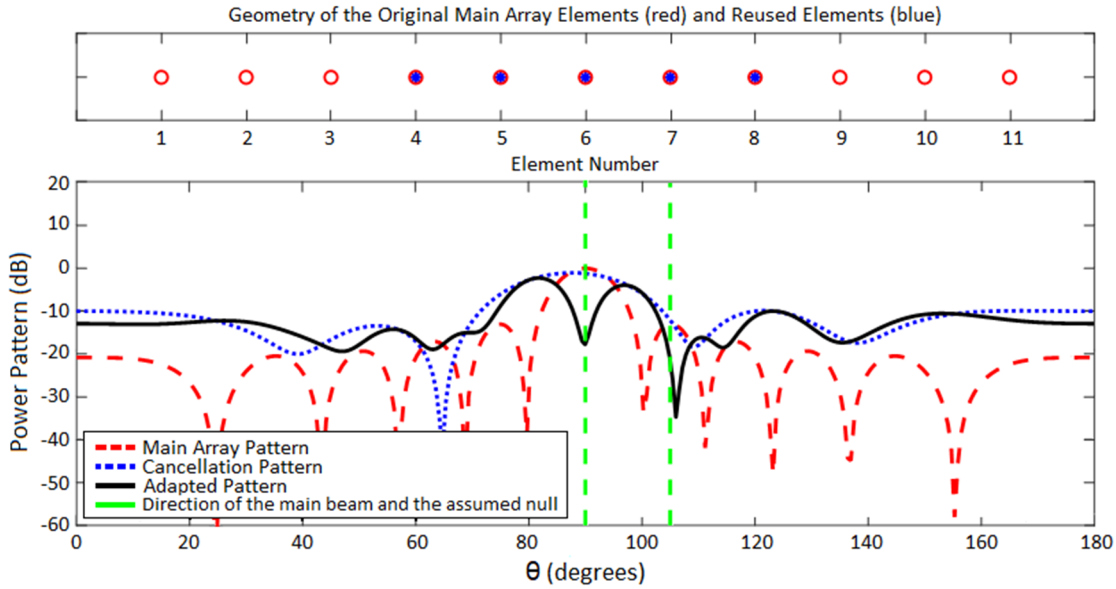

Figure (4.43) Geometry of the main and auxiliary elements and the beam pattern at N = 11, M = 5, and SIR = 0 dB.

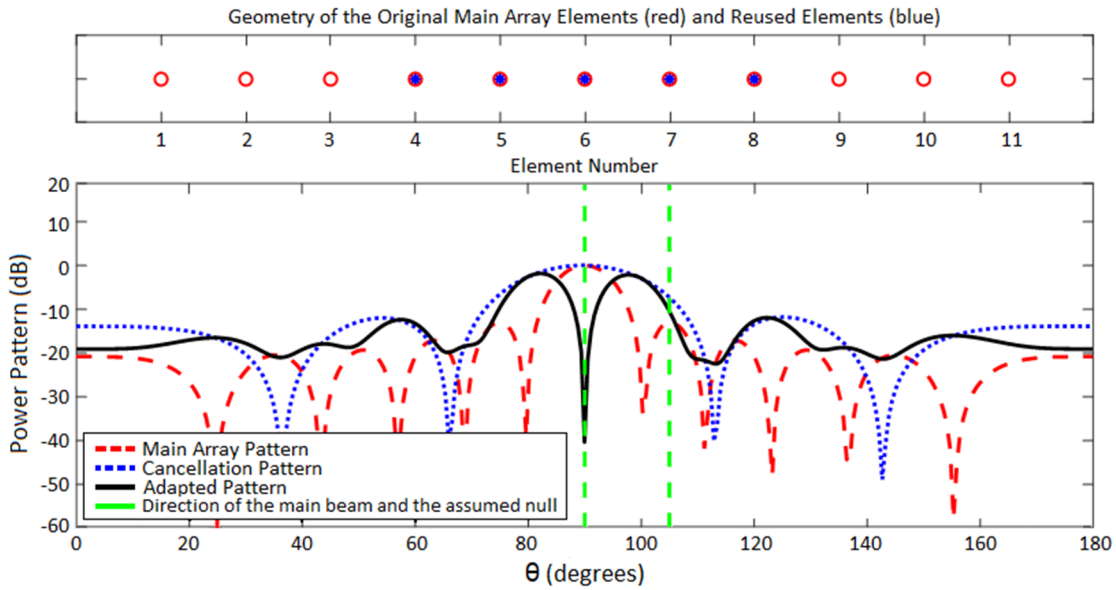

Figure (4.44) Geometry of the main and auxiliary elements and the beam pattern at N = 11, M = 5, and SIR = 30 dB.

Figures (4.45), (4.46) and (4.47) illustrate the ASLL for the ASLC method at 0.2λ, 0.4λ and 0.5λ, respectively. With the increase of array size,

the ASLC achieves lower ASLL of about -4.5dB than that of uniform array. It can be seen that, when the distance between the elements are increased the performance is not affected.

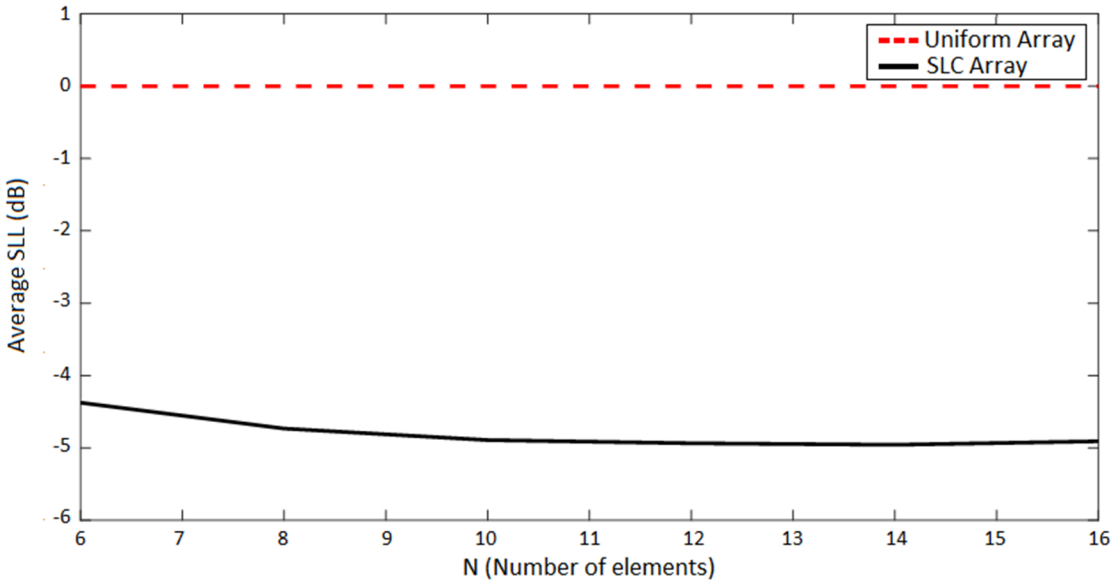

Figure (4.45) ASLL comparison between ASLC and uniform arrays at d=0.2λ

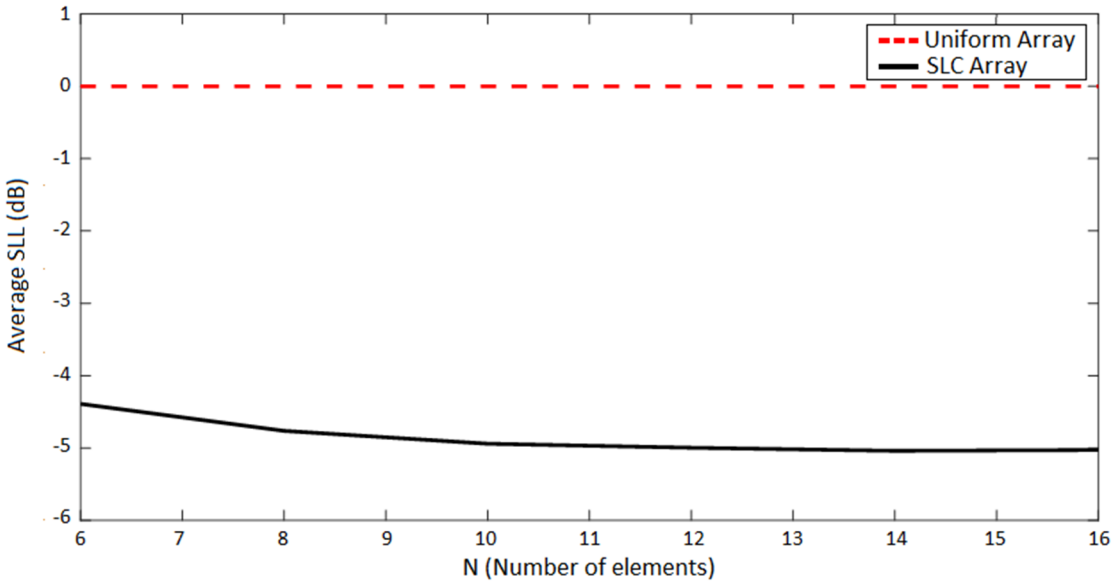

Figure (4.46) ASLL comparison between ASLC and uniform arrays at d=0.4λ

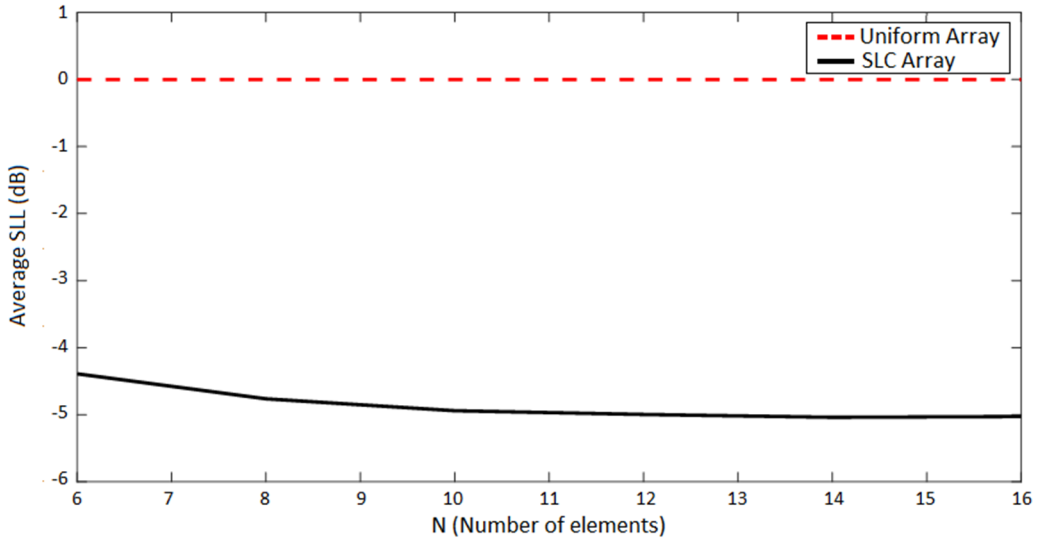

Figure (4.47) ASLL comparison between ASLC and uniform arrays at d=0.5λ

The performance in terms of Taper efficiency is also evaluated at various distances 0.2λ, 0.4λ and 0.5λ, respectively. Figures (4.48), (4.49) and (4.50) show the Taper efficiency compared to the uniform array. It can be noticed that at lower array size, the ASLC Taper efficiency is higher to that in uniform of about 0.8, 1.25 and 1.75 at distances 0.2λ, 0.4λ and 0.5λ, respectively and N=6. At higher array's size, the ASLC Taper efficiency approaching for uniform array.

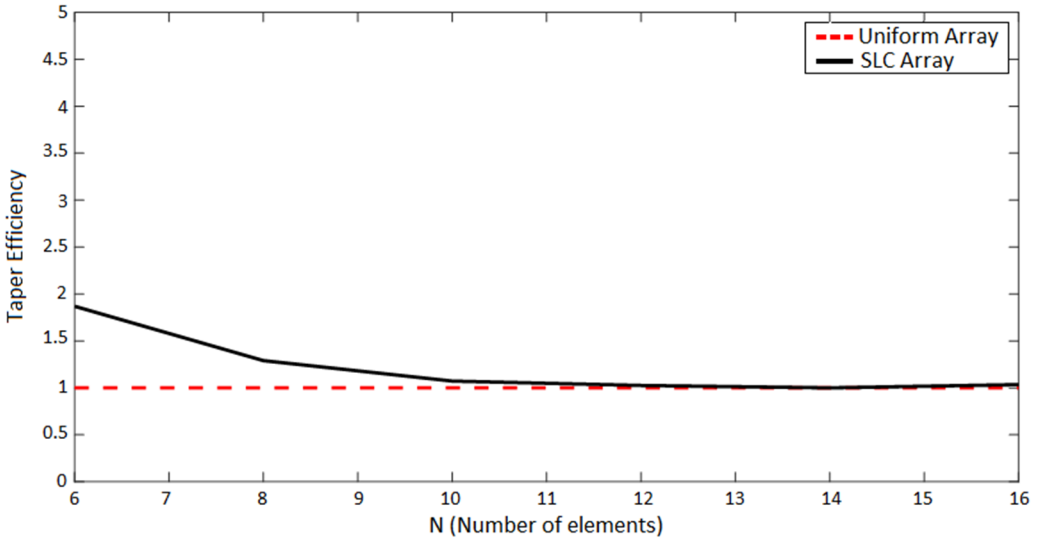

Figure (4.48) Taper efficiency comparison between ASLC and uniform arrays at d=0.2λ

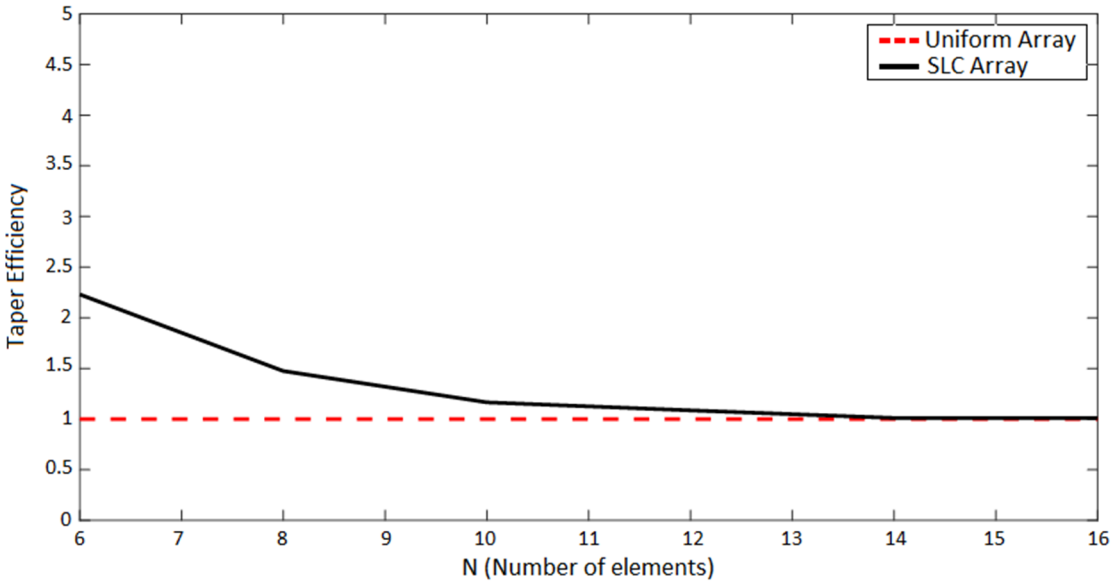

Figure (4.49) Taper efficiency comparison between ASLC and uniform arrays at d=0.4λ

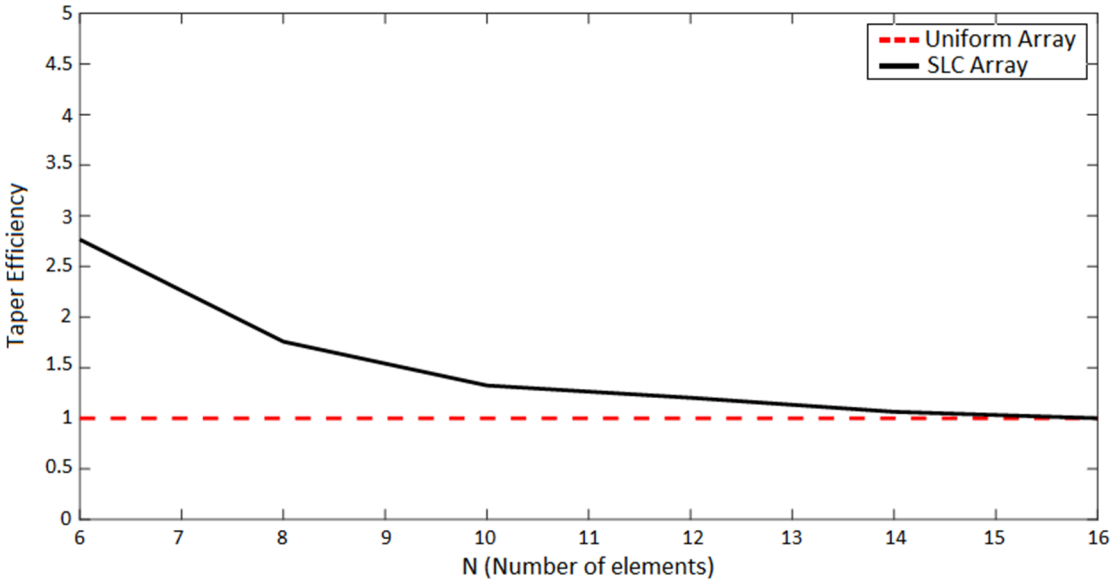

Figure (4.50) Taper efficiency comparison between ASLC and uniform arrays at d=0.5λ

4.5 Null Steering Method Maximum Directivity Result

For the three null steering methods that introduced in this dissertation, the maximum directivity (D) are measured and listed in Table (4.2). It can be seen that, the directivities in Schelkunoff method is decreased with increasing of the distance between the elements, while in Godara method, the performance is different, the directivities are increased with increasing of the distance between the elements. Also, the performance of ASLC are the same of that in Godara.

Table (4.2) Null Steering Methods Directivity

Method	**d**	**N**	**Uniform D (dB)**	**Non-uniform D (dB)**
Schelkunoff	0.2λ	6	3.225	7.515
	0.2λ	11	4.614	9.576
	0.4λ	6	4.774	5.47
	0.4λ	11	6.138	8.284
	0.5λ	6	2.27	1.992
	0.5λ	11	3.615	1.763
Godara	0.2λ	6	4.1928	4.3865
	0.2λ	11	6.6381	6.4168
	0.4λ	6	6.9131	6.8174
	0.4λ	11	9.5013	9.278

	0.5λ	6	7.7932	7.6369
	0.5λ	11	10.4252	10.2032
ASLC	0.2λ	6	15.24	15.52
	0.2λ	11	12.61	13.67
	0.4λ	6	15.24	16.38
	0.4λ	11	12.61	15.97
	0.5λ	6	15.24	17
	0.5λ	11	12.61	15.46

When the number of elements is increased, the directivity is increased in Schelkunoff and Godara, while it decreases in ASLC. The maximum directivities are achieved at ASLC and the minimum directivities at Schelkunoff method.

The directivities in Schelkunoff method are greater than that in uniform at 0.2λ and 0.4λ, while at 0.5λ, the directivity is decreased. For Godara method, the directivity is a slightly higher in that of uniform array. In ASLC the directivities are increased to that in uniform for all the specified distances.

4.6 Results Discussion

In this section, the discussion of the obtained results is introduced for the utilized techniques.

4.6.1 Regarding to Schelkunoff Method

In comparison to the uniform excited array, the Schelkunoff method has the ability to produce the nulls in the visible region. The main beam is

widen in comparison to uniform array when the distance d is increased between the elements and at d=0.5λ, null is created at the 90˚ for each of N=6 and N=11 as shown in Figures (4.5), (4.6), (4.7), (4.8), (4.9), and (4.10). The Schelkunoff method achieves lower ASLL than that in uniform array at 0.2λ and 0.4λ, while the ASLL is increased when d equal to 0.5λ as shown in Figures (4.11), (4.12) and (4.13). Higher tapering efficiency are achieved to that in uniform when d= 0.2λ and d=0.4λ as shown in Figures (4.14) and (4.15), while at 0.5λ, the taper efficiency is decreased as shown in Figure (4.16). It can be observed that the distance 0.2λ achieved the best performance compared to 0.4λ and 0.5λ. The directivity is increased in Schelkunoff method in comparison to that in uniform.

4.6.2 Regarding to Godara method

In comparison to the uniform excited array, the Godara method has the ability to create nulls at the specified angles at distance 0.5λ as shown in Figures (4.23) and (4.26). The Godara method achieved the same ASLL performance of the uniform array as shown in Figures (4.27), (4.28), and (4.29) for d equal to 0.2λ, 0.4λ and 0.5λ, respectively. Higher tapering efficiency were achieved in comparison to uniform array as shown in Figures (4.30), (4.31), and (4.32). The directivity is a slight increase in Godara method to that in uniform. In addition, when the array size is increased the directivity is increased as shown in Table (4.2).

4.6.3 Regarding to Adapted Side Lobe Canceller (ASLC)

The ASLC method achieved the desired null position and minimum of main beam distortion at N=11, M=5, SIR=-30 dB and d=0.5λ as shown in Figure (4.42), while for the same specifications, but at SIR=0 dB and

SIR=30 dB there is a distortion in the main beam as shown in Figures (4.43) and (4.44). The ASLC method achieved lower ASLL in comparison to uniform array as shown in Figures (4.45), (4.46), and (4.47). In addition, the Taper efficiency is increased at smaller array size and approaching to uniform performance at larger array size as shown in Figures (4.48), (4.49), and (4.50). The directivity is increased in comparison to the uniform array and the ASLC directivity decreased at N=11 in comparison to that at N=6 elements as shown in Table (4.2).

CHAPTER FIVE

CONCLUSIONS AND FUTURE WORKS

5.1 Conclusion

Null steering techniques are important in the wireless communication to cancel the unwanted signals in the desired direction. In this study, the investigation of three null steering methods are introduced Schelkunoff, Godara, and ASLC methods using the Matlab software program and at different simulation parameters. The conclusion obtained from this study are:

1. Schelkunoff method achieved N-1 nulls in the visible array pattern region. The main beam is widen in comparison to uniform array when the distance d is increased between the elements.
2. The Schelkunoff method achieves lower ASLL than uniform array at 0.2λ and 0.4λ, while the ASLL is increased when d equal to 0.5λ.
3. The Schelkunoff method achieves higher Taper efficiency in comparison to uniform array at 0.2λ and 0.4λ, while it decreased when d = 0.5λ.
4. The Godara method can achieve nulls at specified angles at d= 0.5λ, and can achieve the same ASLL performance to the uniform array. In addition, higher Taper efficiency is obtained in compared with uniform array.
5. The ASLC achieved the desired nulls using auxiliary array. ASLC method achieved lower ASLL in comparison to uniform array. As well as, the Taper efficiency is increased at smaller array size and approaching to uniform performance at larger array size
6. When the distance between the elements is increased, the directivities for both Godara and ASLC methods are increased, while

in Schelkunoff, the directivity is decreased with the increment of distance.

7. The ASLC method achieved higher directivity compared with Godara and Schelkunoff methods.

5.2 Future Works

1. Using other types of null steering methods.
2. Optimizing the results using Genetic algorithm (GA) or other optimizing methods.
3. Using another type of arrays such as planar or crossed arrays.
4. Using artificial intelligence techniques to improve the performance.
5. Applying the investigated methods to 5G base station arrays.

REFERENCES

[1] Quintessence of Nano-Satellite Technology: SMALL IS BIG. Planet Aerospace India. 2020

[2] C. A. Balanis, *Antenna Theory: Analysis and Design*, 3rd ed. New York: Wiley, 2005.

[3] "Smart antenna systems," International Engineering Consortium. [Online]. Available: www.iec.org/online/tutorials/smart antennas

[4] P.-J. Wan, "Capacity expansion: Sectorized cellular systems." [Online]. Available: http://www.csam.iit.edu/$\sim$wan/lecture05.pdf

[5] Constantine A. Balanis, Panayiotis I. Ioannides, *Introduction to Smart Antennas,*

[6] S. Bellofiore, "Smart antenna systems for mobile platforms," Ph.D. dissertation, Arizona State University, Dec. 2002

[7] Ram, Gopi, D. Suneel Varma, and G. Arun Kumar. "Memetic Flower Pollination Algorithm-Based Radiation Pattern in Time-Modulated Linear Antenna Arrays." In *Soft Computing for Problem Solving*, pp. 187-196. Springer, Singapore, 2021.

[8] R. T. Compton Jr., R. Huff, W. G. Swarner, and A. A. Ksienski, "Adaptive arrays for communication systems: An overview of research at the ohio state university," *IEEE Trans. Antennas Propagat.*, vol. AP-24, no. 5, pp. 599–607, Sept. 1976. doi:10.1109/TAP.1976.1141413

[9] R. A. Monzingo and T. W. Miller, *Introduction to Adaptive Arrays*. Scitech Publishing Inc., Oct. 2003, Mendham, NJ. ISBN 1-891121-24-3.

[10] S. P. Applebaum, “Adaptive arrays,” *IEEE Trans. Antennas Propagat.*, vol. AP-24, no. 5, pp. 585–598, Sept. 1976. doi:10.1109/TAP.1976.1141417

[11] Z. Fu, “Adaptive arrays antenna systems,” Ithaca, NY 14850, USA. [Online]. Available: http://people.cornell.edu/pages/zf24/Adaptive arrays.htm

[12] H. Steyskal, "Simple method for pattern nulling by phase perturbation," in *IEEE Transactions on Antennas and Propagation*, vol. 31, no. 1, pp. 163-166, January 1983, doi: 10.1109/TAP.1983.1142994

[13] T. B. Vu, “Method of null steering without using phase shifters’, In IEE Proceedings H (Microwaves, Optics and Antennas), vol. 131, no. 4, pp. 242-245), 1984.

[14] H. Steyskal, R. Shore and R. Haupt, "Methods for null control and their effects on the radiation pattern," in *IEEE Transactions on Antennas and Propagation*, vol. 34, no. 3, pp. 404-409, March 1986, doi: 10.1109/TAP.1986.1143816.

[15] M. M. Dawoud, and T. H. Ismail, “A new method for null steering by element position perturbations,” In1990 Symposium on Antenna Technology and Applied Electromagnetics, pp. 123-128, Aug 1990.

[16] T. H. Ismail and M. M. Dawoud, "Null steering in phased arrays by controlling the element positions," in *IEEE Transactions on Antennas and Propagation*, vol. 39, no. 11, pp. 1561-1566, Nov. 1991, doi: 10.1109/8.102769.

[17] I. Chiba and S. Mano, “Null beam forming by phase control of selected elements in phased-array antennas,” Electronics and Communications in Japan (Part I: Communications) vol. 74, no.12, pp. 23 32, 1991, doi:10.1002/ecja.4410741203.

[18] M. M. Dawoud, “Null steering in scanned linear arrays by element position perturbations,” International Journal of Electronics, vol. 78, no. 4, pp. 743-757, 1995, doi: 10.1080/00207219508926207.

[19] T.H. Ismail and M.J. Mismar, “Null Steering With Arbitrary Phase Perturbations Using Dual Phase Shifters,” Journal of Electromagnetic Waves and Applications, vol. 13, no. 8, pp. 1021-1029, 1999, doi: 10.1163/156939399X01159.

[20] R. Vescovo, “Null control for linear arrays by phase-only or amplitude only modification of the excitations,” IEEE Antennas and Propagation Society International Symposium. 1999 Digest. Held in conjunction with: USNC/URSI National Radio Science Meeting (Cat. No.99CH37010).

[21] Y. C. Chung and R. L. Haupt, “Amplitude and Phase Adaptive Nulling With a Genetic Algorithm,” Journal of Electromagnetic Waves and Applications, vol.14, no.5, pp. 631-649, 2000, doi: 10.1163/156939300X01337.

[22] R. Vescovo, “Null synthesis by phase control for antenna array,“ Electronics Lett., vol. 36, no. 33, pp. 198-199, 2000.

[23] Mohammed, J. R., “An investigation into Side Lobe Reduction and Cancellation Techniques”, M.Sc. Thesis, Mosul University, 2000.

[24] J. A. Hejres, "Null steering in phased arrays by controlling the positions of selected elements," in *IEEE Transactions on Antennas*

and Propagation, vol. 52, no. 11, pp. 2891-2895, Nov. 2004, doi: 10.1109/TAP.2004.835128.

[25] M. Moctar, P. Vaudon, and M. Rammal. "Smart antenna array patterns synthesis: Null steering and multi-user beamforming by phase control," Progress In Electromagnetics Research, vol. 60, pp. 95-106, 2006.

[26] M.J. Mismar, T.H. Ismail, and D.I. Abu-Al-Nadi, "Analytical array polynomial method for linear antenna arrays with phase-only control," vol. 61, no. 7, pp. 485–492, 2007, doi:10.1016/j.aeue.2006.06.009

[27] J. A. Hejres, A. Peng and J. Hijres, "Fast Method for Sidelobe Nulling in a Partially Adaptive Linear Array Using the Elements Positions," in *IEEE Antennas and Wireless Propagation Letters*, vol. 6, pp. 332-335, 2007, doi: 10.1109/LAWP.2007.900955.

[28] R. Ghayoula, N. Fadlallah, A. Gharsallah, and M. Rammal, "Phase-only adaptive nulling with neural networks for antenna array synthesis," IET Microw. Antennas Propag., vol. 3, no. 1, pp. 154–163, 2009.

[29] R. A. Qamar and N. M. Khan, "Null steering, a comparative analysis," *IEEE 13th International Multitopic Conference*, pp. 1-5, 2009 .doi: 10.1109/INMIC.2009.5383130.

[30] Nihad I. Dib Sotirios K. Goudos Hani Muhsen, "Application of Taguchi's Optimization Method and Self-Adaptive Differential Evolution to the Synthesis of Linear Antenna Arrays," Progress In Electromagnetics Research, vol. 102, pp. 159-180, 2010. doi:10.2528/PIER09122306.

[31] K. H. Sayidmarie and J. R. Mohammed, “Null steering method by controlling two elements,” IET Microwaves, Antennas & Propagation, vol. 8, no.15, pp. 1348–1355, 2014, doi:10.1049/iet-map.2014.0213.

[32] Al Zubaidy, Mahmod A., and Shatha M. Ali. "Study and Evaluation of The Uniform and Nonuniform Beam forming Systems for Reduction the Noise and Interference.", International Journal of Engineering and Innovative Technology, Volume 7, Issue 2, August 2017.

[33] J. R. Mohammed, “Obtaining Wide Steered Nulls in Linear Array Patterns by Optimizing the Locations of Two Edge Elements. AEU - International Journal of Electronics and Communications, vol. 101, no. 1, pp.145-151, 2019, doi:10.1016/j.aeue.2019.02.004.

[34] J. R. Mohammed, R. H. Thaher, A. J. Abdulqader, “ Linear and Planar Array Pattern Nulling via Compressed Sensing,” Journal of Telecommunictions and Information Technology, vol. 3. pp. 50-55, 2021, doi:10.26636/jtit.2021.152921.

[35] S. Rahman, Q. CAO, M. M. Ahmed, and H. Khalil “Analysis of linear antenna array for minimum side lobe level, half power beamwidth, and nulls control using PSO,” Journal of Microwaves, Optoelectronics and Electromagnetic Applications, vol. 16, pp. 577-91, 2017.

[36] C. A. Balanis, Antenna Theory Analysis And Design, 4th Edi. Hoboken, New Jersey: John Wiley & Sons, Inc., 2016.

[37] Electronics Club website, https://electronics-club.com/antenna-array/

[38] https://www.cdeep.iitb.ac.in/slides/A16/EE609/EE609-L6.pdf

[39] https://www.allaboutcircuits.com/technical-articles/antenna-basics-field-radiation-patterns-permittivity-directivity-gain/

[40] https://cnj.atu.edu.iq/wp-content/uploads/2020/03/lec-2-1.pdf

[41] https://www.qsl.net/va3iul/Antenna/Phased_Array_Antennas/Phased_Array_Antennas.pdf

[42] Anjaneyulu, G., Siddartha Varma, J. (2020). Synthesis of Low Sidelobe Radiation Patterns from Embedded Dipole Arrays Using Genetic Algorithm. In: Karrupusamy, P., Chen, J., Shi, Y. (eds) Sustainable Communication Networks and Application. ICSCN 2019. Lecture Notes on Data Engineering and Communications Technologies, vol 39. Springer, Cham https://doi.org/10.1007/978-3-030-34515-0_84

[43] Mailloux, Robert J. Phased array antenna handbook. Artech house, 2017

[44] Yadav, Kuldeep & Rajak, Amit & Singh, H.. (2015). Array Failure Correction with Placement of Wide Nulls in the Radiation Pattern of a Linear Array Antenna Using Iterative Fast Fourier Transform. Proceedings - 2015 IEEE International Conference on Computational Intelligence and Communication Technology, CICT 2015. 471-474. 10.1109/CICT.2015.33.

[45] K. Guney and A. Akdagli, "Null steering of linear antenna arrays using a modified tabu search algorithm," Progress In Electromagnetics Research, vol, 33, pp.167-82, 2001.

[46] D. D. Helmut, E. Schrank,and G. E. Evans, Radar Hanbook, 2nd Ed., San Francisco: McGraw-Hill, 1990.

[47] H.O. Quispe, “Implementation Of Null Steering Algorithms In a Compact Analog Array,” Phd. dissertation, Montana State University, 2014.

[48] L. Godara, "Application of Antenna Arrays to Mobile Communications, Part II: Beam-Forming and Direction-of-Arrival Considerations," Proceedings of the IEEE, vol. 85, no. 8, pp. 1195-1245, Aug. 1997.

[49] T. Hong,” Design of an Adaptive Sidelobe Cancellation Algorithm for Radar,” Journal of Physics: Conference Series, vol. 1754, no. 1, p. 012217 Feb. 2021, doi:10.1088/1742-6596/1754/1/012217

[50] B. D. Van Veen and K. M. Buckley, "Beamforming: a versatile approach to spatial filtering," in *IEEE ASSP Magazine*, vol. 5, no. 2, pp. 4-24, April 1988, doi: 10.1109/53.665.

[51] J. R. Mohammed, K. H. Sayidmarie, “Performance evaluation of the adaptive sidelobe canceller system,” Electronics and Communications, vol. 80, pp. 179–185, 2017, doi:10.1016/j.aeue.2017.06.039

الخلاصة

دفعت التداخلات المتزايدة للبيئة الكهرومغناطيسية إلى دراسة تقنيات إبطال أنماط المصفوفة. هذه التقنيات مهمة للغاية في أنظمة الاتصالات لتقليل الانحلال في أداء نسبة الإشارة إلى الضوضاء بسبب التداخل غير المرغوب فيه، والذي يحفز التقدم في هوائيات مستقبل الاتصالات وبالتالي طرق التركيب.

تبحث هذه الرسالة في ثلاثة أنواع من طرائق توجيه القيم الفارغة، هي: طريقة Schelkunoff وطريقة Godara وطريقة Adapted Side Lobe Canceller (ASLC) باستخدام برنامج الـ Matlab. تم استخدام حجمين لمصفوفة الهوائي بعدد عناصر N=6 و N=11، والمسافات (d) بين العناصر هي 0.2λ و 0.4λ و 0.5λ للطرائق الثلاث المستخدمة. تمت مقارنة أداء طرائق توجيه القيم الفارغة بأداء المصفوفة الخطية المنتظمة واسعة النطاق.

تظهر نتائج المحاكاة أنّ طريقة Schelkunoff لديها القدرة على إزاحة (N-1) من القيم الفارغة إلى المنطقة المرئية عند d=0.2λ، بينما تُنشئ طريقة Godara قيمًا فارغة عند الزوايا المحددة عند d=0.5λ. حققت طريقة ASLC الاتجاه المطلوب للحزمة الرئيسية وموقع القيمة الفارغة عند نسبة إشارة إلى ضوضاء التداخل (SIR) قيمتها 30 dB-، وتراجع أداؤها عندما كانت الـ SIR مساوية لـ 0 dB و 30 dB.

حققت طريقتا Schelkunoff و ASLC متوسط مستوى فص جانبي (ASLL) أعلى مما هو عليه في المصفوفة المنتظمة، بينما حققت طريقة Godara متوسط مستوى فص جانبي (ASLL)مماثلًا لما هو عليه في المصفوفة المنتظمة. وحققت التقنيات الثلاث كفاءة تناقصية (Taper Efficiency) أعلى مقارنةً بالمصفوفة المنتظمة. أخيرًا، تبيّن أنّ مصفوفات الطرائق الثلاث المستخدمة تحقق اتجاهية أعلى مما في المصفوفات المنتظمة، وأقصى اتجاهية تم الحصول عليها تحققت بطريقة ASLC.

وزارة التعليم العالي والبحث العلمي
جامعة نينوى
كلية هندسة الالكترونيات
قسم هندسة الاتصالات

استقصاء أداء تقنيات توجيه القيم الفارغة في مصفوفات الهوائي الخطية

رسالة تقدم بها

محمد أزهر فخري

إلى
مجلس كلية هندسة الالكترونيات
جامعة نينوى
كجزء من متطلبات نيل شهادة الماجستير
في
هندسة الاتصالات

بإشراف

أ.د. جعفر رمضان محمد

وزارة التعليم العالي والبحث العلمي
جامعة نينوى
كلية هندسة الالكترونيات
قسم هندسة الاتصالات

استقصاء أداء تقنيات توجيه القيم الفارغة في مصفوفات الهوائي الخطية

محمد أزهر فخري

رسالة ماجستيرعلوم في هندسة الاتصالات

بإشراف

أ. د. جعفر رمضان محمد

1444 هـ

2022 م